AD-760 583

INVESTIGATION OF THERMAL FATIGUE IN NON-TUBULAR REGENERATIVELY COOLED THRUST CHAMBERS. VOLUME II

D. Fultons

Rockwell International Corporation

Prepared for:

Air Force Rocket Propulsion Laboratory

May 1973

AFRPL-TR-73-10
VOLUME II

INVESTIGATION OF THERMAL FATIGUE IN NON-TUBULAR REGENERATIVELY COOLED THRUST CHAMBERS

FINAL REPORT
VOLUME II

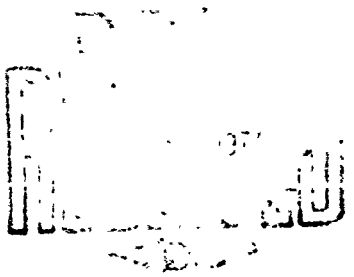

D. FULTON
ADVANCED PROGRAMS

ROCKETDYNE DIVISION, ROCKWELL INTERNATIONAL
6633 Canoga Avenue, Canoga Park, California

TECHNICAL REPORT AFRPL-TR-73-10, VOLUME II

May 1973

Air Force Rocket Propulsion Laboratory
Director of Science & Technology
Air Force Systems Command
United States Air Force
Edwards, California

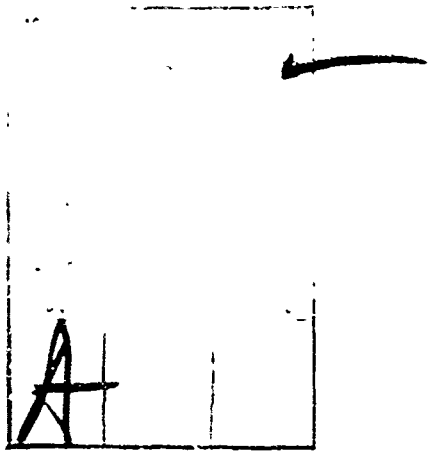

"When U. S. Government drawings, specifications, or other data are used for any purpose other than a definitely related Government procurement operation, the Government thereby incurs no responsibility nor any obligation whatsoever, and the fact that the Government may have formulated, furnished, or in any way supplied the said drawings, specifications, or other data, is not to be regarded by implication or otherwise, or in any manner licensing the holder or any person or corporation, or conveying any rights or permission to manufacture, use, or sell any patented invention that may in any way be related thereto."

Unclassified

Security Classification

DOCUMENT CONTROL DATA - R & D

Security classification of title, body of abstract and indexing annotation must be entered when the overall report is classified.

1. ORIGINATING ACTIVITY (Corporate author) ROCKETDYNE DIVISION ROCKWELL INTERNATIONAL CORPORATION 6633 Canoga Avenue, Canoga Park, California 91304	2a. REPORT SECURITY CLASSIFICATION Unclassified 2b. GROUP

3. REPORT TITLE

Investigation of Thermal Fatigue in Non-Tubular Regeneratively Cooled Thrust Chambers, Volume II

4. DESCRIPTIVE NOTES (Type of report and inclusive dates)

5. AUTHOR(S) (First name, middle initial, last name)

Donald L. Fulton

6. REPORT DATE	7a. TOTAL NO. OF PAGES	7b. NO. OF REFS
May 1973	114	0

8a. CONTRACT OR GRANT NO	9a. ORIGINATOR'S REPORT NUMBER(S)
F04611-70-C-0014	R-9093
b. PROJECT NO 3058	
c. Task 305810	9b. OTHER REPORT NO(S) (Any other numbers that may be assigned this report) AFRPL-TR-73-10 Volume II
d.	

10. DISTRIBUTION STATEMENT

Approval for public release; distribution unlimited

11. SUPPLEMENTARY NOTES	12. SPONSORING MILITARY ACTIVITY
	Air Force Rocket Propulsion Laboratory

13. ABSTRACT

Long life non-tubular teneratively cooled thrust chambers were fabricated and hot-fire cyclic tested to verify the life prediction techniques established in Volume I of this report.

Chambers incorporating copper alloy (NARloy-Z and zirconium copper) and nickel for the hot gas wall material and electroformed nickel closures were fabricated by Rocketdyne and hot fire cyclic tested by the AFRPL. Propellants were LO_2/H_2 at a nominal mixture ratio of 6:1. Chamber pressure was 750 psia and thrust (corrected to vacuum and with a full area ratio nozzle) was 3300 pounds. A calorimeter thrust chamber assembly (calorimeter thrust chamber and coaxial injector) were also fabricated and hot-fire tested to establish the heat flux profile.

Post-test analysis and metallurgical evaluation of the chamber were performed to locate and define fatigue cracks.

DD FORM 1 NOV 65 1473

Unclassified

Security Classification

14 KEY WORDS	LINK A		LINK B		LINK C	
	ROLE	WT	ROLE	WT	ROLE	WT
Thermal Fatigue Prediction Analysis						
Parametric Heat Transfer Analysis						
Life of Non-Tubular Chambers						
Material Properties						
Isothermal Fatigue Data						
Chamber Designs						
Fatigue and Panel Testing						
Copper Alloys for Chambers						
Nickel for Chambers						

AFRPL-TR-73-10

INVESTIGATION OF THERMAL FATIGUE IN NON-TUBULAR REGENERATIVELY COOLED THRUST CHAMBERS

FINAL REPORT

VOLUME II

D. FULTON
ADVANCED PROGRAMS

ROCKETDYNE DIVISION, ROCKWELL INTERNATIONAL
6633 Canoga Avenue, Canoga Park, California

TECHNICAL REPORT AFRPL-TR-73-10, VOLUME II

May 1973

Air Force Rocket Propulsion Laboratory
Director of Science & Technology
Air Force Systems Command
United States Air Force
Edwards, California

FOREWORD

The information reported herein was prepared under sponsorship of the Rocket Propulsion Laboratory at Edwards Air Force Base under Contract F04611-70-C-0014, Project 3058, Task 305810. Testing at the AFRPL was accomplished under in-house project 305810RY.

Acknowledgment is made to the many North American Rockwell personnel who contributed to this effort. Major contributors were:

Thermal Analysis	- R. D. Tobin J. M. Shoji
Structural and Life Analysis	- R. A. Cooper N. E. Bergstresser
Design	- L. R. Russell R. G. Barnsdale
Materials and Processes	- J. G. Somerville R. G. Cron

The Air Force Project Engineer was Mr. C. D. Penn, AFRPL/LKCG.

This report (R-9093) has been reviewed and is approved

Carleon D. Penn
Project Engineer
Liquid Rocket Division
Air Force Rocket Propulsion Laboratory
Edwards, California

ABSTRACT

Long life non-tubular regeneratively cooled thrust chambers were fabricated and hot fire cyclic tested to verify the life prediction techniques established in Volume I of this report.

Chambers incorporating copper alloy (NARloy Z and zirconium copper) and nickel for the hot gas wall material and electroformed nickel closures were fabricated by Rocketdyne and hot fire cyclic tested by the AFRPL. Propellants were LO_2/H_2 at a nominal mixture ratio of 6:1. Chamber pressure was 750 psia and thrust (corrected to vacuum and with a full area ratio nozzle) was 3300 pounds. A calorimeter thrust chamber assembly (calorimeter thrust chamber and coaxial injector) were also fabricated and hot-fire tested to establish the heat flux profile.

Post-test analysis and metallurgical evaluation of the chamber were performed to locate and define fatigue cracks.

CONTENTS

ILLUSTRATIONS

TABLES

INTRODUCTION

The next generation of liquid rocket engine thrust chambers will employ non-tubular construction methods and will have a requirement for long life and multiple reuse. The practicality of producing non-tubular thrust chambers of the candidate materials has been demonstrated in a range of thrust and chamber pressure levels. However, very little effort has been expended in evaluating the long life characteristics of such chambers.

The Air Force Rocket Propulsion Laboratory (AFRPL) awarded the Rocketdyne Division, Rockwell International, a contract to analytically and experimentally explore the long life characteristics of non-tubular thrust chambers. This program was entitled "Investigation of the Thermal Fatigue Characteristics of Non-Tubular Regeneratively Cooled Thrust Chambers."

The objective of this program was to (1) define design criteria for the thermal cycling capability of non-tubular regeneratively cooled thrust chambers and (2) to demonstrate this cycling capability.

The results of Phase II - Thermal Cycling Demonstration are presented herein. The results of Phase I - Development of Design Criteria are presented in Volume I.

SUMMARY

Phase II of this program, entitled Thermal Cycling Demonstration, consisted of three tasks:

Task I - Fabrication and Structural Testing
Task II - Test
Task III - Post-Test Analysis

In Task I a total of three regeneratively cooled thrust chambers were fabricated:

NARloy-Z Regeneratively Cooled Chamber
Zirconium Copper Regeneratively Cooled Chamber
Nickel 200 Regeneratively Cooled Chamber

All chambers incorporated an annealed electroformed nickel closure and were fabricated as follows.

A forged disk was spun to chamber shape, the internal and external surfaces were machined, the coolant passages were machined into the outer surface and the electroformed nickel closure deposited in place. Subsequently, flanges and manifolds were TIG brazed onto either end of the chambers and appropriate instrumentation added.

The copper alloy chambers were of identical design and incorporated 40 constant width, variable depth coolant passages. The nickel 200 chamber incorporated 7? step width, variable depth channels with transition occurring at a plane ~ 2.9 inches upstream of the throat.

Also fabricated was a calorimeter thrust chamber to be used to establish the heat flux profile and a 40 element coaxial injector to be tested with the calorimeter thrust chamber and used in the cyclic test effort.

A total of 654 cycles were accumulated on the NARloy-Z chamber and 587 cycles were accumulated on the zirconium copper chamber. At the end of the cyclic test series the NARloy-Z chamber had 5 cracks through the wall and the zirconium copper chamber had 16 through cracks.

The hot gas surface of the NARloy-Z chamber was in good condition after testing; however, the zirconium copper chamber showed substantial surface roughness. This was attributed to its coarse grain structure when compared to the NARloy-Z. The nickel 200 chamber accumulated approximately 50 cycles with no evidence of fatigue cracking when a facility malfunction damaged the chamber.

Post-test evaluation of the two copper alloy chambers showed that generally the cracks were associated with small zirconium oxide inclusions. These inclusions are formed as small spherical globules during ingot processing and are subsequently worked into long narrow stringers by the forging and spinning operation.

The chambers both demonstrated good life characteristics even with these small inclusions. In addition, processing techniques are available which will produce ingots free of these inclusions to improve life even further.

DISCUSSION

This program was undertaken with the objective of defining design criteria for the thermal cycling capability of non-tubular regeneratively cooled thrust chambers and to demonstrate this cycling capability. The program effort was divided into two phases:

Phase I - Development of Design Criteria
Phase II - Thermal Cycling Demonstration

The results of the Phase I effort are presented in Volume I of this report. Phase II results are presented herein.

PHASE II - TASK I - FABRICATION AND STRUCTURAL TESTING

In this task the hardware designed as a part of the Phase I effort was fabricated, laboratory tested and delivered to the AFRPL for hot-fire testing. The hardware that was fabricated included:

Nickel 200 Regeneratively Cooled Thrust Chamber
NARloy-Z Regeneratively Cooled Thrust Chamber
Zirconium-Copper Regeneratively Cooled Thrust Chamber
Calorimeter Thrust Chamber Assembly
    Water Cooled Calorimeter Thrust Chamber
    Co-axial Element Injector

A discussion of the fabrication and structural test history of each follows.

Nickel 200 Thrust Chamber

The nickel 200 chamber consisted of a spun and machined nickel 200 liner, an electroformed nickel closure, and welded-on stainless steel flanges and manifolds.

The liner was hot-spun from ultrasonically inspected nickel 200 plate stock as shown schematically in Fig. 1. After spinning, the liner was annealed at 1500 F for 30 minutes and then ultrasonic and dye-penetrant inspected preparatory to machining into the final configuration. A typical as-spun liner is shown in Fig. 2.

Machining of the liner consisted of cutting three contours; the A mold line (thrust chamber internal contour), the B mold line (bottom of the coolant channel), and C mold line (chamber external contour). Each of these operations constituted a tracer lathe or mill procedure. To insure maximum tolerance control, the templates for the three operations were manufactured as a coordinated set, with the B template matched to the A for control of wall thickness, and the C template matched to the B for control of channel depth.

The first step in liner machining was to maching the internal contour to net dimensions using the A template. The liner was then installed on a mandrel, all void areas filled with wax and the external contour machined to its net dimensions using the C template. Coolant channels were then machined into the liner using the B template. The initial slotting operation consisted of adding the 0.080 channels into the combustion zone (Fig. 3), followed by machining of the 0.040 wide channels in the throat region. The as-slotted liner is shown in Fig. 4 and a closeup view of the transition from 0.040 wide channels to 0.080 wide channels is shown in Fig. 5. The channels were then deburred and the liner removed from the mandrel for inspection.

After verifying dimensional acceptability, the liner was prepared for electroforming of the nickel closure. The liner was reinstalled on the mandrel. The channels were filled with wax and the surface hand sanded to the proper conditions. A conductive copper power was added over the wax. The liner was placed inside its plexiglass shielding (Fig. 6) and taken through its activation and electroforming cycles. The as-electroformed closure is shown in Fig. 7. After electroforming the outer contour was machined to the prescribed thickness using a fourth, or D template. This machining was also accomplished using a tracer lathe. The manifold configuration was also machined into each end, and the liner was cut to the final length. The liner was then removed from the mandrel and

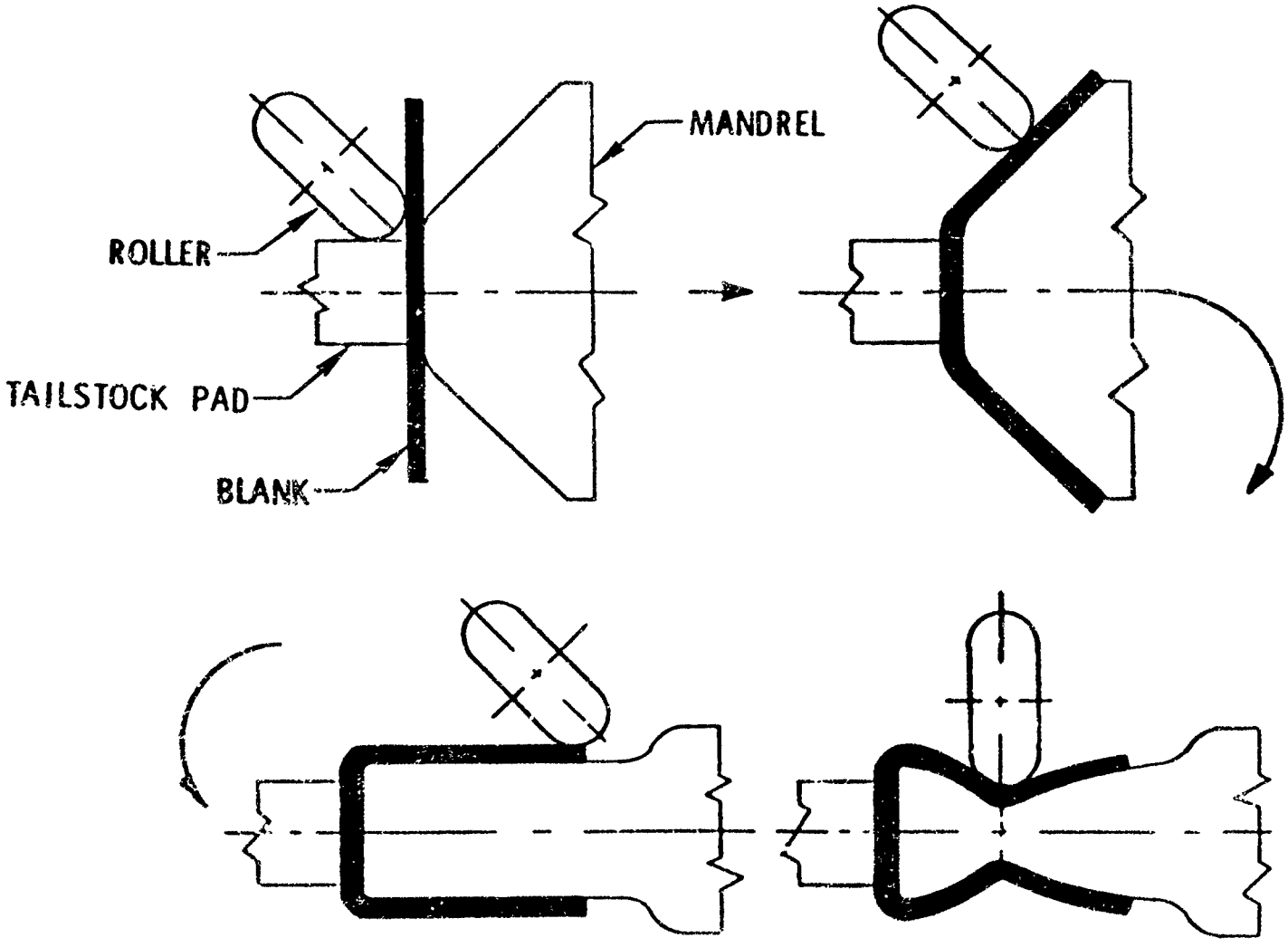

Figure 1. Fabrication Process - Form Spinning

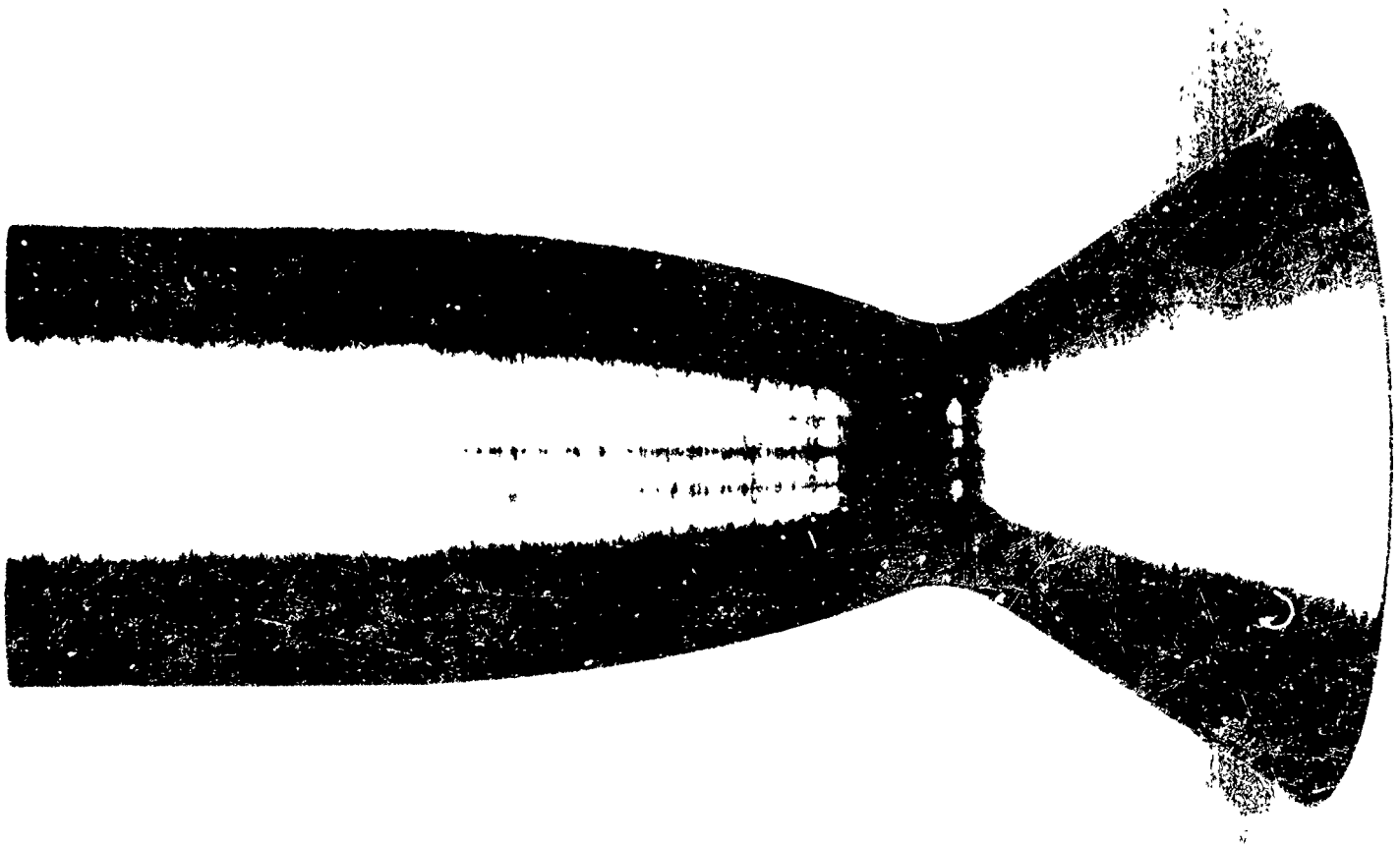

Figure 2. Nickel-200 Spinning

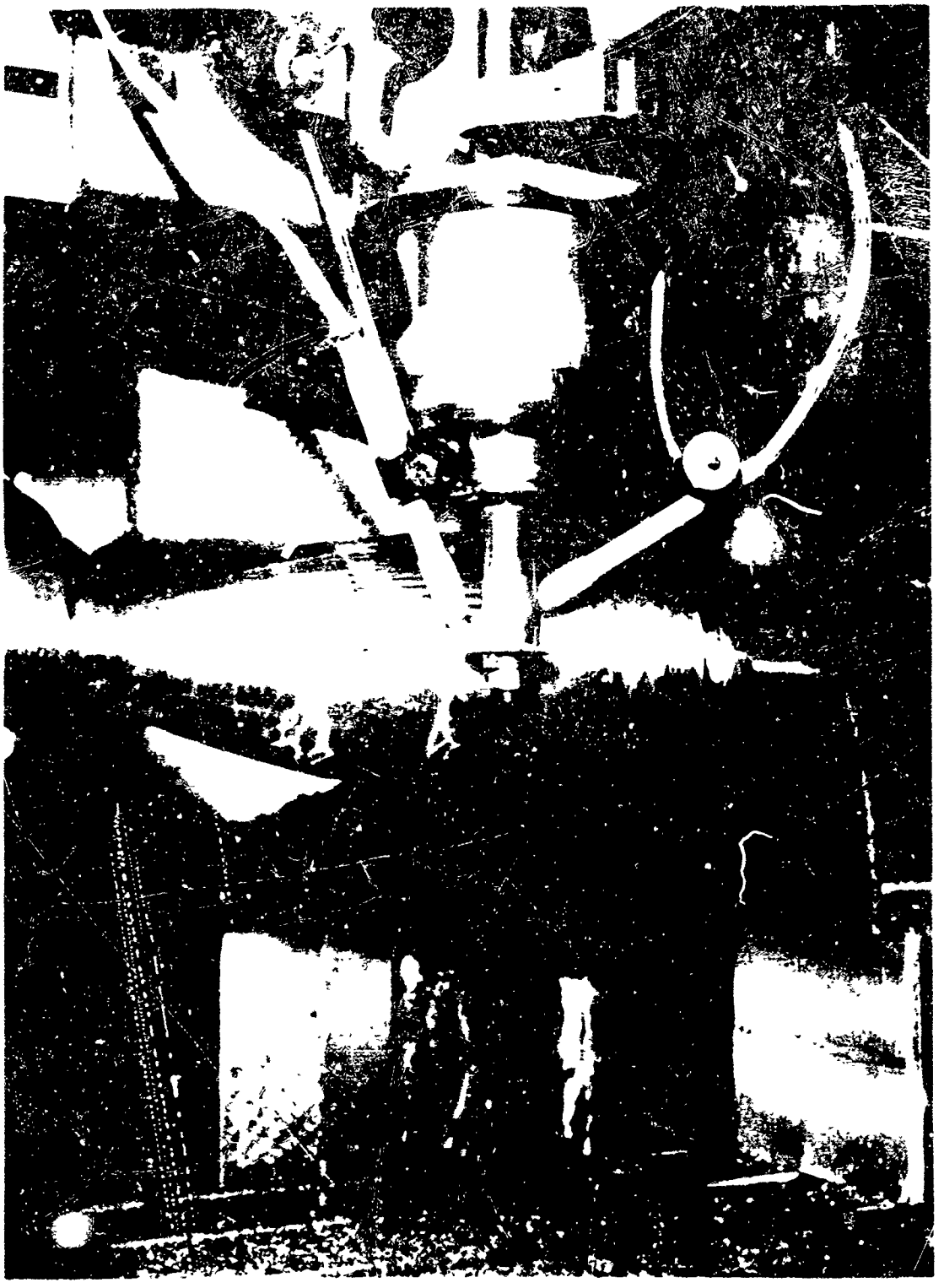

1X232-3/19/71-C1A

Figure 3. View Showing Slotting Operation on Nickel-200 Chamber

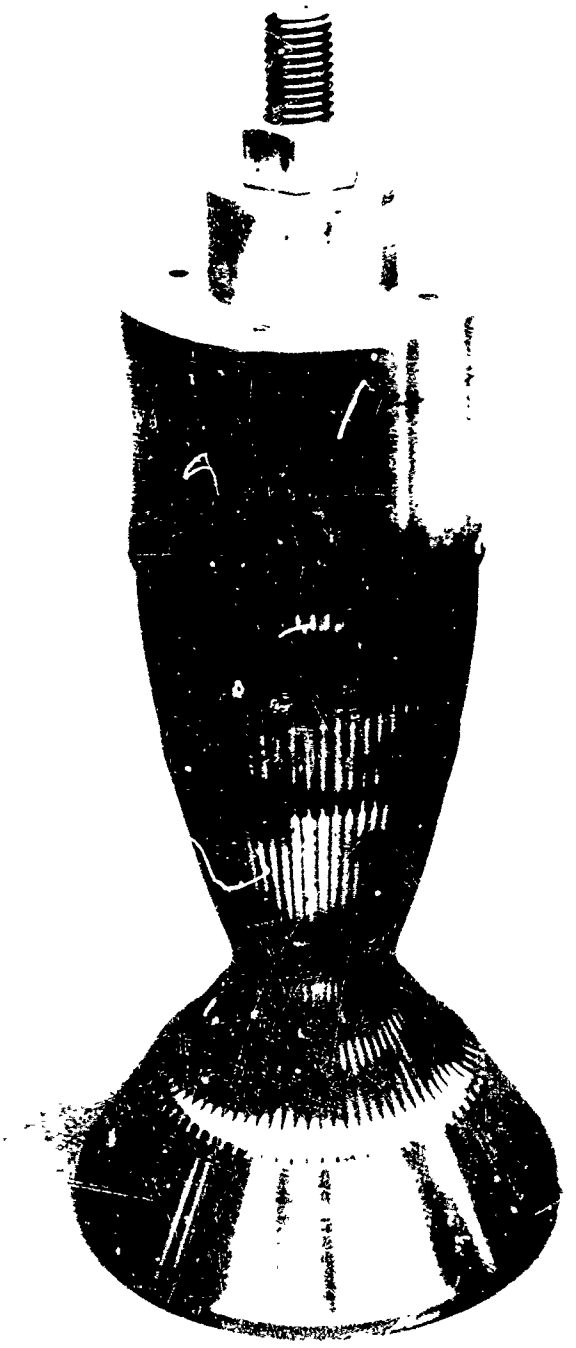

1XZ32-3/25/71-C1C

Figure 4. View Showing Slotted Nickel-200 Chamber

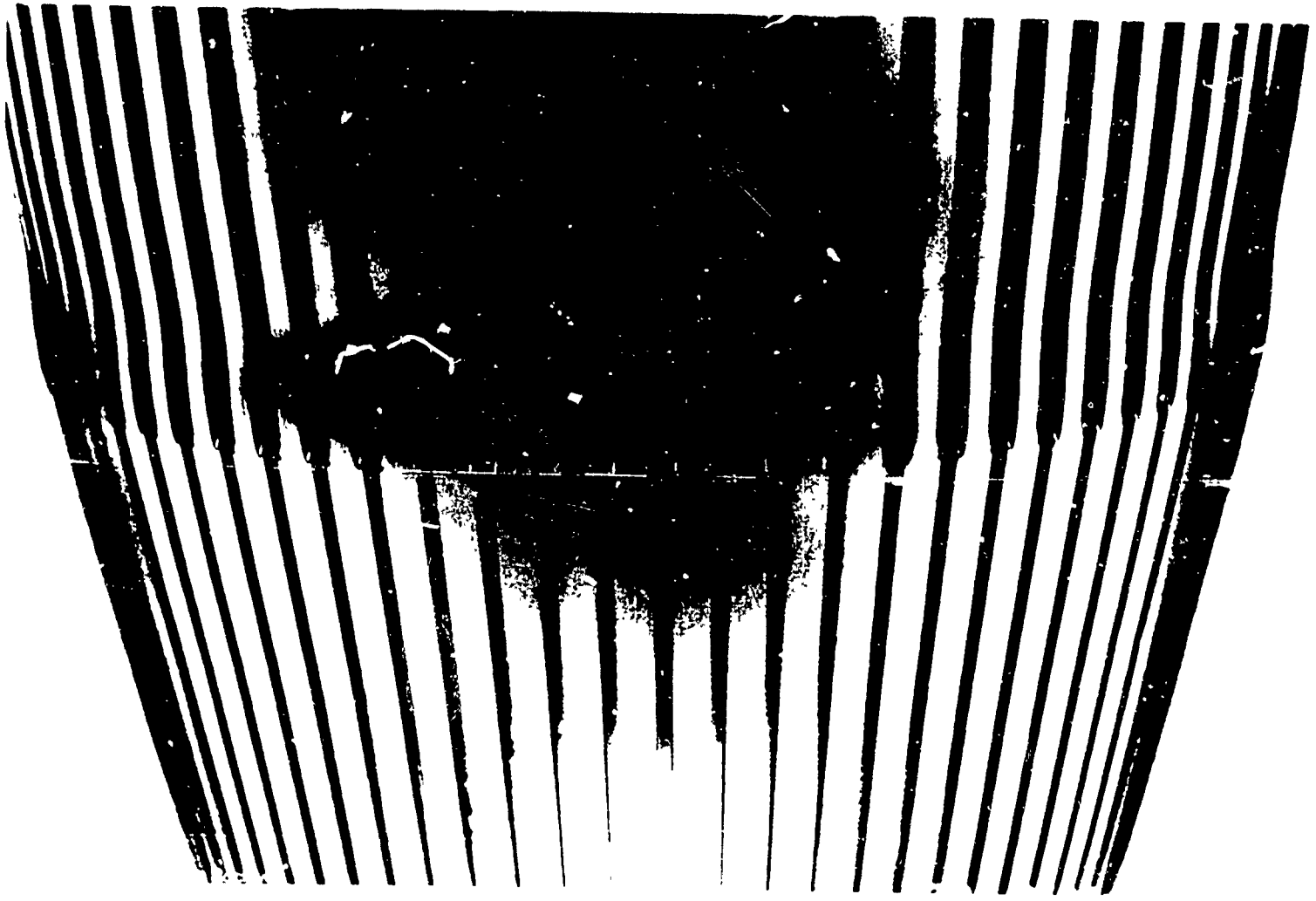

IXZ32-3/25/71-C1A

Figure 5. Close-Up View of Channel Transition on Nickel-200 Chamber

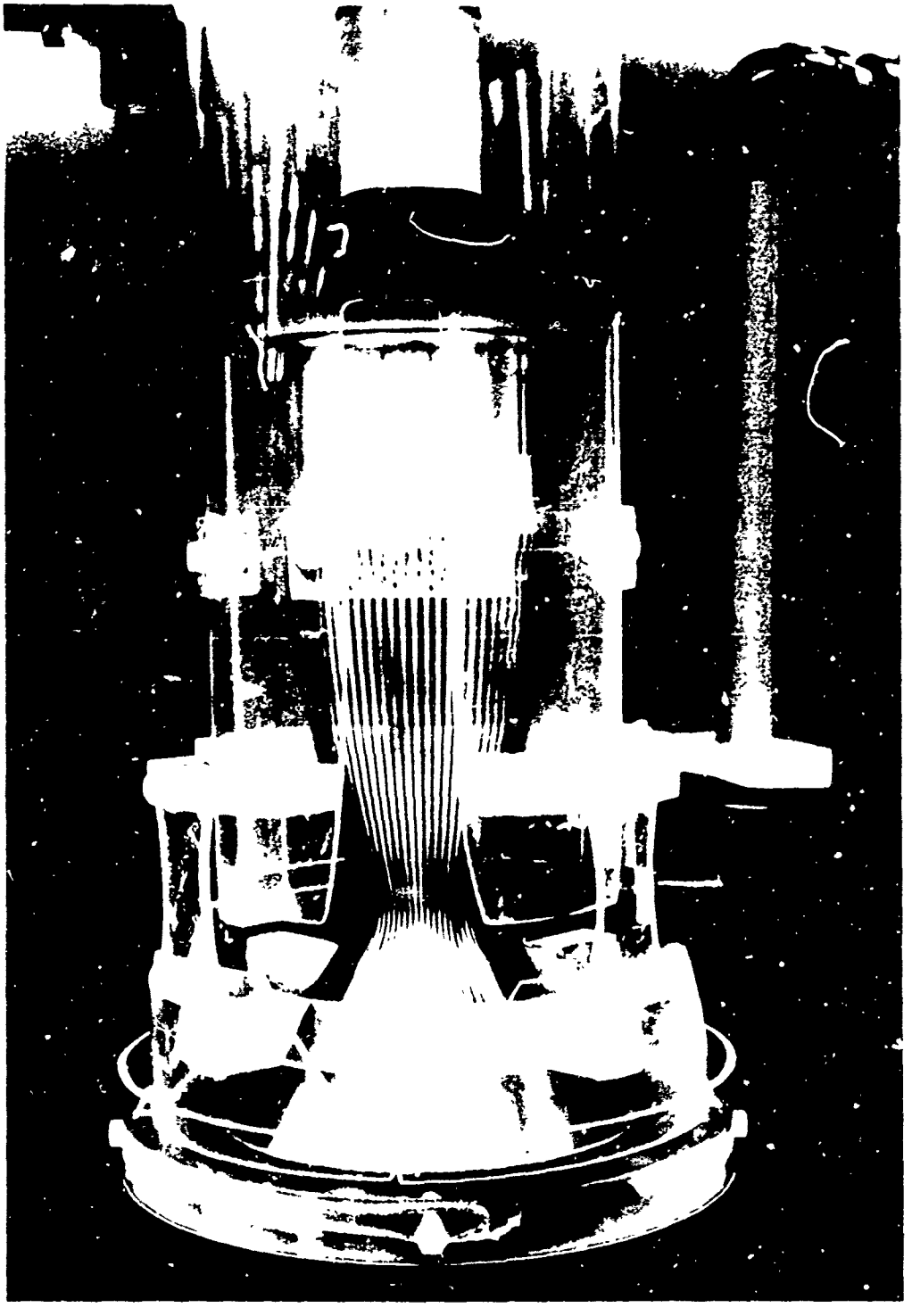

1XW32-4/1/71-C2A

Figure 6. Nickel-200 Chamber Ready for Electroforming

1XW32-4/8/71-C1

Figure 7. As-Electroformed Nickel-200 Chamber

all wax flushed from the channels. A visual inspection and flow test was run at this time to assure that all channels were open and flowing properly. The chamber is shown in this condition in Fig. 8. The liner was then annealed at 900 F for 30 minutes in argon to improve the hydrogen resistance capability of the electroformed nickel closeout. Subsequently, the 304L stainless steel flanges, which had been prepared as subassemblies were TIG brazed to chamber body. The final operation then consisted of finish machining these flanges to establish sealing surfaces, etc. The completed chamber, shown in Fig. 9, was then waterflow checked to assure proper coolant distribution, proof pressure tested to 2400 psig and delivered to the AFRPL for hot fire testing.

Copper Alloy Thrust Chambers

Fabrication of the two copper alloy chambers was virtually identical in process to the nickel chamber fabrication. The major exception being that the fabrication process started with the procurement of cast ingots which were subsequently processed into plate stock for spinning.

The NARloy-Z ingot was melted using the procedures Rocketdyne had previously developed for producing this company proprietary alloy. After casting, the ingot was hot forged into a disk and ultrasonically inspected to verify that it was free of zirconium oxide inclusions. This inspection conducted to a Rocketdyne specification was used to verify that there were no inclusions larger than 0.050 inch in diameter.

This forged disk was then hot spun into the chamber shape, heat treated, and aged (900 F for 4 hours). The completed liner was again ultrasonic inspected and penetrant inspected to verify quality.

The NARloy-Z liner was then machined using the same procedures and types of templates as those employed on the nickel chamber. The major difference was that the NARloy-Z chamber incorporated 40 constant width (.080 inches wide) channels rather than the step width channels employed in the nickel chamber. A completed NARloy-Z liner is shown in Fig. 10 and 11. The liner, ready for

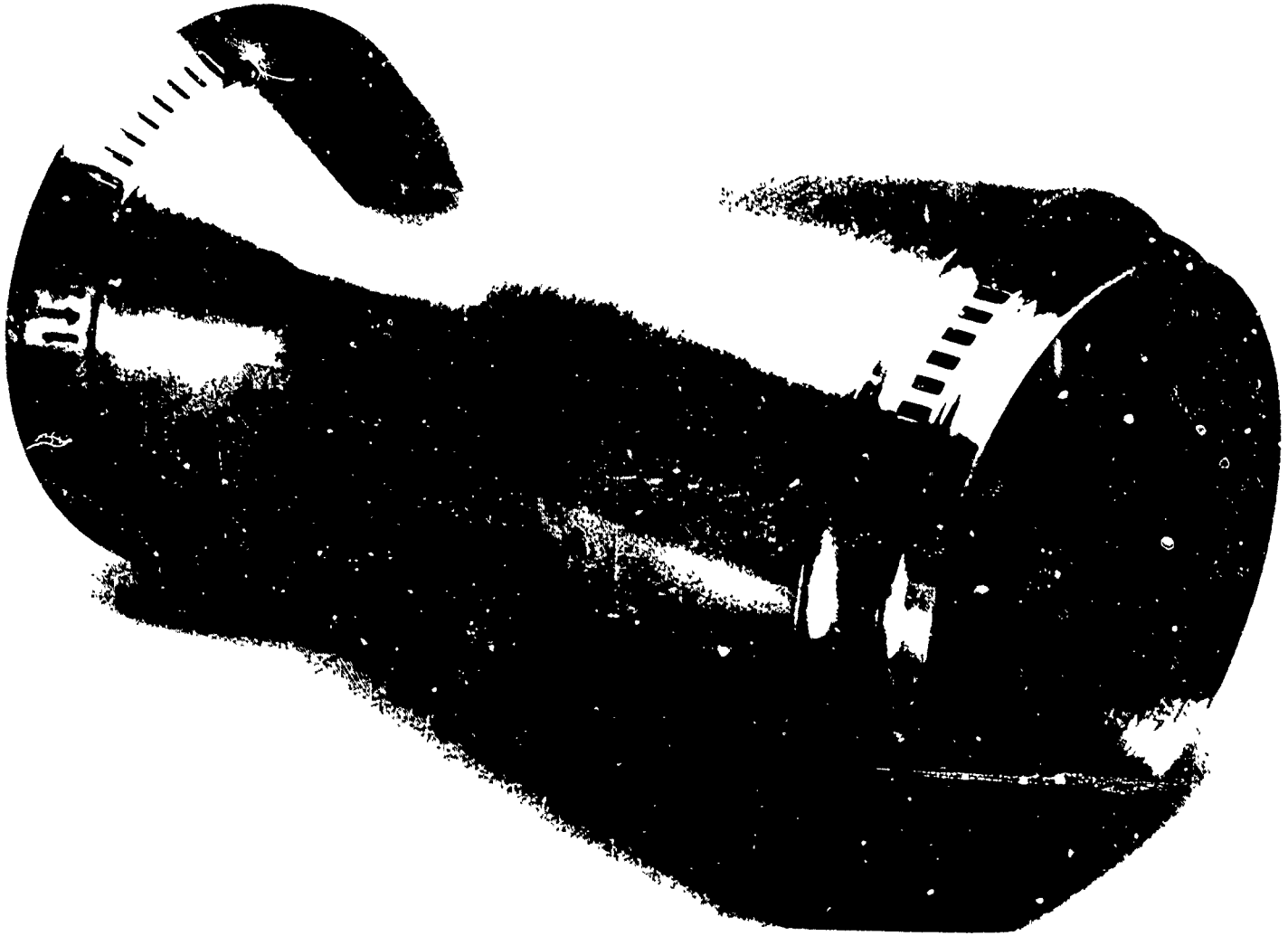

1XZ31-5/5/71-C18

Figure 8. Nickel-200 Chamber Prior to Addition of Flanges

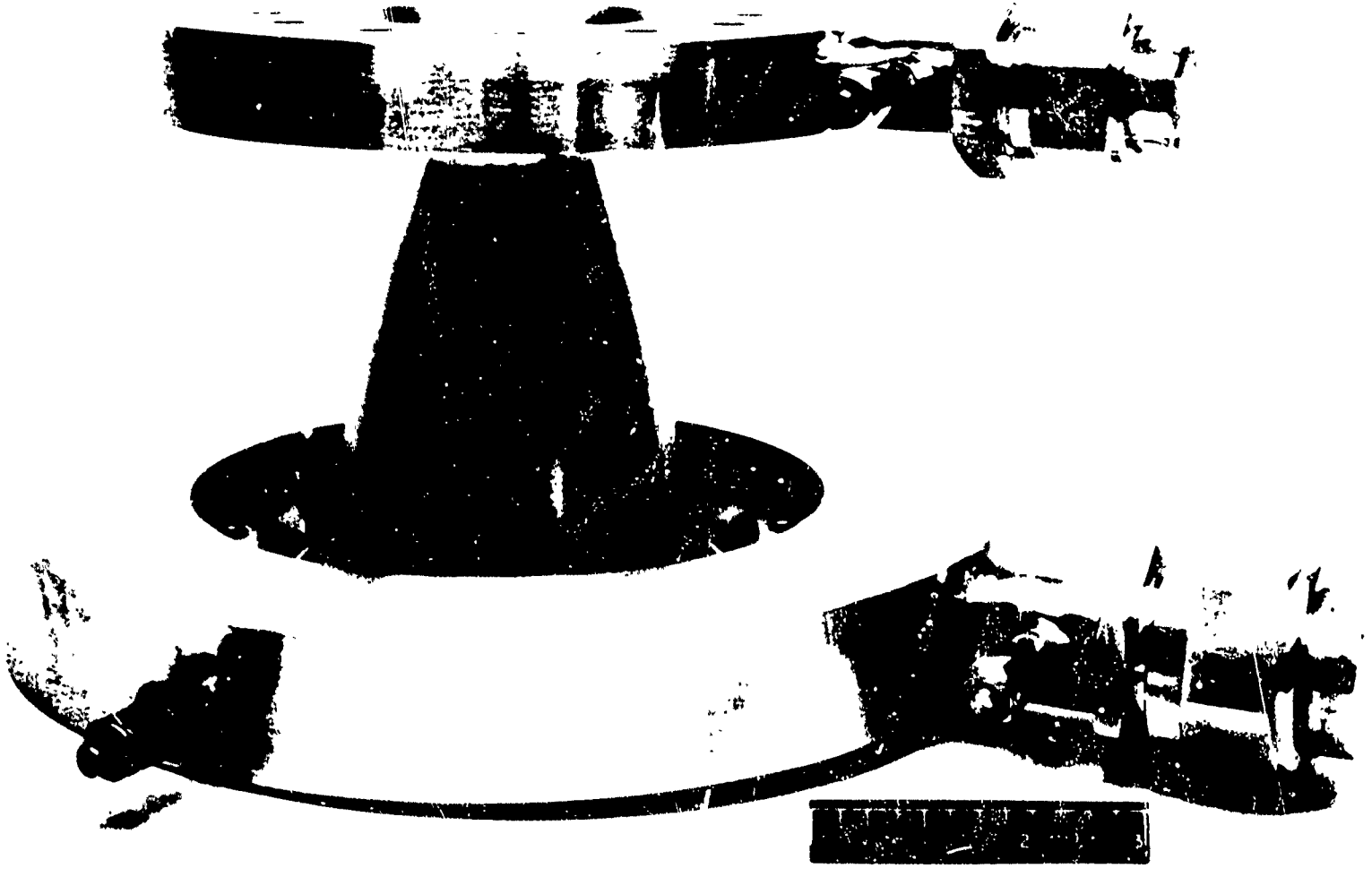

1XZ32-6/1/71-C1A*

Figure 9. Completed Nickel-200 Chamber

1XZ32-9/1/71-C1B*

Figure 10. Machined NARloy-Z Liner

IXZ32-9/1/71-GIA

Figure 11. View Showing Internal Surface of NARloy-Z Liner

electroforming of the nickel closure is shown in Fig. 12 and the completed NARloy-Z chamber is shown in Fig. 13 and 14.

In addition, to improve the data yield from the hot firing tests, thermocouples and strain gages were added to the chamber exterior to record external surface temperatures and strain profiles as a function of time. A photograph of the NARloy-Z chamber showing this instrumentation is presented in Fig. 15 and a closeup of one area showing the thermocouple and the axial and circumferential strain gages is shown in Fig. 16.

The zirconium copper alloy is a commercially available material and it was originally planned to use this material as supplied by the manufacturer. An ingot was purchased, forged into a disk and ultrasonically inspected for oxide inclusions. Results showed the presence of several inclusions greater than the 0.050 flat bottom hole standard The disk was sectioned for metallurgical evaluation which verified the presence of the oxide inclusions. A detailed discussion of this investigation is presented in Appendix A.

It was concluded form this effort that "off-the-shelf" zirconium copper ingots were unsuitable for use as liners in long life thrust chambers. To solve this problem new ingots were procured and then remelted using the consumable electrode process (as discussed in Appendix A). Subsequent forging and ultrasonic inspection revealed that the inclusions had been eliminated to the degree that their presence could be determined by ultrasonics.

The zirconium copper liners were then spun into shape, heat treated and aged (900 F for 4 hours), inspected, and machined using the same tooling and procedures as that employed in the NARloy-Z chamber. The zirconium copper liner is shown in Fig. 17 while a closeup view of the completed chamber is shown in Fig. 18. Pressure and flow testing of this chamber was identical to that used on the NARloy-Z chamber. Instrumentation identical to that shown previously for the NARloy-Z chamber was added and the chamber delivered to the AFRPL for testing.

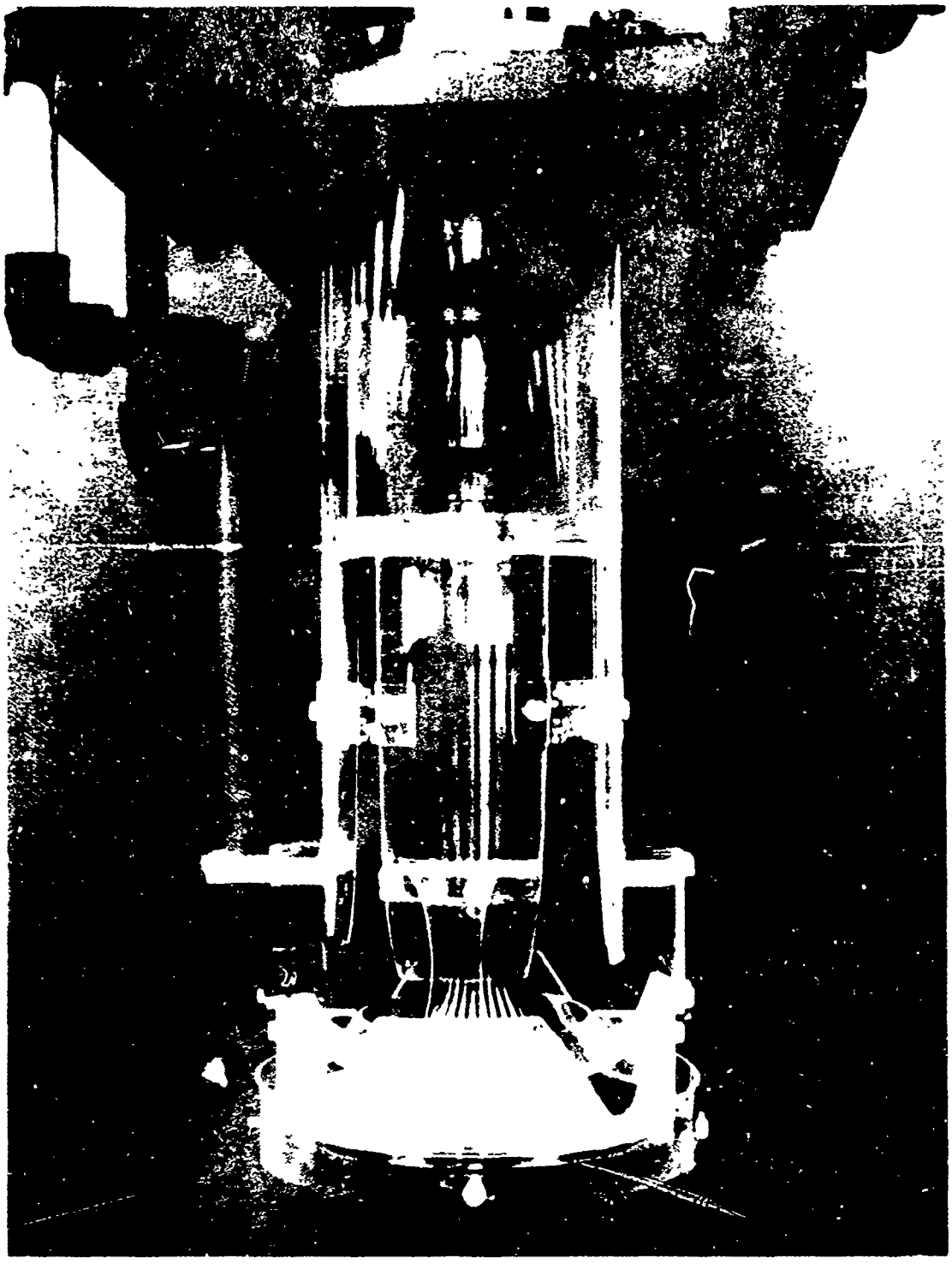

IX232-9/14/71-C1*

Figure 12. NARloy-Z Chamber Ready for Electroforming

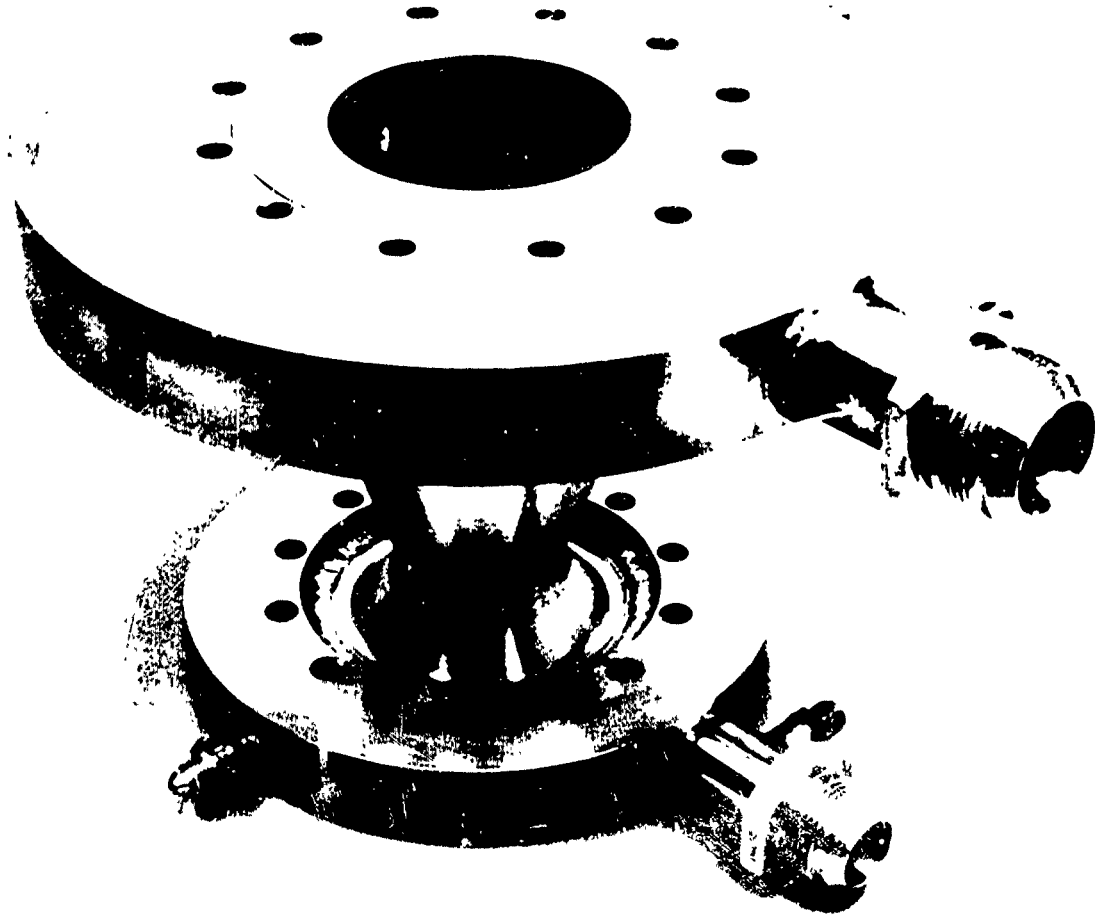

5AG33-12/13/71-C1A*

Figure 13. Completed NARloy-Z Thrust Chamber

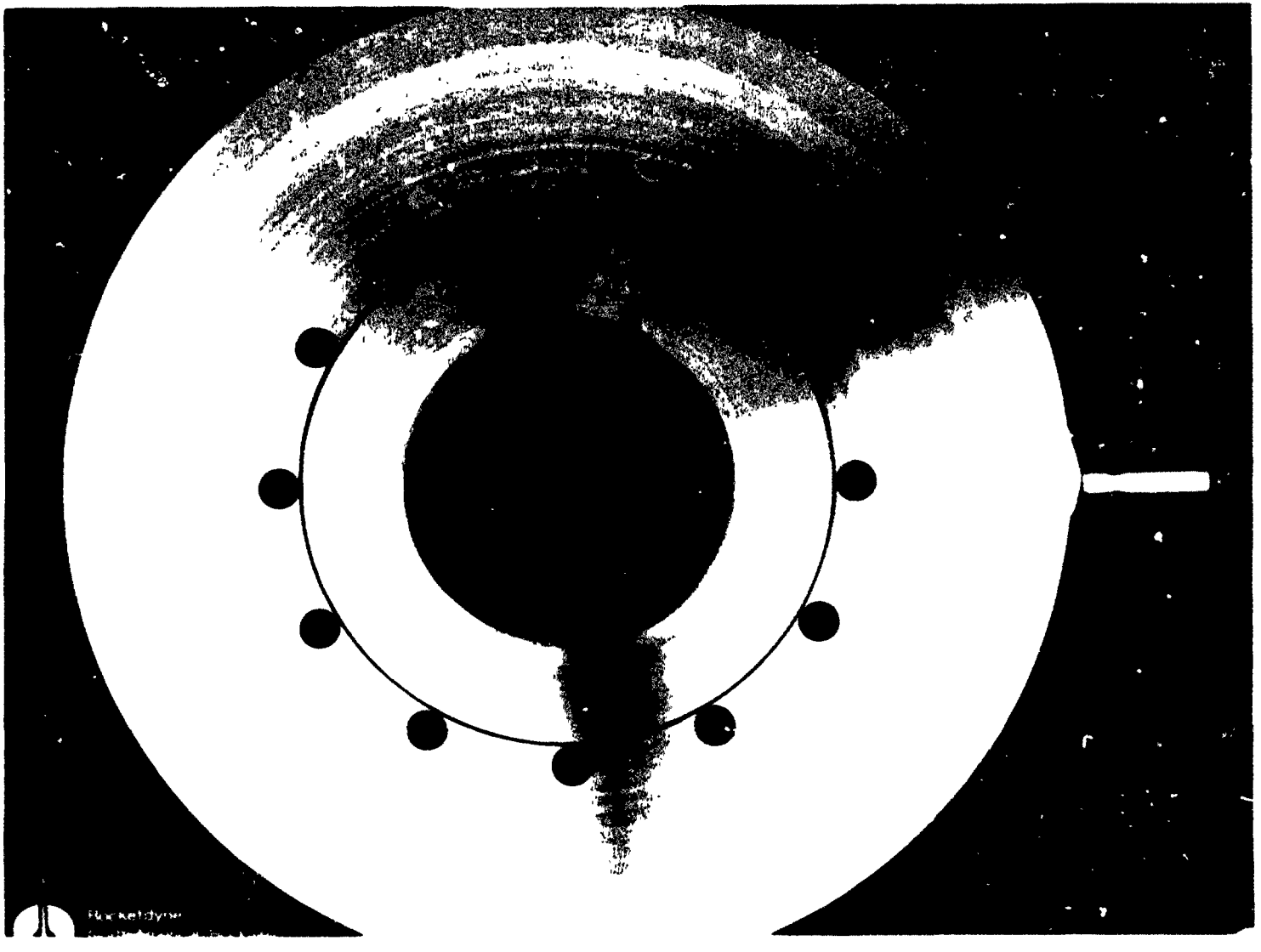

5AG33-12/13/71-C1B*

Figure 14. Close-Up of Throat Region - NARloy-Z Thrust Chamber

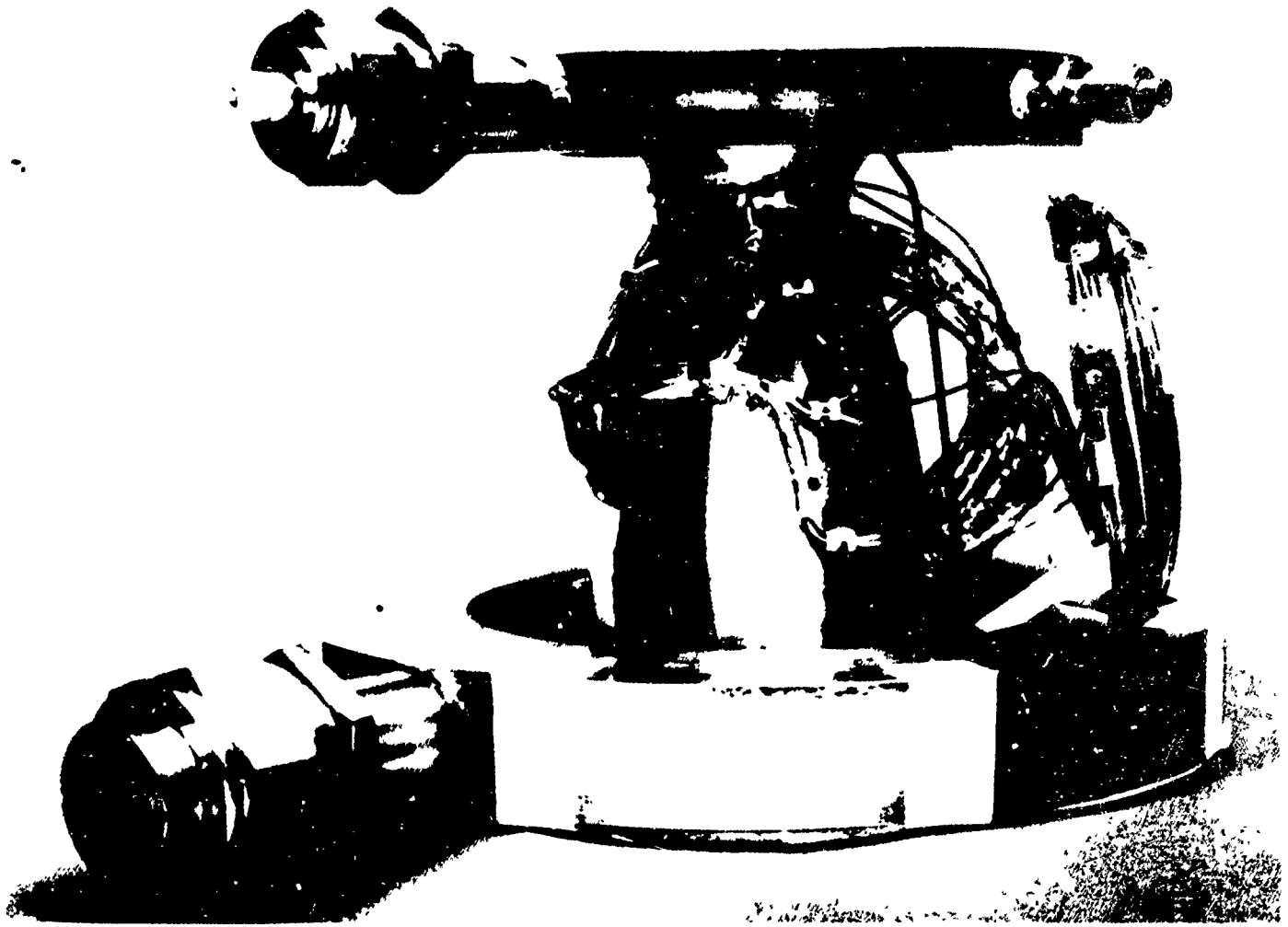

SAG39-5/10/72-C18

Figure 15. Instrumented NARloy-Z Thrust Chamber

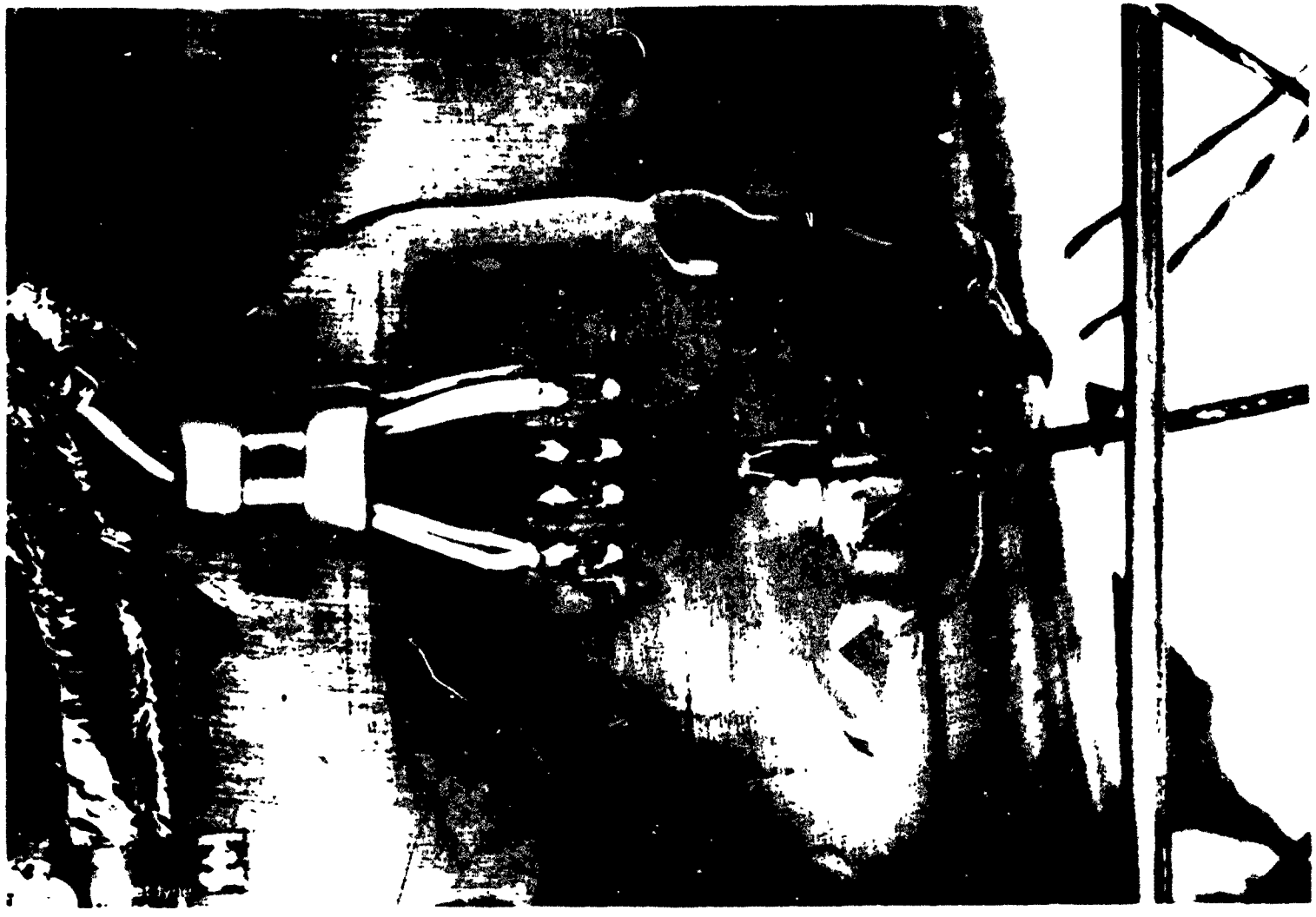

5AG39-5/10/72-C1C

Figure 16. Close-Up View of Instrumentation

1XW32-11/17/71-C1A*

Figure 17. Slotted Zr-Cu Liner

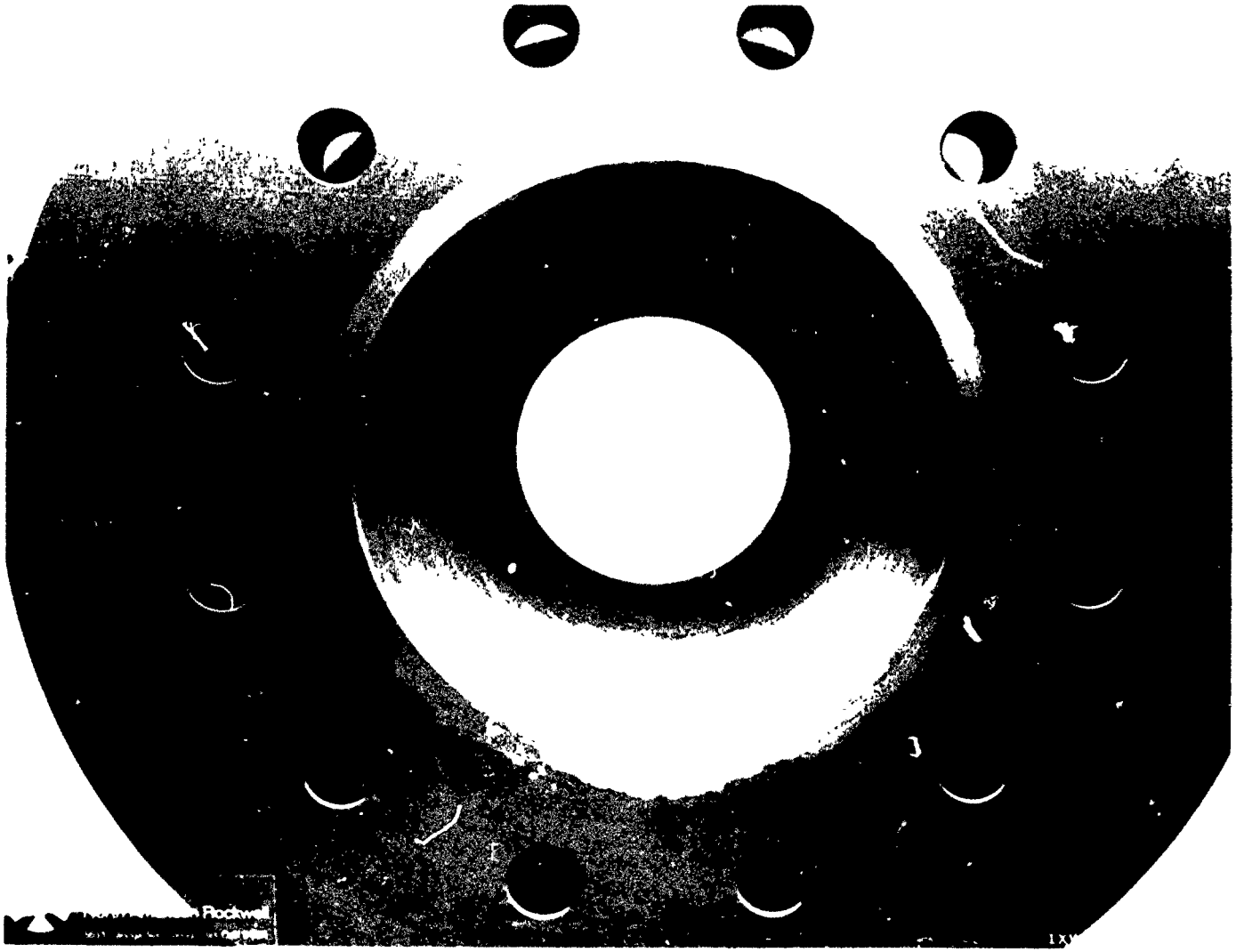

1XW32-1/25/72-C1E*

Figure 18. Close-Up of Zirconium-Copper Thrust Chamber Throat (Nozzle Side)

Calorimeter Thrust Chamber

The calorimeter thrust chamber liner was fabricated from an OFHC copper billet. All machining was accomplished using coordinated templates for dimensional control. The first step in the fabrication process consisted of machining the ID to net dimensions, and then machining the OD to net dimensions. This was followed by the machining of the circumferential water-coolant grooves, Fig. 19. After machining and dimensional inspection, an electroformed nickel closeout was added to this chamber (Fig. 20) and individual water feed and collection tubes TIG brazed to each coolant channel as shown in Fig. 21 and 22.

Injector

The injector was fabricated to AFRPL drawings. Initially the nickel injector body and posts were machined and the rigimesh face and manifold were welded in place, as shown in Fig. 23 through 26. The injector was then water-flow calibrated to verify proper injection parameters and delivered to the AFRPL.

PHASE II - TASK II - TEST

All hot firing effort was accomplished at the AFRPL. A description of the test procedure, test facility and the test program follows.

Test Procedures and Facility

The nickel thrust chamber was tested with coolant in a bypass mode (hydrogen coolant in parallel with injector hydrogen). The copper alloy chambers were cyclic tested with coolant in a regenerative mode (hydrogen coolant in series with injector hydrogen). Hydrogen coolant at -100 to -150 F ran continuously; shuttled between the injector and burn stack by use of a start valve and a bypass valve. Ignition was accomplished by injecting a small quantity of gaseous fluorine into the O_2 side of the injector at startup of each cycle. A simplified system schematic is shown in Fig. 27 and a detailed description of the facility follows.

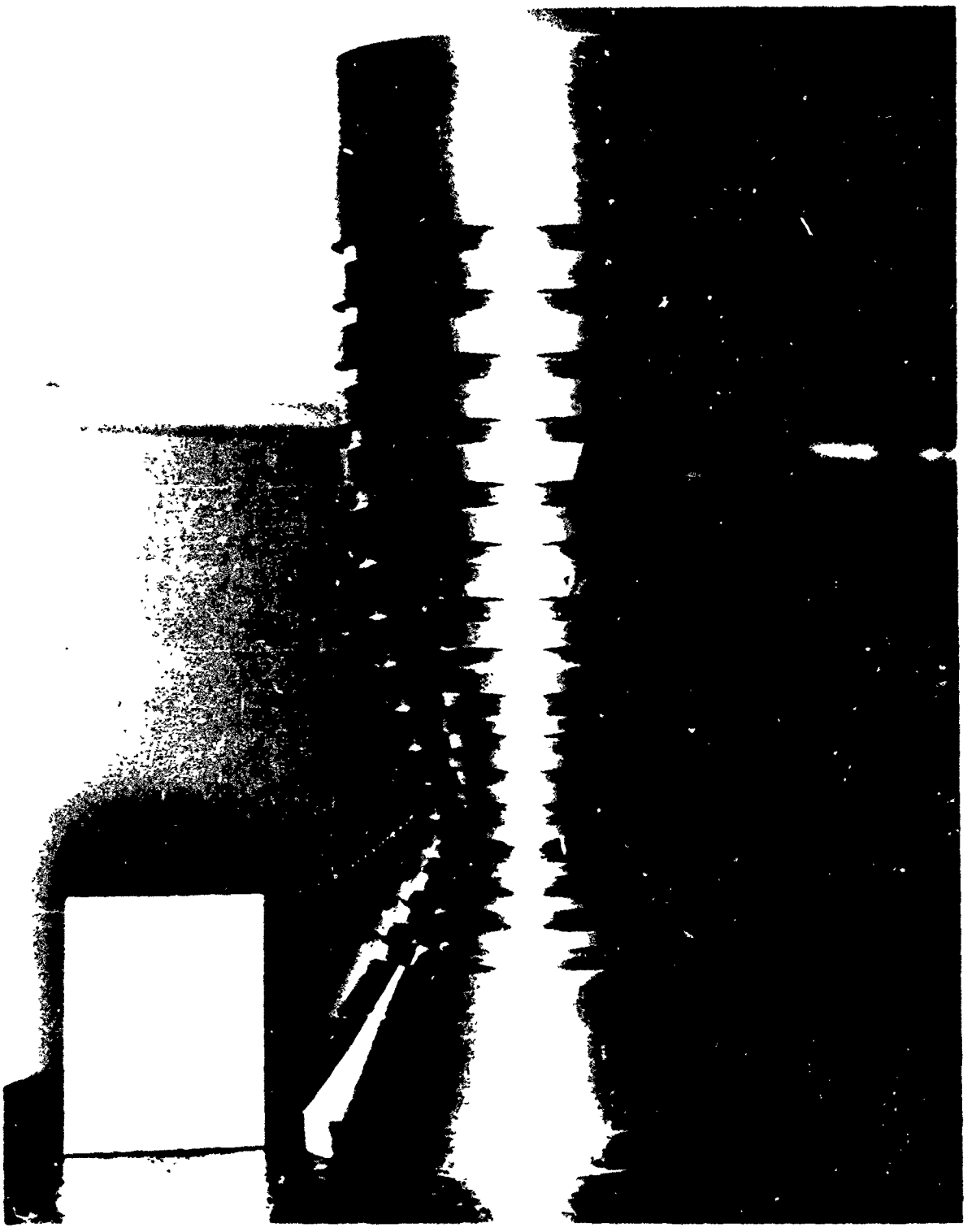

Figure 19. Machined OFHC Copper Liner for Calorimetric Thrust Chamber

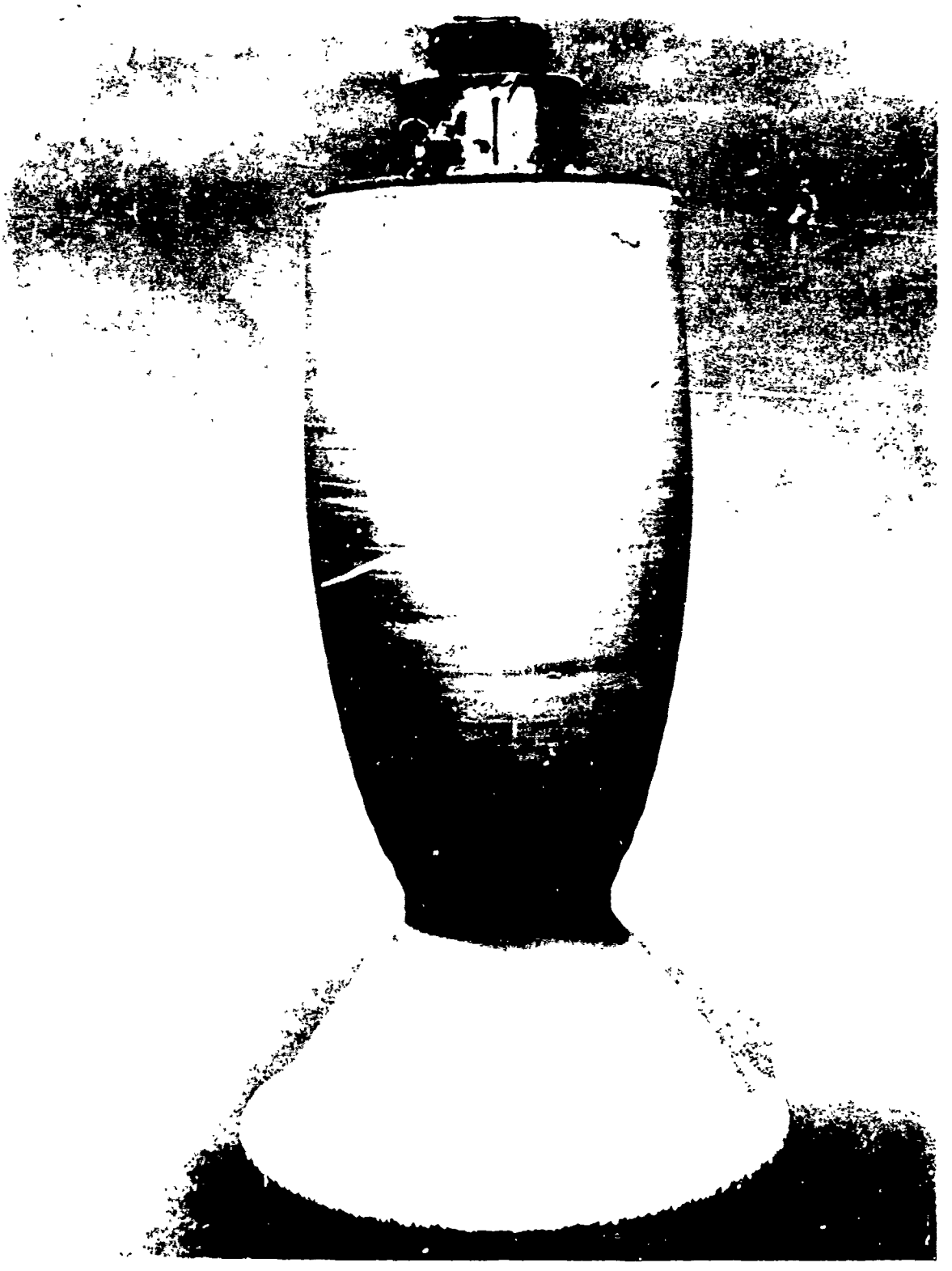

'XZ32-11/2/71-C1

Figure 20. As-Electroformed Calorimetric Thrust Chamber

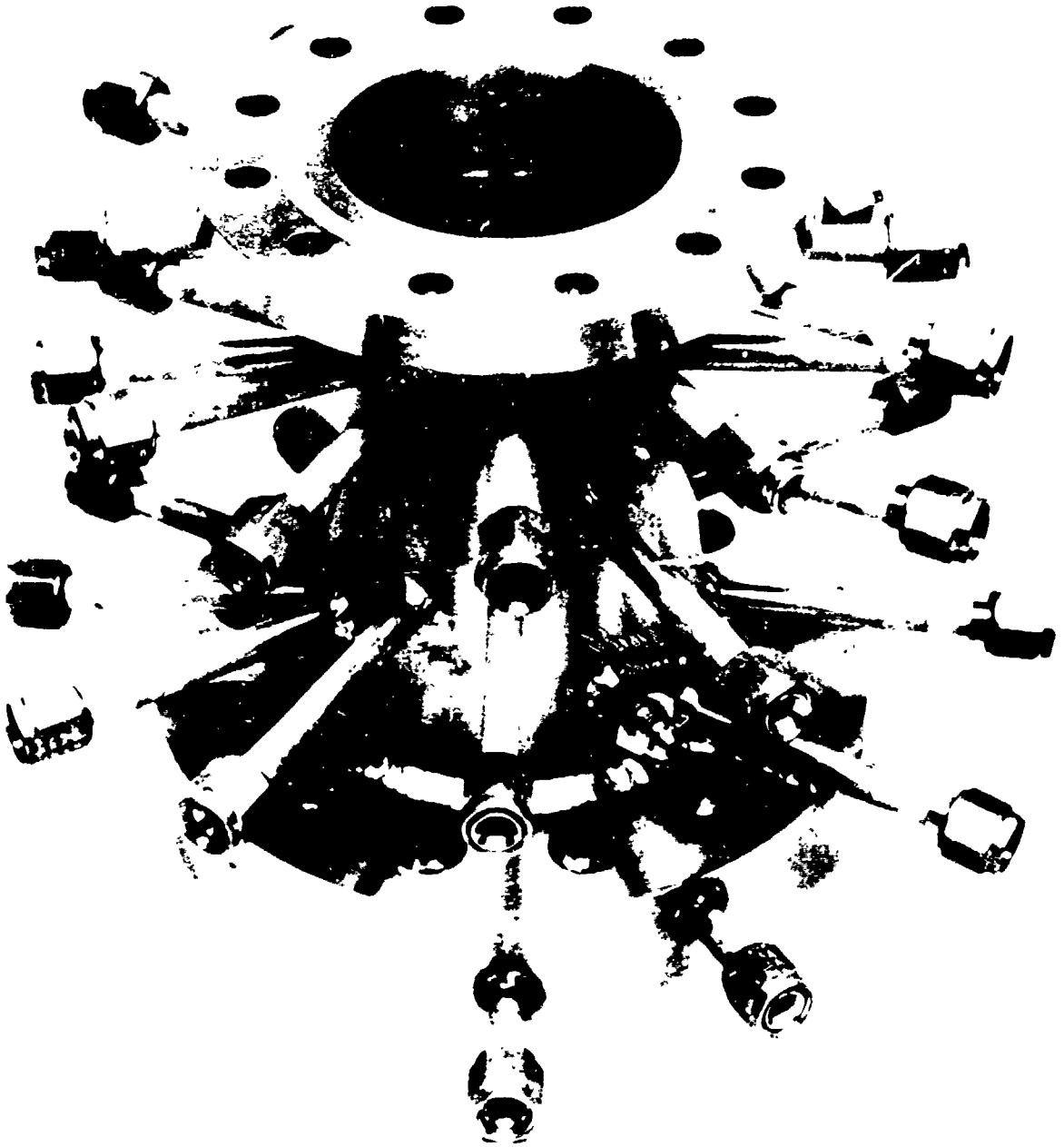

1XW32-12/22/71-C1A*

Figure 21. Calorimetric Thrust Chamber

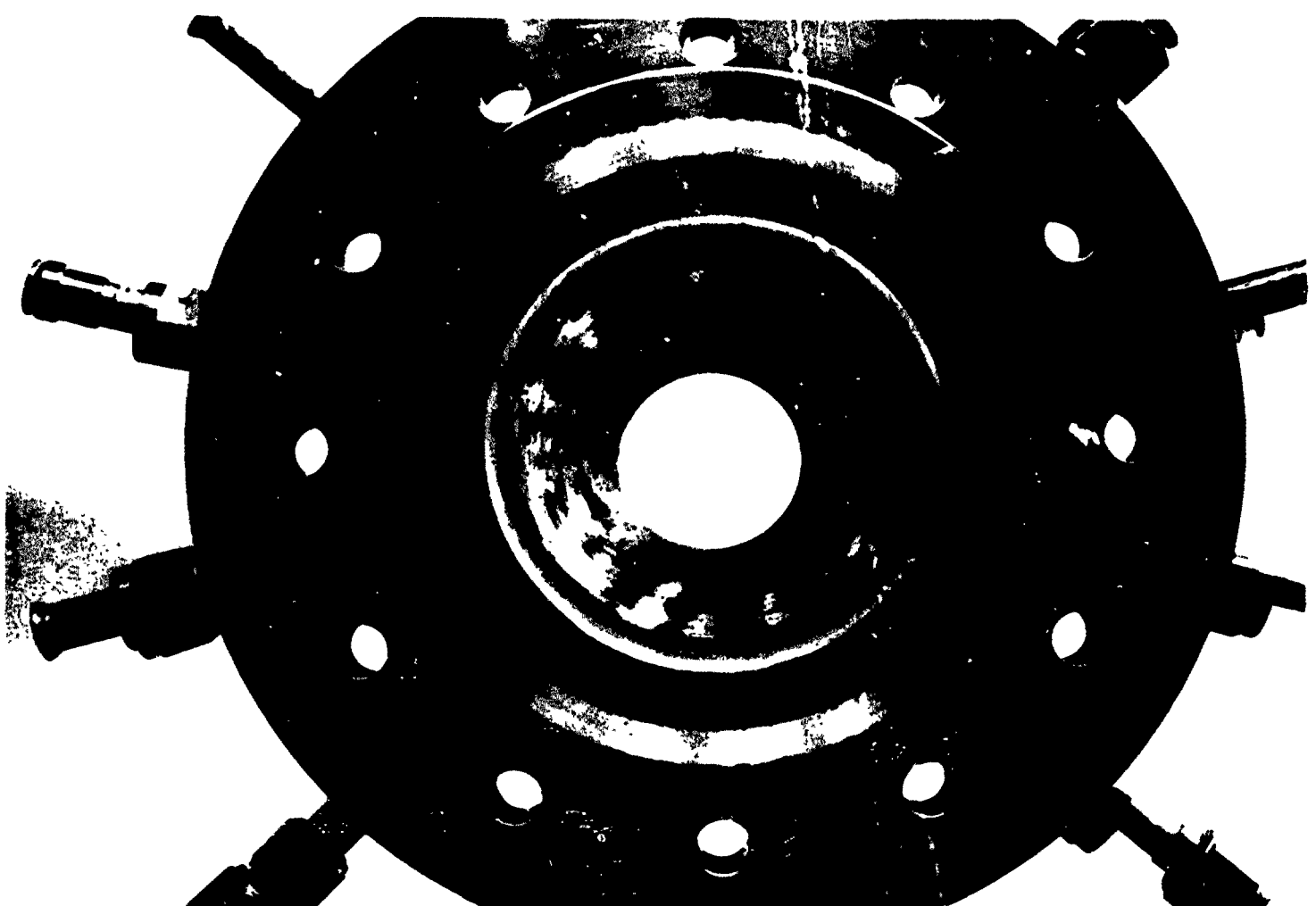

1XW32-12/22/71-C1E*

Figure 22. View Showing Hot Gas Surface of Calorimetric Thrust Chamber

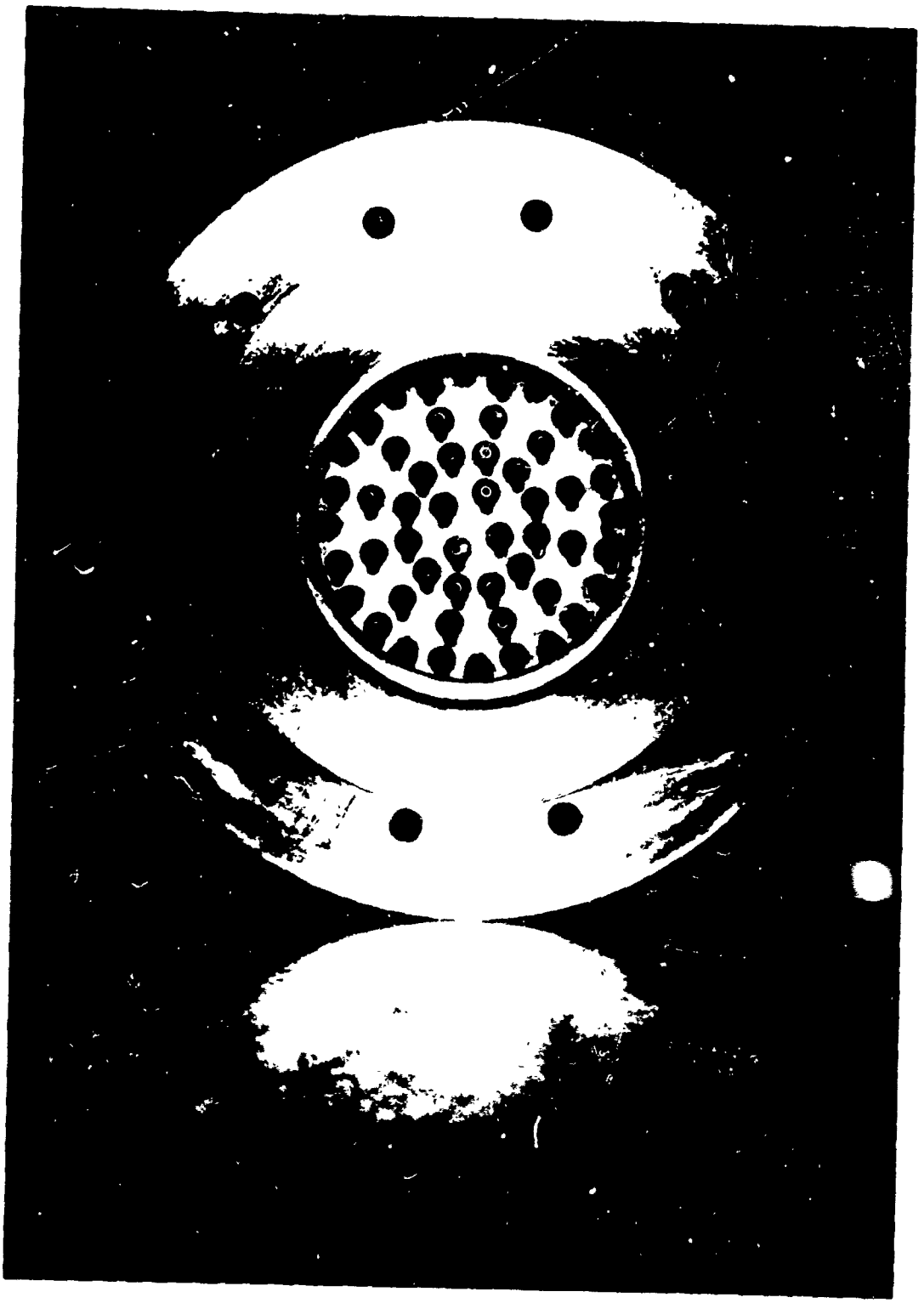

Figure 23. Injector Body

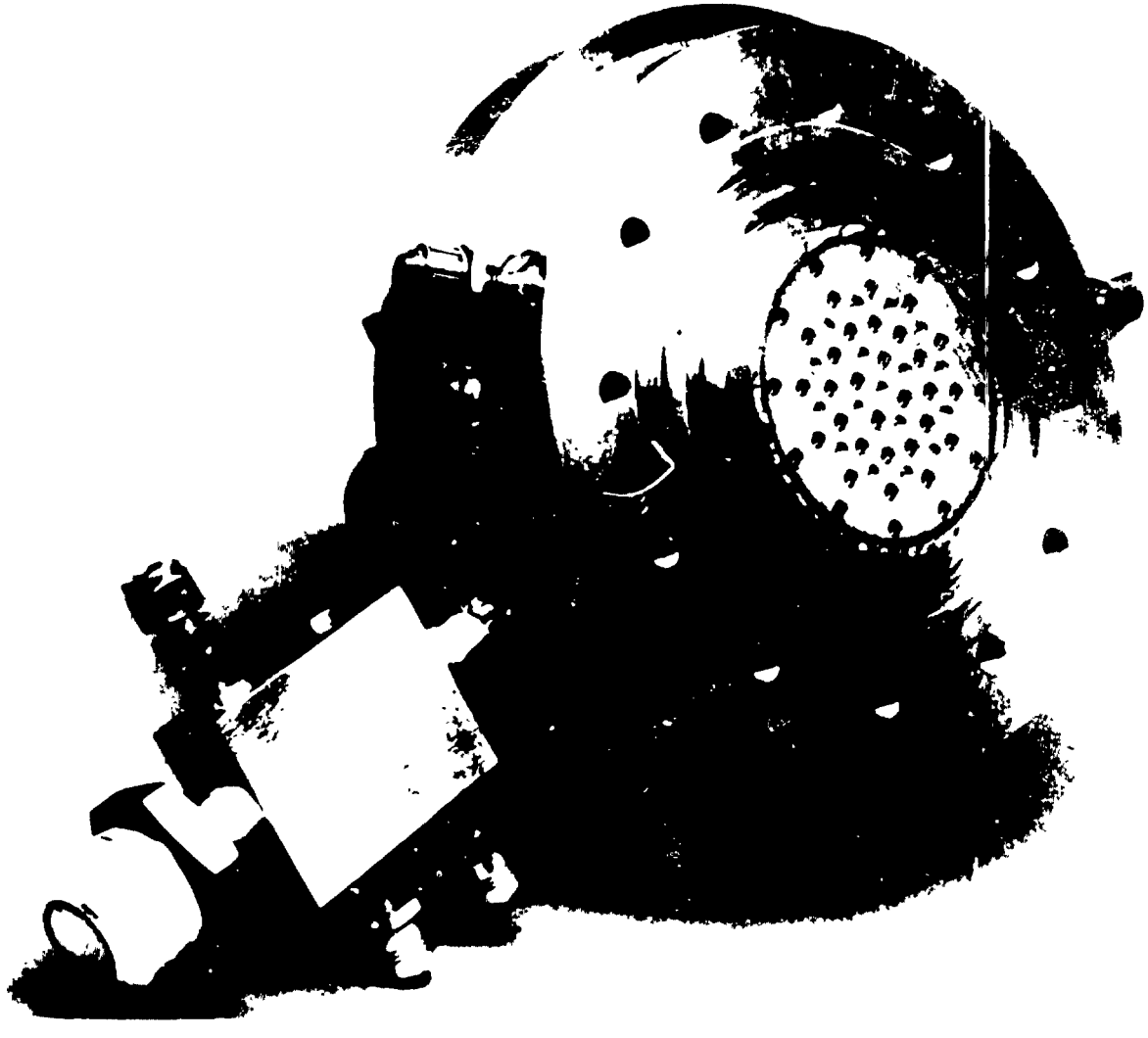

5AG33-11/9/71-C1A

Figure 24. Coaxial Element Injector

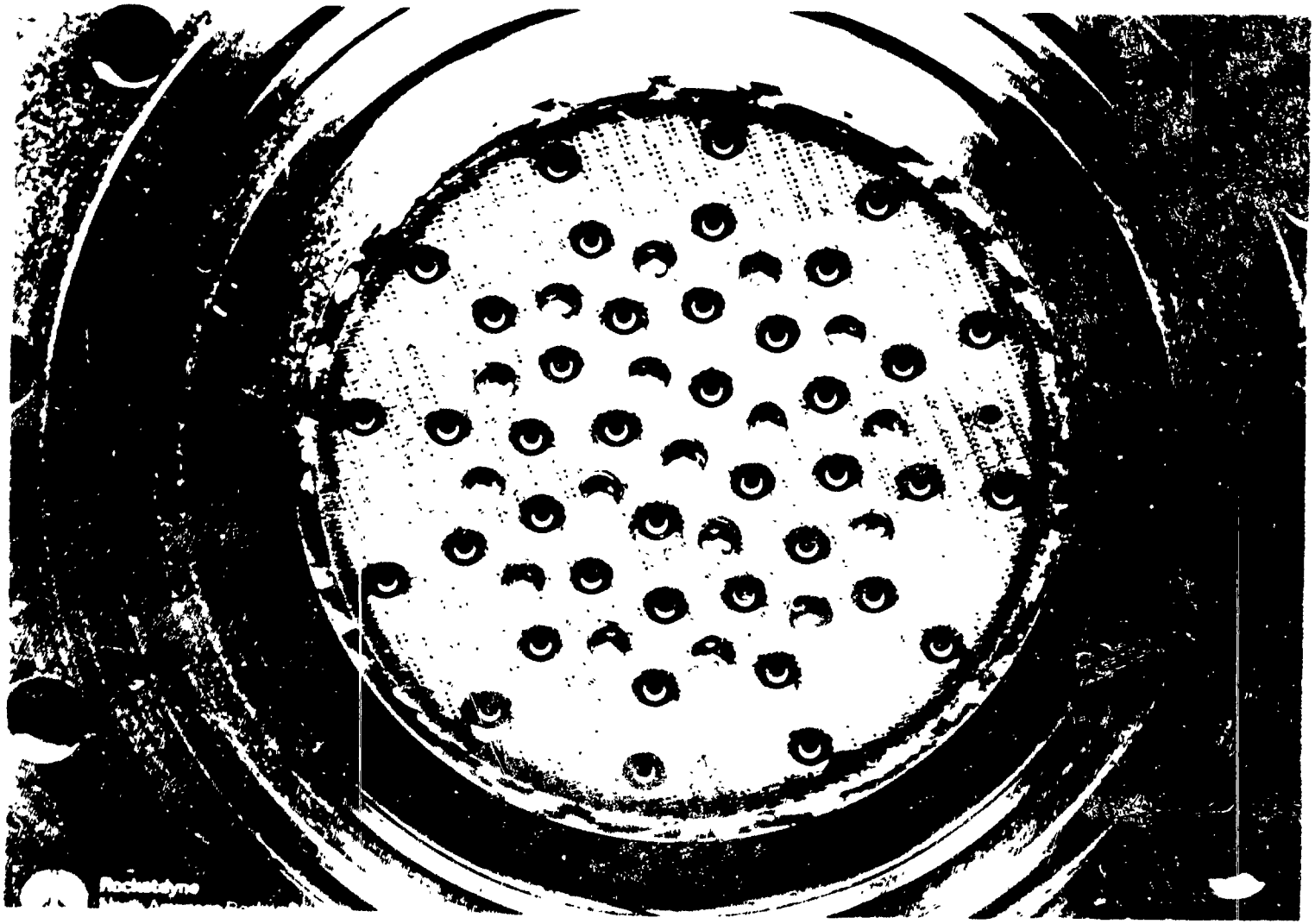

5AG33-11/9/71-C1C

Figure 25. Close-Up of Coaxial Injector Face

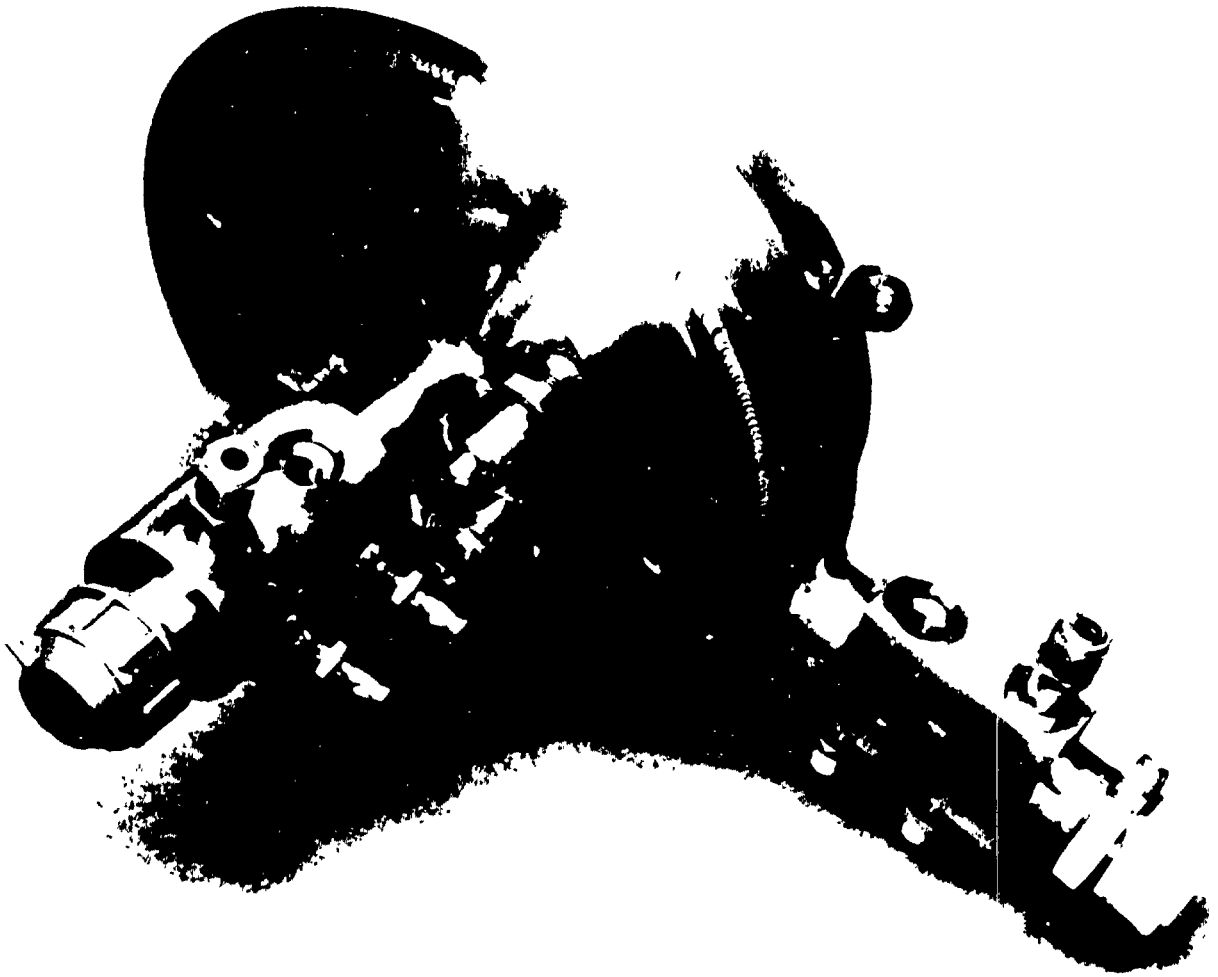

5AG33-11/9/71-C18

Figure 26. Back Side of Injector

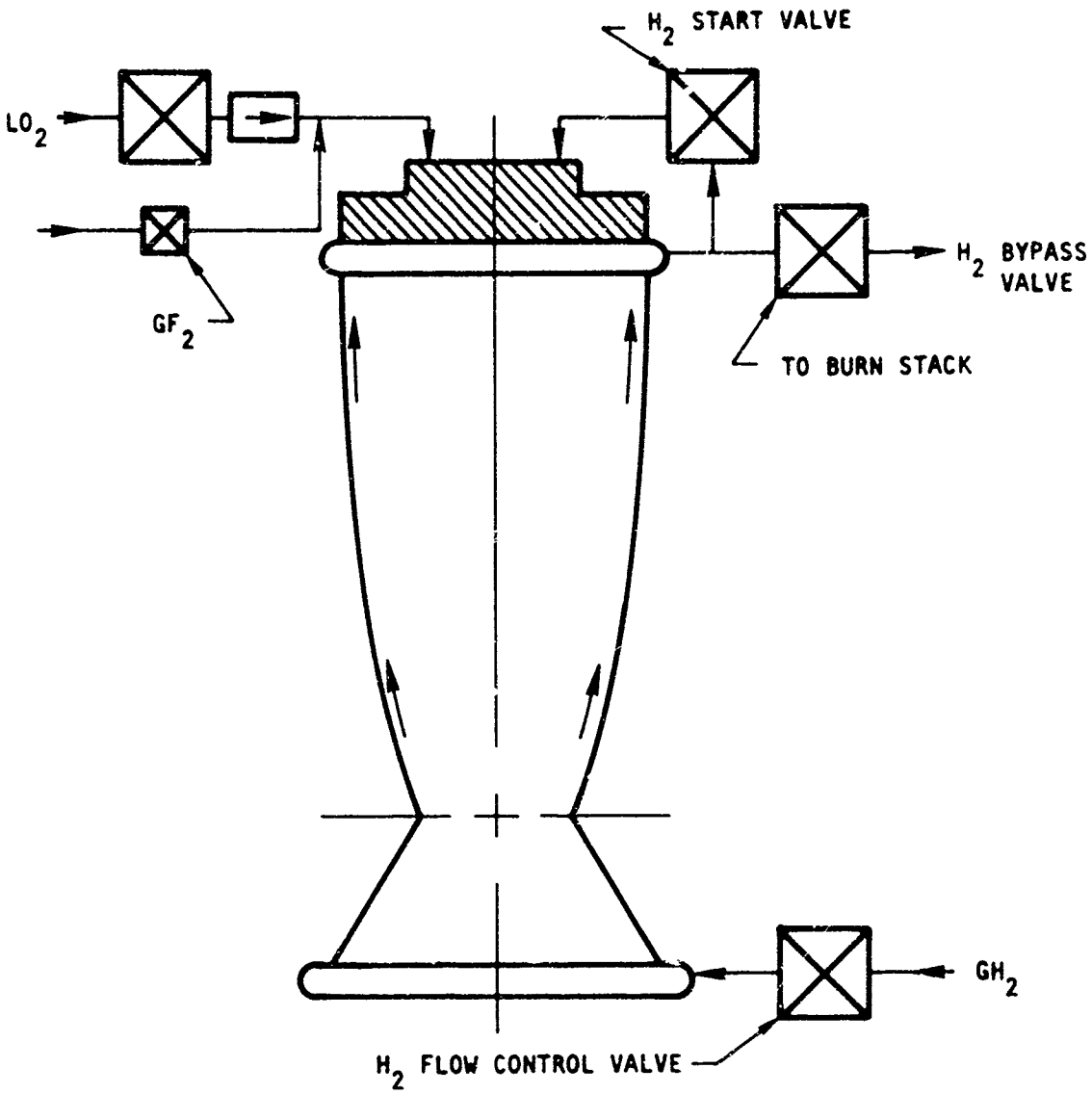

Figure 27. Test Schematic for Copper Alloy Chambers

The test facility at the AFRPL was test stand 1-52A. This stand was originally designed as a 10,000-pound-thrust fluorine/hydrogen facility and needed only minor modifications for use in this program. The liquid oxygen tank is a 1500 psi, 500 gallon vessel. Hydrogen is stored as a liquid, converted to a gas with a cryogenic pump and held in two 6000 psi, 300 cu ft gas bottles for running.

Hydrogen was temperature conditioned by passing it through a heat exchanger containing liquid nitrogen. The LN_2 flows continuously into the heat exchanger during the test to compensate for boiloff. The LN_2 level was controlled by adjusting the height of a runoff pipe.

The fuel flowrate was controlled by regulating an upstream orifice pressure with a hydraulic servo valve. For cycling tests, the engine was regeneratively cooled and a subsonic orifice was used to minimize pressure drops. For checkout tests, a sonic orifice was used to control the fuel flow, and a subsonic orifice was used in a parallel hydrogen loop which cooled the engine. The hydrogen in the cooling loop was burned in an exhaust stack.

Oxygen flowrate was controlled by using a flowmeter signal to regulate the oxidizer start valve. This control signal was biased through an EAI TR-20 analog computer to account for fuel flowrate deviations, as indicated by the pressure in the fuel injector manifold. This was to prevent extreme mixture ratio excursions.

Ignition was achieved by injecting a slug of gaseous fluorine downstream of the oxidizer start valve just prior to opening the start valve. The fluorine is then pushed by the LO_2 into the chamber and ignites the hydrogen which has also just reached the chamber.

Data were recorded on 20 strip charts, 2 oscillographs, a SEL digital tape recorder, and an FM tape recorder. The final data were obtained by processing the digital tape through an IBM 7040 computer. The FM tape was used to check for high frequency pressure oscillations. No such oscillations were seen on the runs when it was used. A detailed facility schematic is shown in Fig. 28.

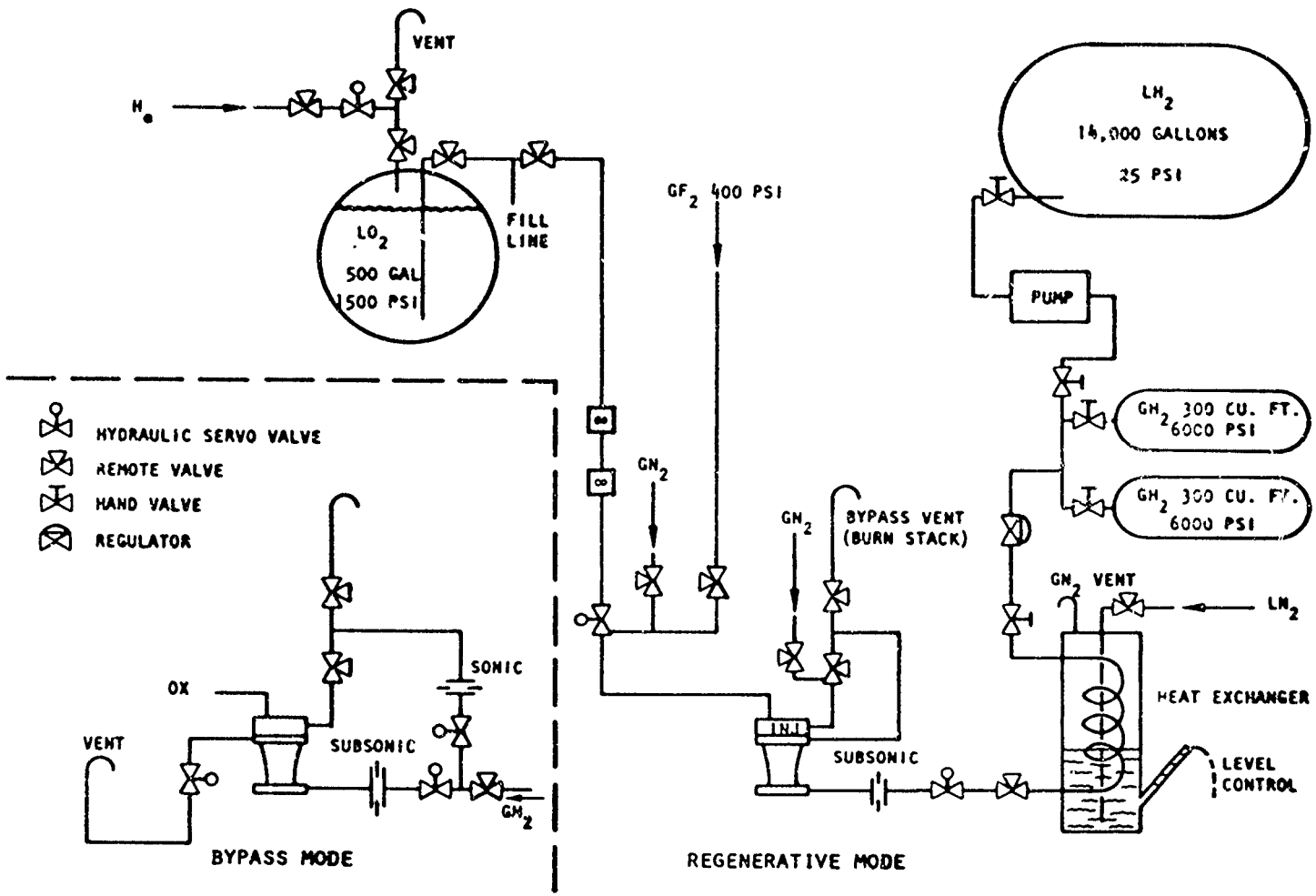

Figure 28. Facility Schematic AFRPL Test Pad 152A

Test Program

The first regeneratively cooled chamber to be hot-fire tested as a part of this program was the powder metallurgy nickel thrust chamber, residual hardware from a previous program. A series of hot-fire checkout tests were conducted with the coolant in a bypass mode, such that it did not go through the injector. Operational parameters and facility checkout were established using this hardware. Effort to cyclic test this hardware was initiated; however, a facility malfunction resulted in hardware damage prior to the accumulation of very many cycles.

The nickel chamber was then installed on the test stand. A series of checkout tests were run and cyclic tests initiated. After approximately 50 cycles, a facility malfunction again occurred which resulted in destruction of the chamber. The chamber is shown post-test in Fig. 29. Although the cyclic life demonstration was not completed on this chamber, 50 cycles were accumulated prior to the malfunction. There were no thermal cracks on the chamber, indicating that this material can be used for chambers having a reasonably long life requirement.

After this, the cyclic test effort was concentrated on the two copper alloy thrust chambers with some testing accomplished on the calorimeter thrust chamber to establish the heat flux profile. The test program is summarized in Table 1, while the range of operating conditions experienced during the test program is presented in Table 2. The actual sequence of events in testing these three chambers is shown in Table 3. The calorimeter thrust chamber was tested 9 times with durations from 1 to 15 seconds to establish a heat flux profile at the nominal operating point (P_c = 750 psia, MR = 6.0). Data from test No. 7 are shown in Fig. 30. For reference the predicted heat flux profile used in the design of the copper alloy chambers is also presented. Comparison of the two shows the experimental profile to be somewhat lower than the predicted value indicating that the chambers were somewhat overdesigned in that they would run with lower wall temperature and bulk temperature rise than predicted. Subsequently, the zirconium copper chamber was installed, and a series of tests run to establish cooling and operational parameters. These tests were of 1 to 6 seconds duration, with hydrogen coolant supplied in a bypass mode. The coolant

Figure 29. Nickel-200 Chamber Post-Test

TABLE 1. HOT FIRE TEST PROGRAM SUMMARY

CHAMBER	TEST NUMBER	TEST OBJECTIVE	TEST DURATION, SECONDS	COMMENTS
ZIRCONIUM COPPER	1-14	CHECKOUT	1.0 TO 6.0	COOLING AND OPERATIONAL REQUIREMENTS ESTABLISHED.
	15-312	CYCLING	3 ON/2 OFF	ROUGHNESS NOTED. CHAMBER RETURNED TO ROCKETDYNE FOR EVALUATION (NO CRACKS).
	313-529	CYCLING	2.0 TO 2.5 SEC ON/ 1.5 TO 2.0 SEC OFF	THROUGH CRACK AFTER 398 CYCLES. AFTER 512 CYCLES RETURNED TO ROCKETDYNE FOR EVALUATION.
	530-587	↓	↓	TEST ANAMOLIES CAUSED HIGHER WALL TEMPERATURES. SEVERAL ADDITIONAL CRACKS.
NARloy-Z	1-10	CHECKOUT	1.0 TO 15.0	OPERATIONAL REQUIREMENTS ESTABLISHED
	11-615	CYCLING	2.0 TO 2.5 SEC ON/ 1.5 TO 2.0 SEC OFF	THROUGH CRACK AFTER 410 CYCLES. AFTER 615 CYCLES RETURNED TO ROCKETDYNE FOR EVALUATION.
	615-654	↓	↓	TEST ANAMOLIES CAUSED HIGHER WALL TEMPERATURES. INJECTOR EXPERIENCED FACE BURNING.
CALORIMETRIC	1-9	HEAT FLUX	1 TO 15	PROFILE ESTABLISHED.
	10-15		3 TO 20	INJECTOR RETESTED AFTER OBSERVING CHANGES IN HEAT FLUX ON REGENERATIVELY COOLED HARDWARE. VERIFIED HEAT FLUX HAD CHANGED.

Table 2. Typical Test Parameters - Copper Alloy Chambers

Chamber	Test Number	Duration, sec	Chamber Conditions			Coolant Conditions				
			Chamber Pressure, psia	Flowrate, lb/sec	Mixture Ratio	Flowrate lb/sec	Inlet Temp, F	ΔT, F	Inlet Pressure, psia	ΔP, psi
NARloy-Z	3	0.7	700	7.00	5.7	1.05	95	143	1310	450
	5	2.4	705	7.43	5.8	1.08	105	170	1300	465
	11 to 24	2.0	745 to 760	6.70 to 7.07	5.0 to 5.2	1.13 to 1.16	-102 to -120	164 to 174	1380	325
	25 to 114	2.0	735 to 760	7.43 to 7.60	5.5 to 5.7	1.11 to 1.17	- 97 to -127	159 to 188	1310 to 1385	295 to 330
	231 to 351	1.5	740 to 770	7.07 to 7.13	5.5 to 5.7	1.08 to 1.10	-118 to -125	189 to 196	1380	310 to 330
	352 to 483	1.5	730 to 750	7.02 to 7.83	5.1 to 5.6	1.10 to 1.15	-122 to -136	180 to 182	1310 to 13[illegible]	290 to 310
	484 to 615	1.5	745 to 750	7.13 to 7.31	5.3 to 5.6	1.08 to 1.16	-107 to -125	175 to 196	1335 to 1370	300 to 310
	616 to 623	1.5	760 to 770	7.11 to 7.13	5.4 to 5.5	1.11 to 1.13	-135 to -147	185 to 196	1350 to 1370	270 to 280
	643 to 653	1.5	770 to 815	7.13 to 7.84	5.6 to 5.7	1.16 to 1.17	-132 to -147	220 to 230	1545 to 1560	300 to 320
Zirconium Copper	9	8.5	730	7.95	6.8	1.02	81	192	1480	440
	12 to 18	2.8 to 3.4	620 to 780	5.76 to 7.48	4.1 to 5.8	1.10 to 1.13	- 96 to -140	149 to 183	1400 to 1410	310 to 325
	30 to 69	3.4 to 3.5	755 to 780	7.74 to 7.77	6.0 to 6.3	1.06 to 1.11	- 96 to -138	195 to 212	1390 to 1420	310
	70 to 118	3.0	750 to 775	7.60 to 7.62	5.8 to 6.1	1.07 to 1.12	- 92 to -139	198 to 214	1380 to 1420	300 to 315
	209 to 399	1.5 to 2.8	730 to 750	7.06 to 7.25	5.3 to 5.[illegible]	1.07 to 1.14	- 95 to -134	185 to 200	1300 to 1420	300 to 320
	537 to 564	1.4 to 1.5	750 to 770	7.38 to 7.75	5.9 to 6.6	1.02 to 1.07	-102 to -113	225 to 226	1380 to 1400	300
	565 to 588	1.5	760 to 780	7.47 to 7.66	5.6	1.13 to 1.16	-136 to -146	208 to 246	1400 to 1430	300 to 310

TABLE 3. TEST SEQUENCE

Test Series	Chamber	Test No.	Injector No.	Comments
1	Zirconium-Copper	1 thru 312	1	After 312 cycles injector showed some anomalies. Also, chamber surface roughened.
2	Calorimeter	1 thru 9	2	Heat flux profile established.
3	NARloy-Z	1 thru 615	2	After 615 cycles chamber returned to Rocketdyne for NDT.
4	Zirconium-Copper	313 thru 512	2	After 512 cycles chamber returned to Rocketdyne for NDT.
5	Calorimeter	10 thru 16	2	Heat flux profile increased. Injector showing signs of distress.
6	Zirconium-Copper	513 thru 587	2	Coolant bulk temperature rise indicated. considerably higher operating conditions.
7	NARloy-Z	616 thru 654	2	Coolant bulk temperature rise indicated considerably higher operating condition. Injector face eroded.

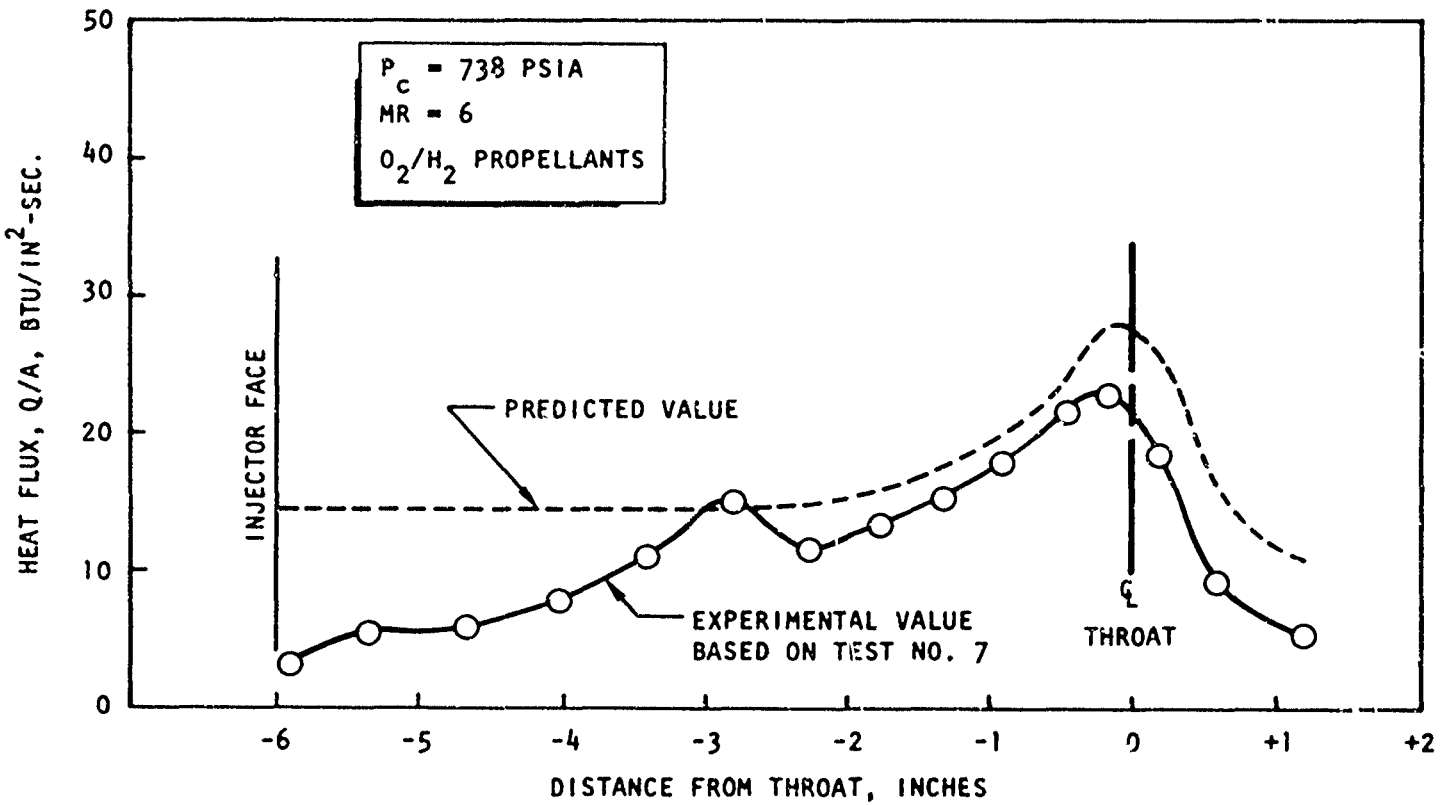

Figure 30. Heat Flux Profile Established by Calorimeter Thrust Chamber Testing

was then rerouted such that the chamber was regeneratively cooled and the cyclic test effort initiated. During the first test series, a total of 312 cycles were accumulated.

These cycles were of 3 seconds on time, 2 seconds off, as noted in Fig. 31. Post-test inspection of the hardware indicated some surface roughing of the hot gas wall; however, a coolant circuit leak test indicated there were no fatigue cracks in the wall (Fig. 32 through 34). After non-destructive evaluation the roughening was attributed to the coarse grain structure and low strength inherent in the zirconium copper material. The chamber was then returned to the AFRPL for additional cycle testing. This next series of cyclic tests consisted of 2 to 2-1/2 seconds on time, followed by 1-1/2 to 2 seconds off time. After 398 cycles, a coolant circuit leak check showed that there was one crack through the hot gas wall. Testing was continued until 512 cycles were accumulated, at which time the chamber was returned to Rocketdyne for further non-destructive evaluation. After this evaluation, the chamber was reinstalled on the test stand and cycled until a total of 587 cycles were accumulated. This last series of tests (530 to 537) had higher wall temperature operation due to some anomalies which occurred in the test facility and a test procedure as will be discussed below. Upon completion of the 587 cycles, a post-test leak check of the coolant circuit showed several additional cracks through the hot gas wall, and the chamber was returned to Rocketdyne for thorough post-test non-destructive and destructive evaluation. Tabulations of reduced data were obtained for all tests. In addition, scale printout of various parameters were obtained as a function of time. Typical examples are shown in Fig. 35 through 37.

A similar procedure was used on the NARloy-Z thrust chamber. The first 10 cycles consisted of checkout to establish operational requirements with the coolant supplied to the chamber in a bypass mode. Test durations of 1 to 15 seconds were run and successfully verified chamber cooling capability. The coolant was then rerouted as discussed previously to run the chamber in a regenerative mode as shown in Fig. 27, and the cyclic test effort initiated. A total of 615 cycles were accumulated, each of 2 to 2-1/2 seconds on and 1-1/2 to 2 seconds off. The coolant circuit leak check after 410 cycles showed one crack had occurred in the

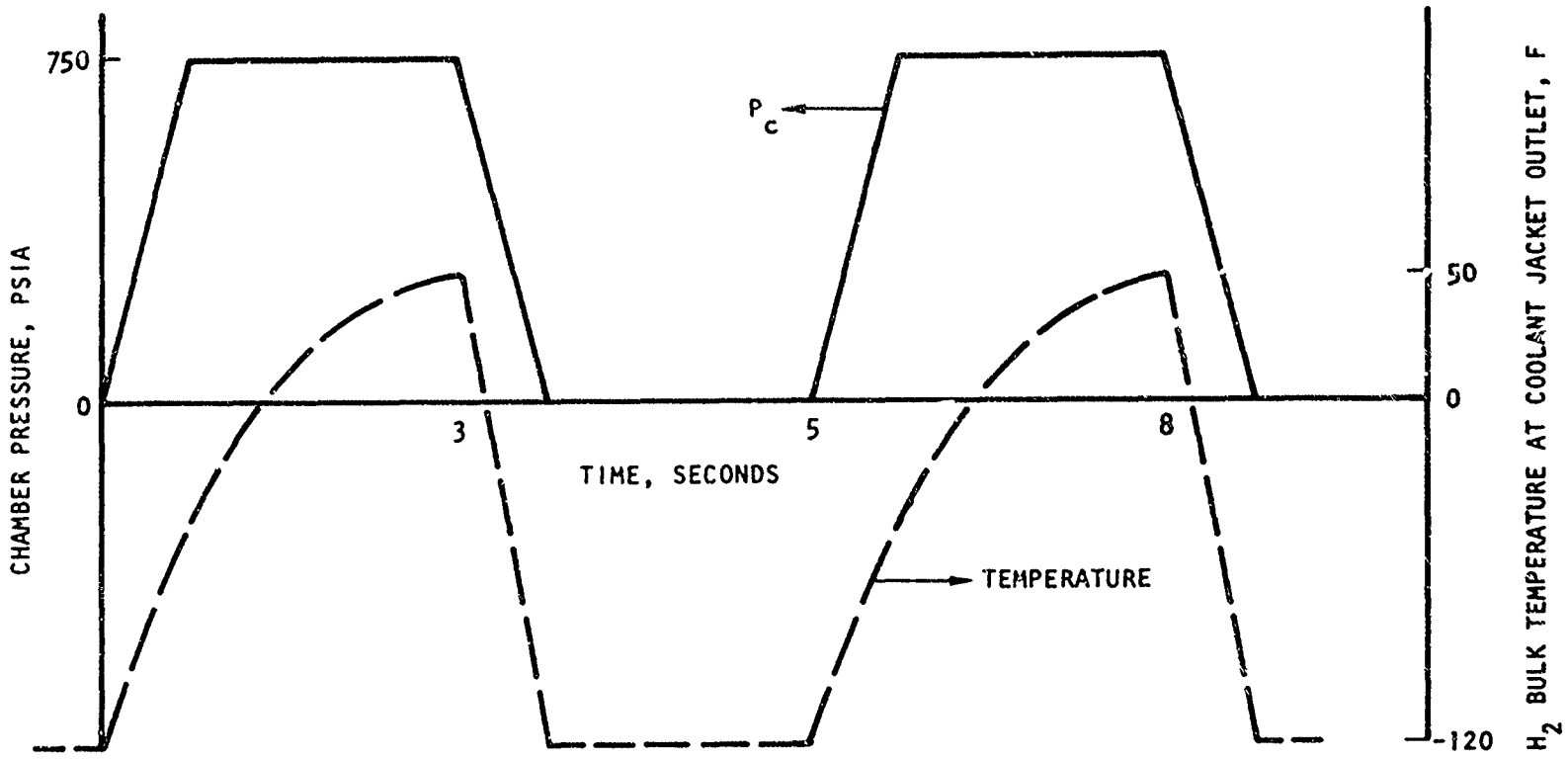

Figure 31. Typical Cycle

5AJ36-4/4/72-C1B

Figure 32. Combustion Zone of Zirconium Copper Chamber Showing Surface Roughness After 312 Cycles

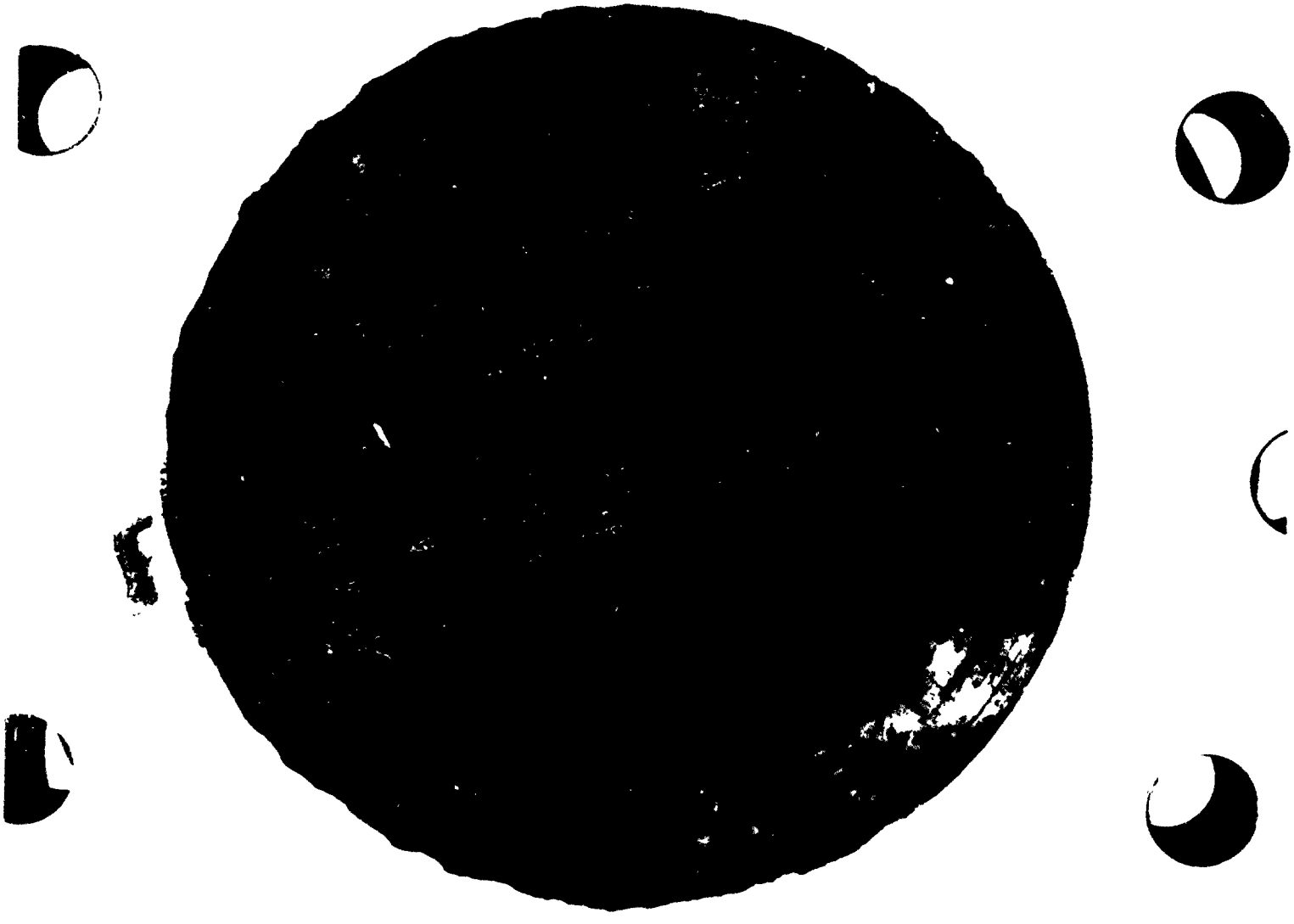

Figure 33. View Showing Coarse Grain Structure of Zirconium Copper Chamber After 312 Cycles

5AJ36-4/4/72-C1D

5AJ36-4/4/72-C1C*

Figure 34. Close Up of Zirconium Copper Chamber Nozzle Region Showing Result of Injector Element Streak

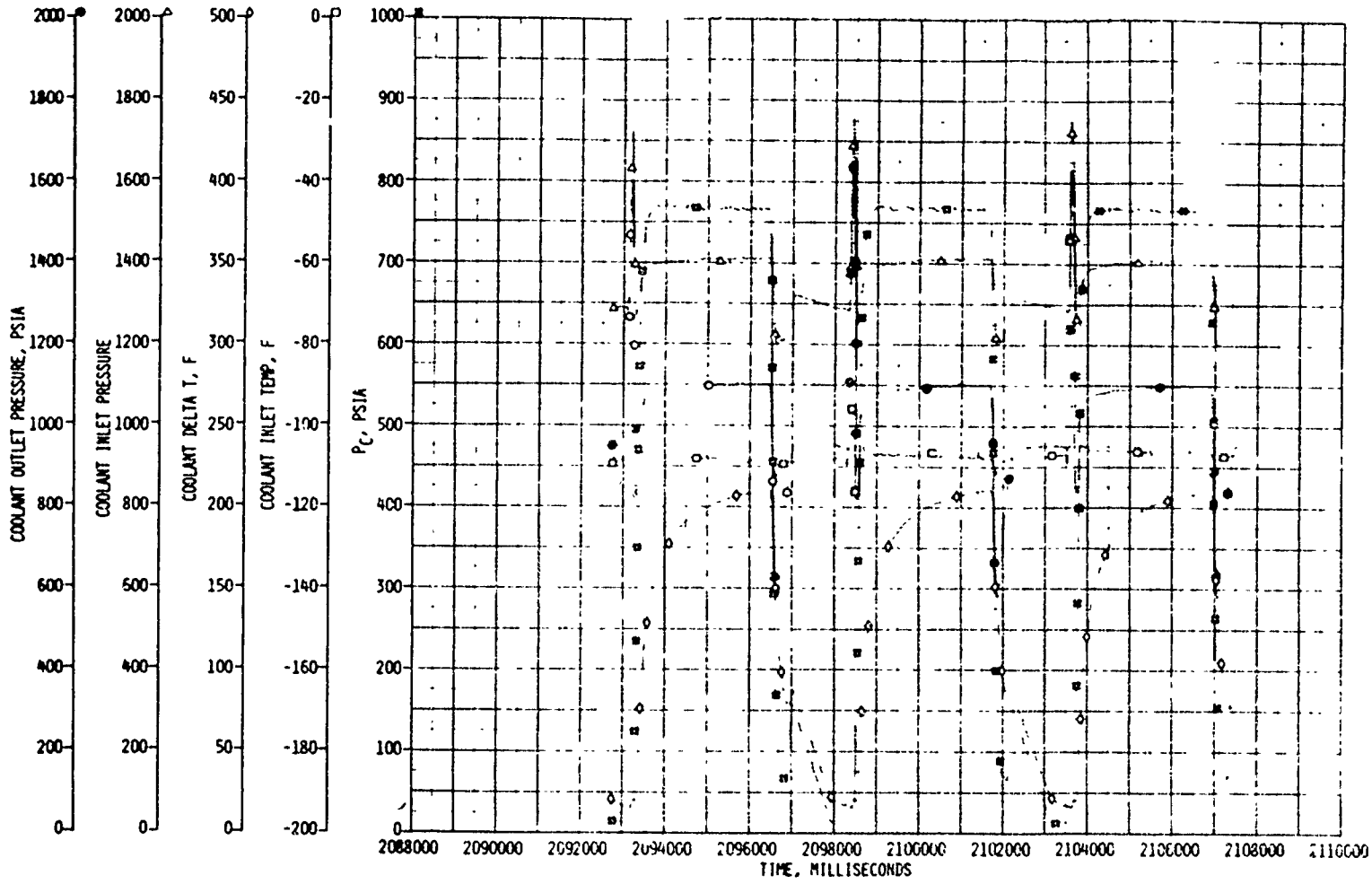

Figure 35. Plot of Various Run Parameters vs Time for Typical Cyclic Test Series - Zirconium-Copper Chamber

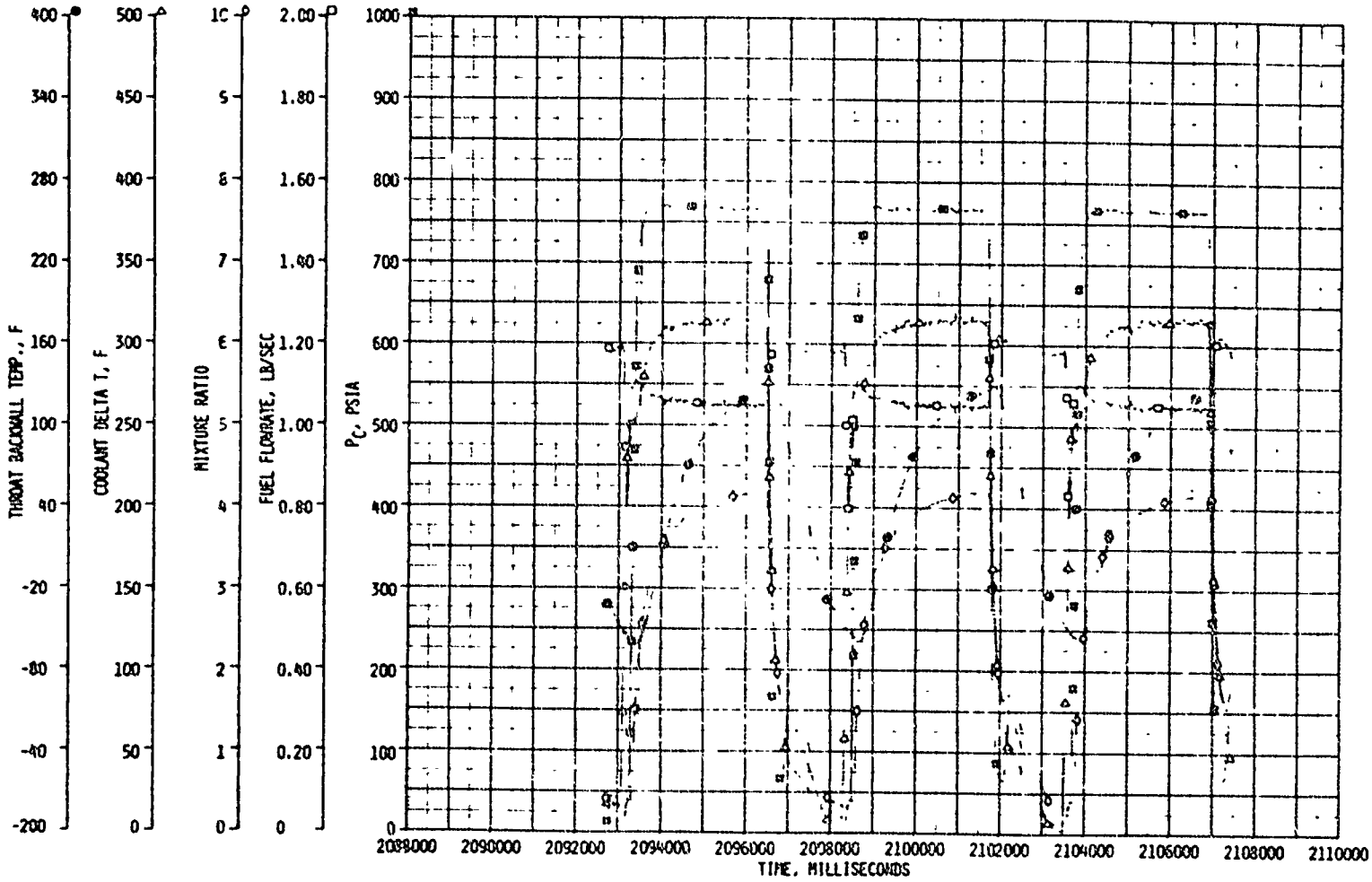

Figure 36. Plot of Various Run Parameters vs Time for Typical Cyclic Test Series - Zirconium-Copper Chamber

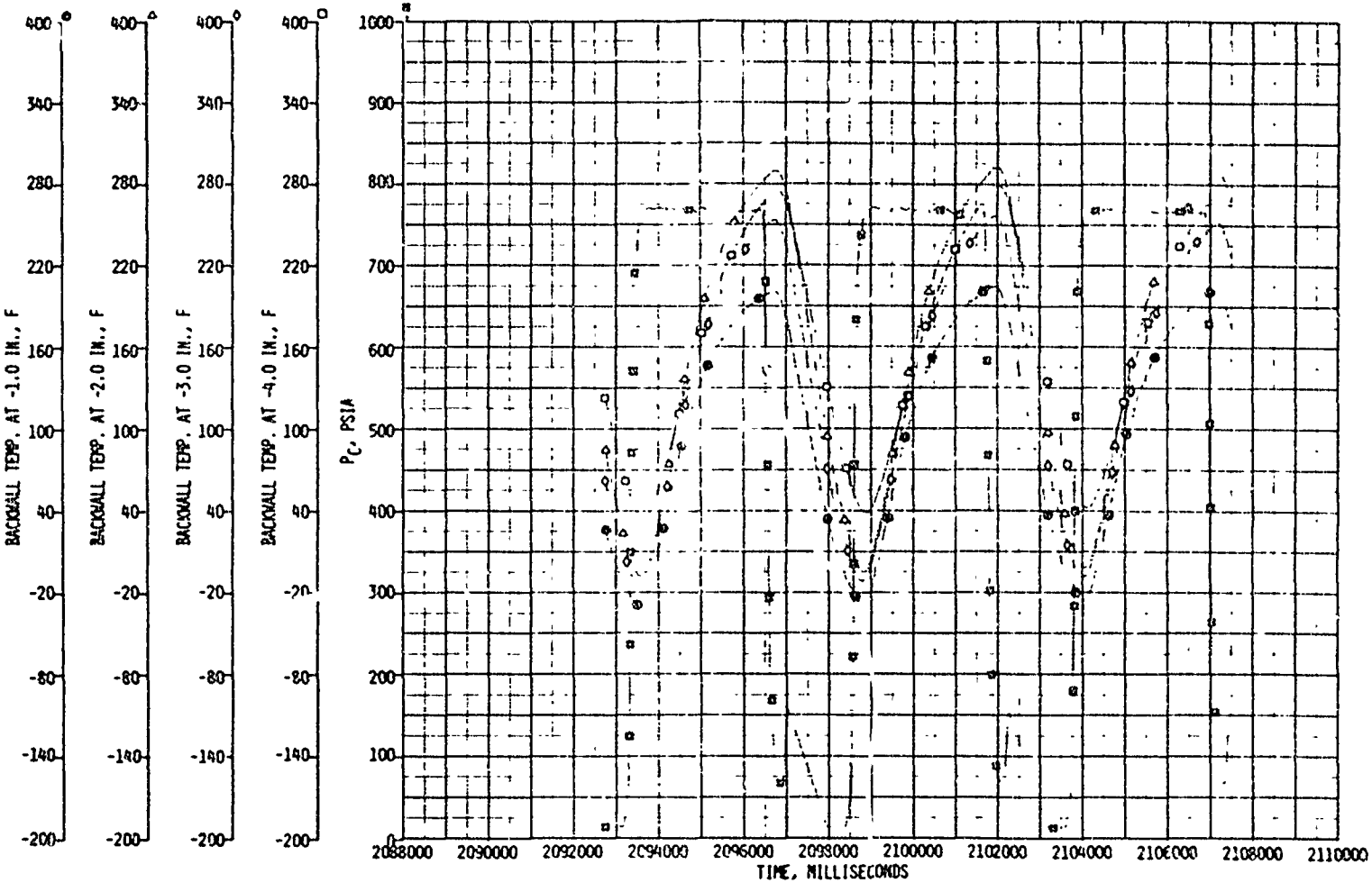

Figure 37. Plot of Various Run Parameters Vs Time for Typical Cyclic Test Series - Zirconium-Copper Chamber

hot gas wall; however, the test effort was continued until 615 cycles were accumulated. At this time the chamber was returned to Rocketdyne for non-destructive evaluation. Following this evaluation, the chamber was reinstalled on the test stand and additional cycles accumulated until 654 cycles had been accumulated on the chamber. Here again, this last series of tests (615 through 654) showed test anomalies reflected in higher wall temperatures. Post-test inspection of the hardware indicated that the injector was experiencing face burning. At this time it was decided to terminate the hot fire test effort on the regeneratively cooled hardware, return the chambers to Rocketdyne for post-test non-destructive and destructive evaluation, and to retest the injector and the calorimetric thrust chamber to establish a post-test heat flux profile.

An additional six tests were completed on the calorimeter thrust chamber assembly with durations as long as 20 seconds. Data showed that the heat flux profile had increased significantly from the pre-test configuration. Typical results are shown in Fig. 38. The real significance of this is that the last series of cycle tests on each of the two copper alloy chambers differs markedly from the first several hundred on each and effected the life somewhat. However, the majority of the testing effort was accomplished under well-controlled conditions and demonstrated the fatigue characteristics of the two copper chambers. Photographs of the hardware at various times during the test and post-test are presented in the following section.

Post-Test Evaluation of Copper Alloy Thrust Chambers

The post-test inspection of the two copper alloy chambers consisted of (1) non-destructive testing; (2) destructive evaluation; and (3) thermal and cyclic life analyses to predict the cyclic life capability of the chambers based on as-tested conditions. A summary of the visual and NDT inspection efforts is presented in Table 4.

Non-Destructive Testing. Part way through the hot fire cycling test effort, both copper alloy thrust chambers were returned to Rocketdyne for non-destructive evaluation of the hot gas wall. This evaluation, which consisted of visual,

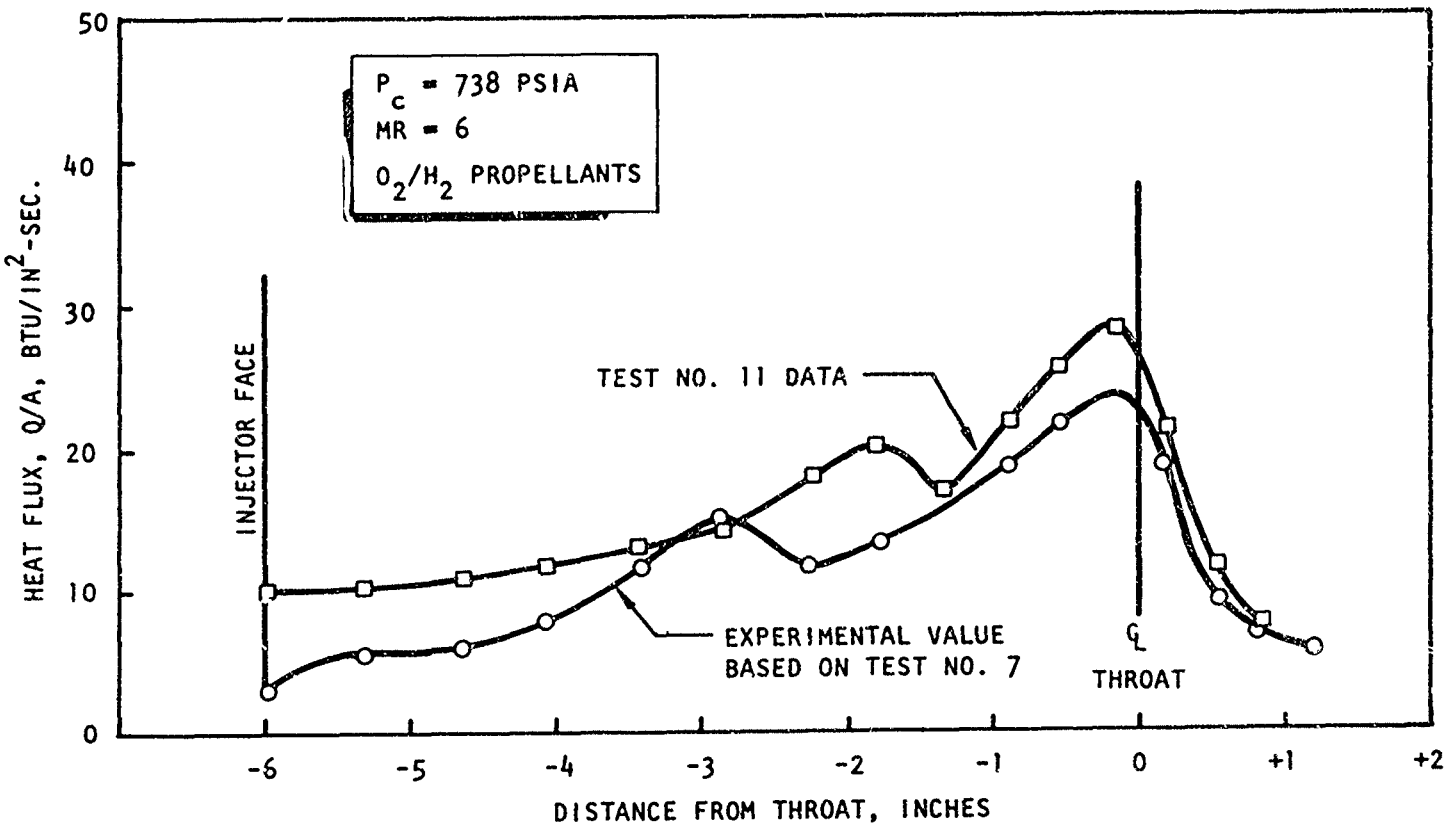

Figure 38. Later Heat Flux Profile as Established by Later Calorimeter Thrust Chamber Tests

TABLE 4. SUMMARY OF COPPER ALLOY CHAMBER NDT EFFORT

	NARLOY-Z CHAMBER	ZIRCONIUM-COPPER CHAMBER
PRE-TEST	SMOOTH SURFACE	SMOOTH SURFACE
AFTER 312 CYCLES	SURFACE LOOKS GOOD -- SLIGHT RIPPLING IN THROAT REGION	SEVERE ROUGHNESS OF SURFACE. TYPICAL OF COARSE GRAIN STRUCTURE -- NO THROUGH CRACKS. DATA INDICATES HOT GAS WALL TEMPERATURE < 300 F. (RETURNED TO ROCKETDYNE FOR EVALUATION)
FIRST THROUGH CRACK	410 CYCLES	398 CYCLES
ADDITIONAL CRACKS	2ND THROUGH CRACK AT 483 CYCLES 3RD THROUGH CRACK AT 543 CYCLES 4TH THROUGH CRACK AT 612 CYCLES RETURNED TO ROCKETDYNE FOR NDT	NO HISTORY OF WHEN ADDITIONAL CRACKS OCCURRED.
ROCKETDYNE NDT (INTERMEDIATE)	615 CYCLES 4 THROUGH CRACKS 3 CRACKS ON COOLANT SIDE OF WALL 2 SURFACE CRACKS ON HOT GAS SIDE	529 CYCLES 9 THROUGH CRACKS 8 CRACKS ON COOLANT SIDE OF WALL 0 SURFACE CRACKS ON HOT GAS SIDE
COMPLETION OF TEST EFFORT	654 CYCLES	587 CYCLES
	ANAMOLY IN TEST PROCEDURE AND/OR INJECTOR RESULTED IN HIGHER THAN PLANNED WALL TEMPERATURES	
POST TEST NDT	654 CYCLES 5 THROUGH CRACKS 3 CRACKS ON COOLANT SIDE OF WALL 1 SURFACE CRACK ON HOT GAS WALL	587 CYCLES 16 THROUGH CRACKS 11 CRACKS IN COOLANT SIDE OF WALL 0 SURFACE CRACKS ON HOT GAS WALL

dye-penetrant, and x-ray examination of the hot gas wall was used to ascertain the location of cracks through the hot gas wall as well as incipient cracking on the hot wall or on the coolant side of the liner. First, the chambers were subjected to a visual inspection to determine areas that showed obvious cracks. Dye penetrant was then added into the coolant passages through the supply manifold, until the channels were completely filled with the dye penetrant solution. Developer was added to the hot gas wall, such that any cracks which existed all the way through the hot wall could be determined. Typical photographs depicting this condition on the NARloy-Z and zirconium copper chambers are shown in Fig. 39 and 40. The next step in the NDT evaluation was to dye penetrant inspect the surface of the hot gas wall. This was not only again located the through cracks but also any cracks on the hot gas wall which were not all the way through the wall. An alternate non-destructive test technique that was used on the chambers was a series of x-rays of the hot gas wall. The x-rays showed not only the cracks through the wall and those on the hot gas surface, but also indicated additional cracks that were located on the coolant side of the liner, but which did not extend all the way through the wall. A compilation of these results conducted part-way through the test effort and upon completion of the test effort is given in Table 5 and 6 and Fig. 41 and 42. It is noted in reviewing the data on these tables, that the cracks did propagate somewhat during the latter portion of the test effort; however, propagation was much less in the NARloy-Z chamber than in the zirconium copper chambers. Typical photographs of the two chambers are presented in Fig. 43 through 50.

Destructive Evaluation of the Hardware. The initial step in this phase of the hardware post-test evaluation was to machine off the forward manifold and water flow the coolant circuit such that the flow from each channel could be evaluated to determine if there were any anomalies in coolant distribution. Results compared quite favorably to the present condition, and led to the conclusion that there was no maldistribution of coolant. Subsequently, the aft flange was machined off and the chambers were split longitudinally to expose the hot gas surface. Sections of each chamber were then metallurgically evaluated to determine the location and effect of the cracks wherever possible.

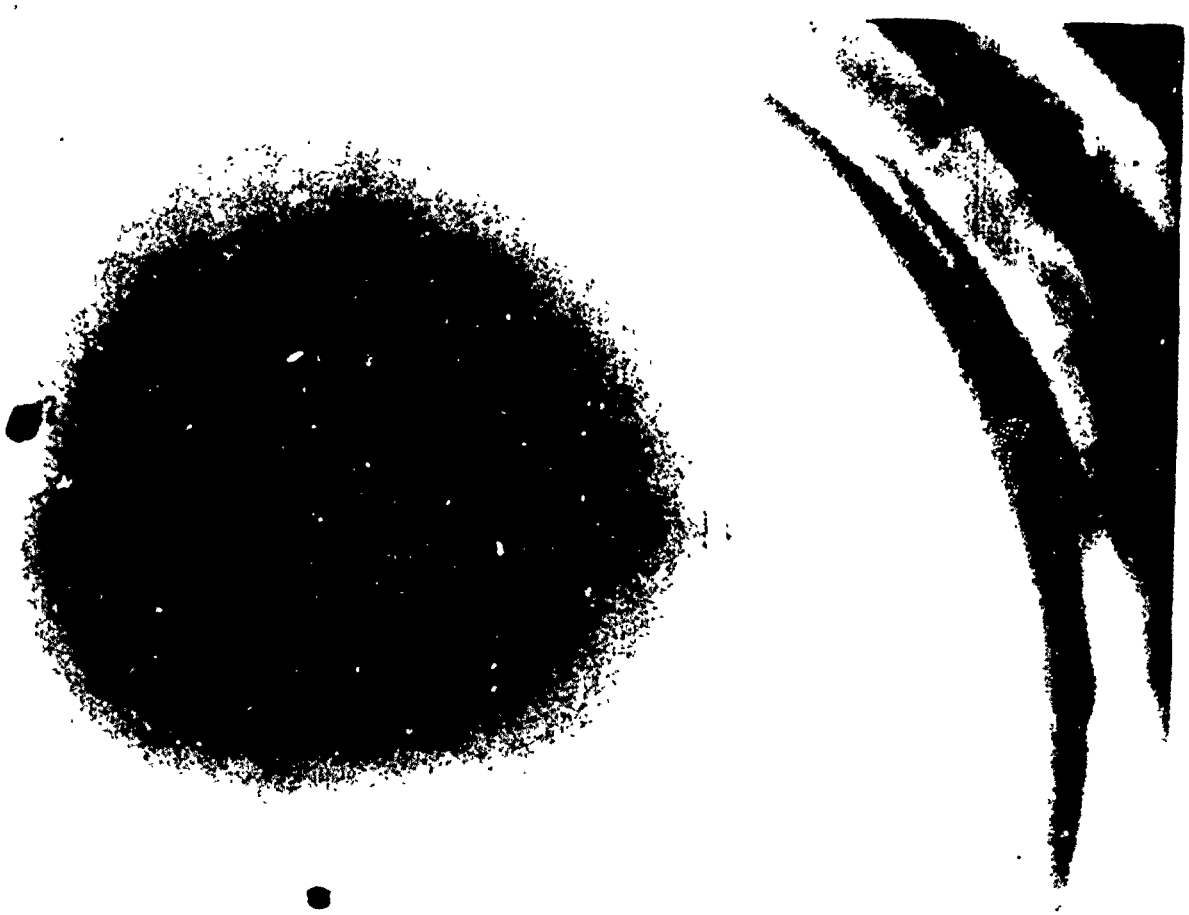

5AJ36-7/5/72-C1D

Figure 39. NARloy-Z Thrust Chamber - 615 Cycles - Dye Penetrant Inspection (in Coolant Channels)

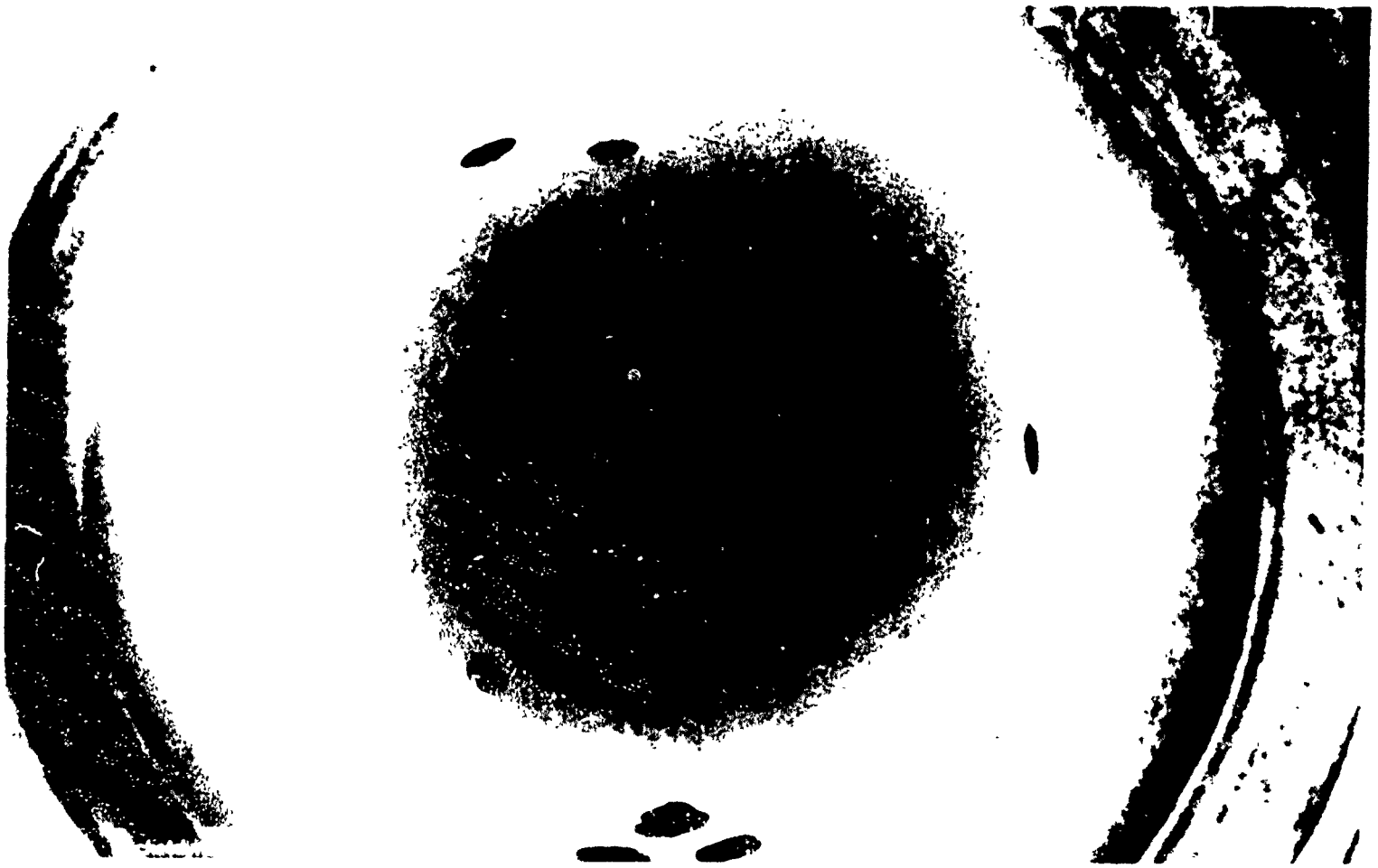

5AJ36-7/5/72-C1A

Figure 40. Combustion Zone of Zirconium Copper Chamber Showing Through Cracks as Determined by Dye Penetrant (in Coolant Channels) After 529 Cycles

Table 5. Summary of Crack Initiation and Growth in NARloy-Z-Chamber

	615 CYCLES							654 CYCLES						
CRACK	☆	○	□	C	H	T	CRACK LENGTH	☆	○	□	C	H	T	CRACK LENGTH
A	X	X	X			X	0.195	X	X	X			X	0.225
B	X	X	X			X	0.185	X	X	X			X	0.225
C		X		?			0.040		X		?			0.050
D		X		?			0.050		X		?			0.050
E	X	X	X			X	0.185	X	X	X			X	0.185
F										X		X		0.040
G		X		?			0.085		X		?			0.085
H	X	X	X			X	0.275	X	X	X		X		0.300
I			X		X		0.025			1				OBSCURED BY INJ. RESIDUE
J			X		X		0.025	X	X	X			X	0.063

☆ DYE INJECTOR
○ X-RAY
□ SURFACE DYE-CHEK
C COOLANT SIDE
H HOT GAS SIDE
T THROUGH CRACK

Table 6. Summary of Crack Initiation and Growth in Zirconium-Copper Chamber

	529 CYCLES							587 CYCLES						
CRACK	☆	○	□	C	H	T	CRACK LENGTH	☆	○	□	C	H	T	CRACK LENGTH
A	X	X	X			X	0.075	X	X	X			X	0.075
B_1	X	X					0.200	X	X	X			X	0.350
B_2		X		?			0.100		X		?			0.100
C									X	-	?			0.300
D									X		?			0.125
E_1								X	X	X			X	0.125
E_2								X	X	X			X	0.125
F_1		X					0.050		X		?			0.050
F_2									X		?			0.100
G									X		?			0.080
H		X		?			0.075	X	X	X			X	0.100
I_1	X	X	X			X	0.175	X	X	X			X	0.500
I_2									X		?			0.300
J_1								X	X	X			X	0.125
J_2		X		?			0.100	X	X	X			X	0.110
J_3	X	X	X			X	0.100	X	X	X			X	0.130
K_1	X		X			X		X	X	X			X	0.175
K_2											?			0.040
L_1		X		?			0.025		X		?			0.040
L_2	X	X	X			X	0.100	X	X	X			X	0.190
M_1		X		?			0.050	X	X	X			X	0.050
M_2											?			0.125
M_3		X		?			0.100	X	X	X			X	0.100
M_4		X		?			0.075		X		?			0.110
N	X	X	X			X	0.075	X	X	X			X	0.075 (ALSO ENTRAPPED DENSE MATERIAL)
O	X		X			X	0.050	X	X	X			X	0.063
P	X	X	X			X	0.150	X	X	X			X	0.150

☆ DYE INJECTOR
○ X-RAY
□ SURFACE DYE-CHEK

C COOLANT SIDE
H HOT GAS SIDE
T THROUGH CRACK

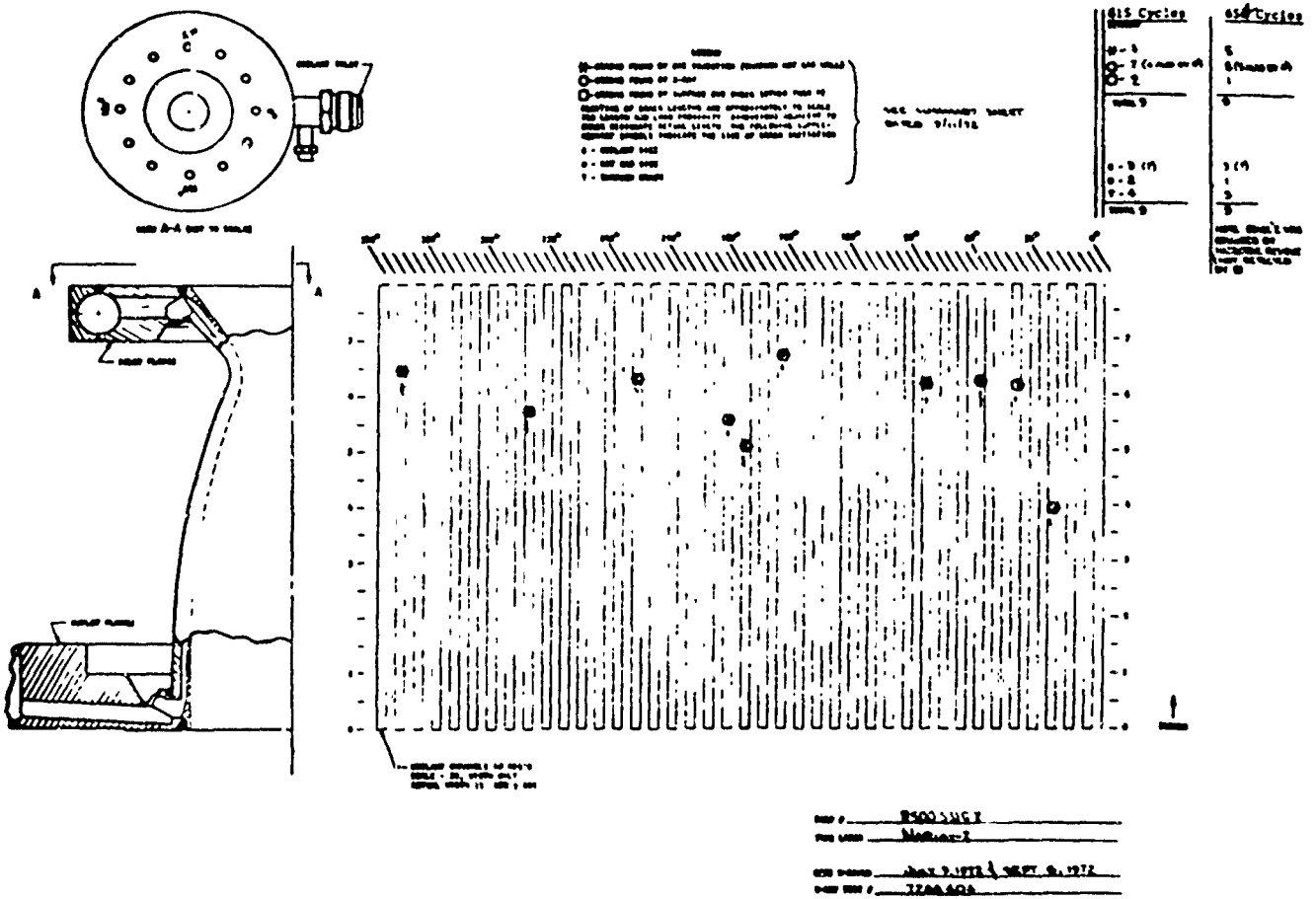

Figure 41. Crack Locations on NARloy-Z Chamber

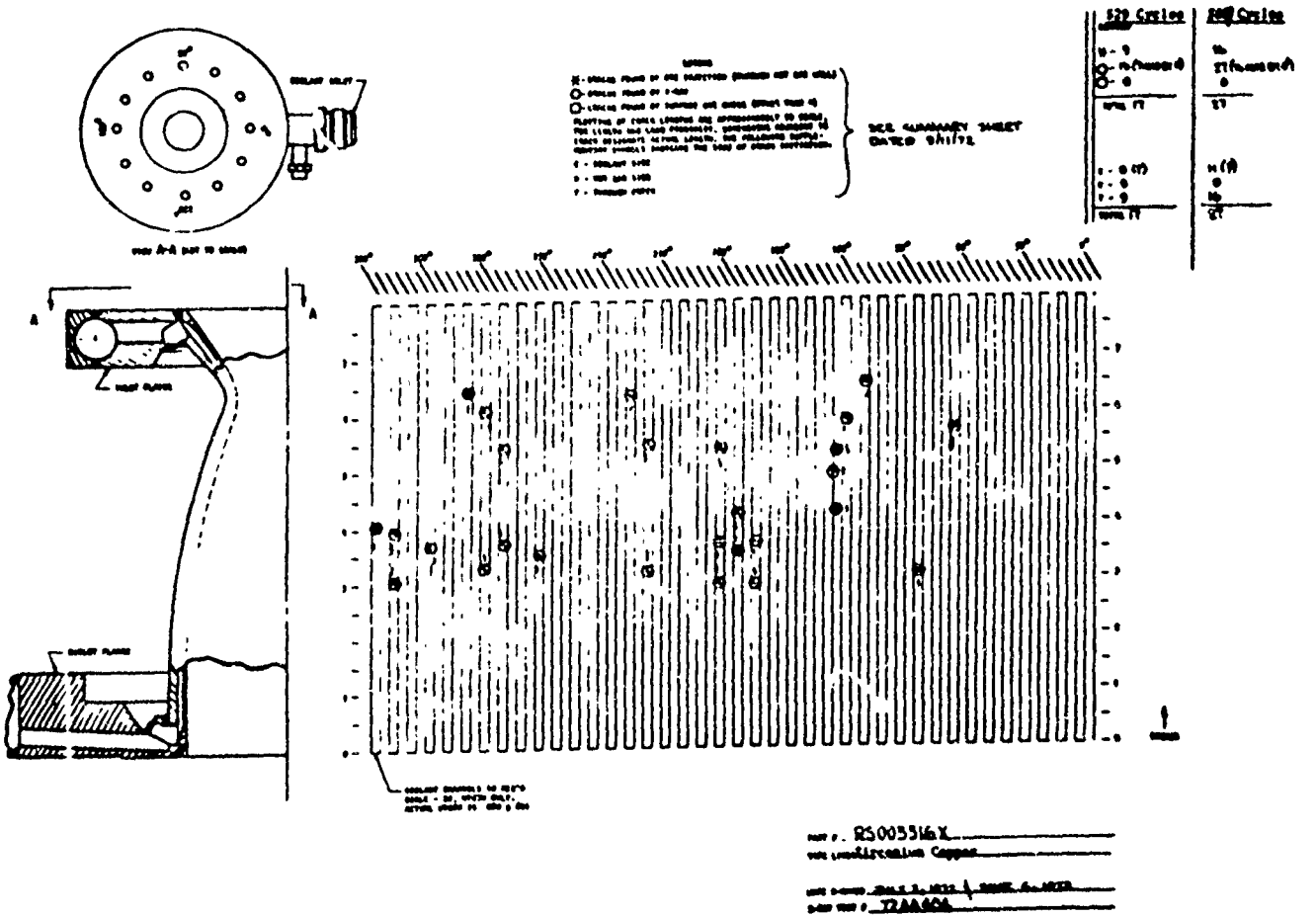

Figure 42. Crack Locations on Zirconium Copper Chamber

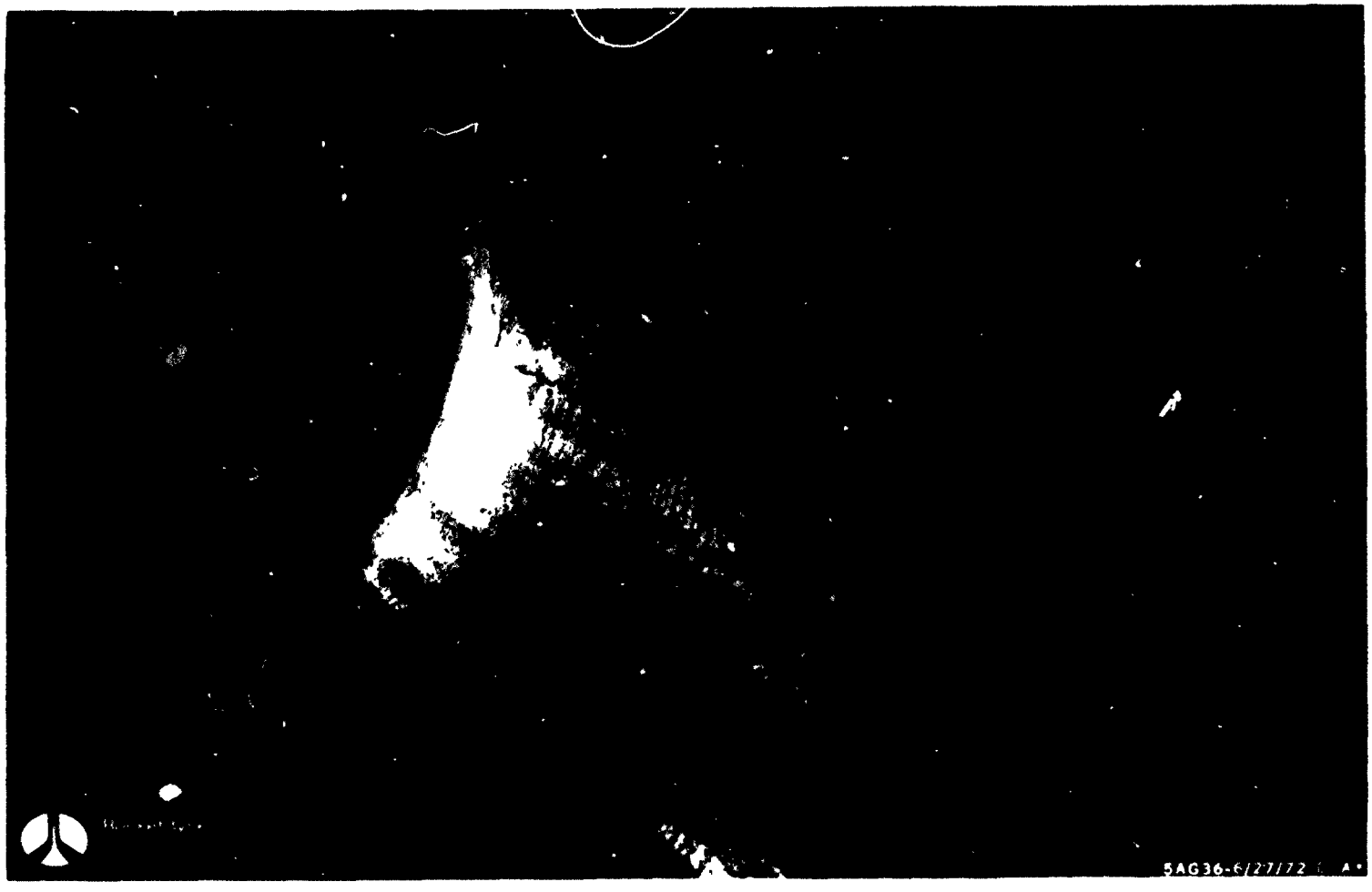

5AG36-6/27/72-C1A

Figure 43. Close Up View of NARloy-Z Chamber Showing Through Cracks in Combustion Zone Following 615 Cycles

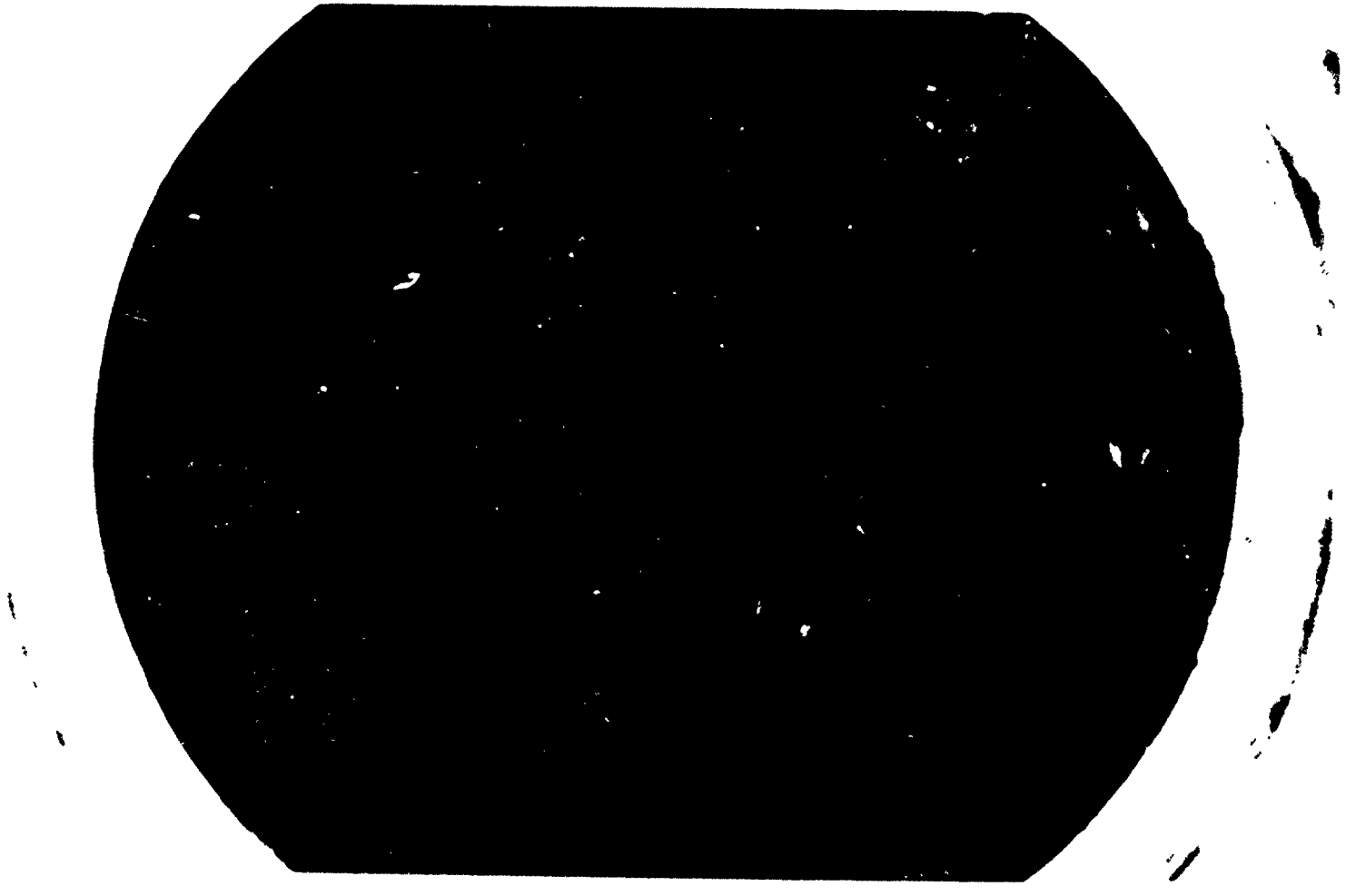

5AG36-6/29/72-C1*

Figure 44. Combustion Zone of NARloy-Z Chamber Showing Through Cracks After 615 Cycles

5AG36-9/12/72-C1A

Figure 45. Combustion Zone of NARloy-Z Chamber Showing Deposit of Nickel from Injector After 654 Cycles

5AG36-9/12/72-C1E

Figure 46. Close Up View of MARIoy-2 Chamber (Nozzle End) After 654 Cycles

IXW35-7/3/72-C1E*

Figure 47. Overall View Showing Combustion Zone of Zirconium Copper Chamber After 529 Cycles

1XW35-7/3/72-C18

Figure 48. Combustion Zone of Zirconium Copper Chamber Showing Typical Through Cracks After 529 Cycles

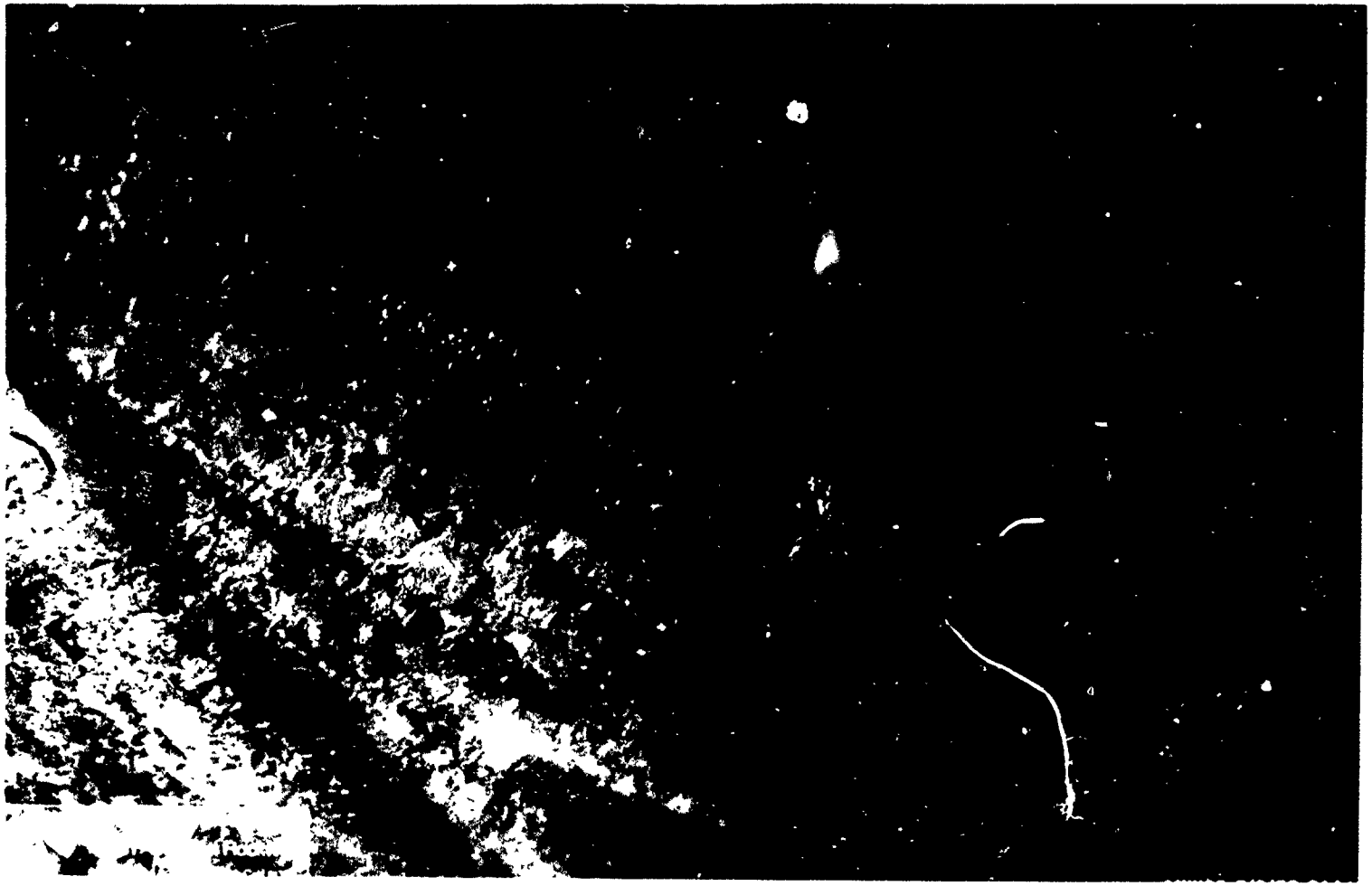

1XW35-7/3/72-C1A*

Figure 49. Close Up View of Zirconium Copper Chamber Combustion Zone Showing Typical Through Cracks and Surface Roughness

5AG36-9/12/72-C1B

Figure 50. Close Up View of Zirconium Copper Chamber Showing Roughness After 589 Cycles

Metallurgical evaluation of the chamber has revealed two types of cracks in the copper alloy liners. These are (1) stringer cracks, related to an inclusion, and (2) linear tears associated with machining of the coolant channels.

Stringer Cracks in NARloy-Z. All of the cracks which extended through the wall, other smaller cracks that were detected by non-destructive test methods, and a large number of much smaller cracks visible at 30X magnification were all oriented with the chamber axis. These were all further characterized by the slightly erratic path of a typical crack.

A number of these cracks were examed metallographically by polishing the surface on which the crack appeared and also by polishing a section cut transverse to this plane. By either method the originating oxide stringer could be detected by removing small increments of material and examining the crack edges. The transverse method was found to involve many more successive cuts because of the greater length of the cracks in relation to their depth. When the plane under examination was completely within the fatigue extension zone no stringer was visible.

A number of large and small cracks were also investigated by bending to expose the fracture faces as a more rapid and certain method of finding the origin. All cracks exposed in this manner clearly originated in an inclusion.

Chemical analysis was performed by dispersive X-ray fluoroscopy and by electron beam microprobe on the crack faces after breaking them open and also upon stringers that were evident in polished microspecimens adjacent to cracks. The dispersive X-ray fluoroscopic qualitative analysis detected zirconium, titanium, aluminum, silicon, and copper on the exposed crack face and principally zirconium in the stringers in microspecimens. The quantitative analysis of stringer material adjacent to a crack in a polished specimen obtained by electron beam microprobe is presented in Table 7 for the NARloy-Z chamber. The analysis of the metallic second phase particles is included for reference.

TABLE 7. ELECTRON BEAM MICROPROBE ANALYSIS OF THE NARloy-Z CHAMBER

1. BLACK INCLUSIONS IN FORM OF STRINGERS

	Near Hot Wall	Near Cold Wall
Zr	44 percent	52 percent
Cu	"High"	28 percent
Ag	4 percent	1 percent
Al	---	1 percent
O_2	10 percent	10-15 percent

2. GRAY-BLACK INCLUSIONS IN STRINGERS

Si	9 percent
O_2	45 percent
Al	23 percent
Cu	1 percent
Zr	Nil
Ag	Nil

3. ROUNDED GRAY PARTICLES CONSIDERED TO BE THE NORMAL METALLIC PHASE

	Near Hot Wall	Near Cold Wall
Zr	16 percent	18 percent
Ag	10 percent	1. percent
Cu	Balance	70 percent

Note: The slight difference shown for the metallic second-phase particles on the hot wall and the cold wall are really insignificant and are within the accuracy of the microprobe.

Linear Tears. Grinding off the electroformed nickel closure on the NARloy-Z chamber revealed pronounced linear marks on the bottom of some of the machined channels in an area starting approximately 1/2 inch above the throat and extending 2 inches towards the injector. Under magnification it became apparent that these had started as very fine, regular machine marks from the slitting saw but had been enlarged in width and depth. Transverse microspecimens through a number of these locations showed a maximum depth of approximately 0.005 inch and a width of 0.0005 inch. Examination at high magnification after exposing the surfaces by bending clearly showed the striations of fatigue propagation. The original machined surface outside the affected area was 30-50 microinches RMS and showed no evidence of deep markings. The hot gas surface on the other hand showed relatively deep circumferential machining marks but no evidence was found of propagation. Although not examined, the zirconium copper chamber should exhibit similar characteristics since all machining parameters were identical.

Photomicrographs of Liner Sections. Both stringer initiated cracks and linear tears due to machining marks on the NARloy-Z chamber are seen in Fig. 51. This is a view looking down into the channel after the electroformed nickel closeout had been machined away. The cracks occurred earlier than the linear tears (or seams). As shown in this figure the tears did not develop in the areas relieved by cracks. Later metallographic preparation verified the presence of the non-metallic stringer material in both of the cracks.

The originating stringers are difficult to detect by polishing a material sample at a crack. They are readily seen on the fracture surfaces after they are exposed by bending as illustrated in Fig. 52. The original crack surfaces in this example were darkened by exposure to the combustion atmosphere but the stringer was clearly visible. Several small stringers which had not cracked open are more evident against the light background of the fresh break.

Figure 53 shows the cold wall in two separate channels after bending to expose two very small cracks. The dark stringer material which initiated the cracks is most easily found by this method. It is noted that the machining marks tend to tear open when the material is bent in this manner.

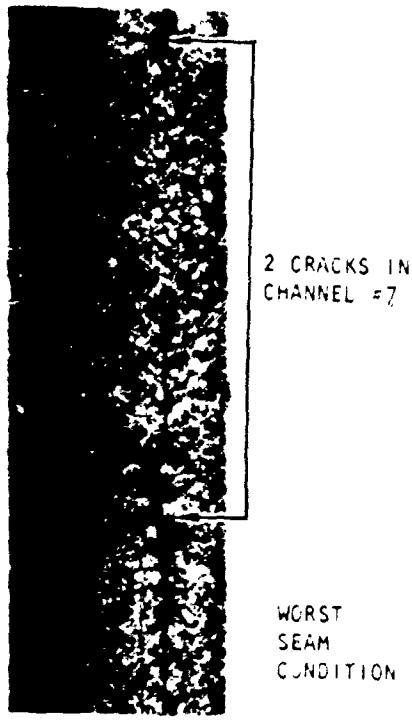

CHANNEL 7 15X

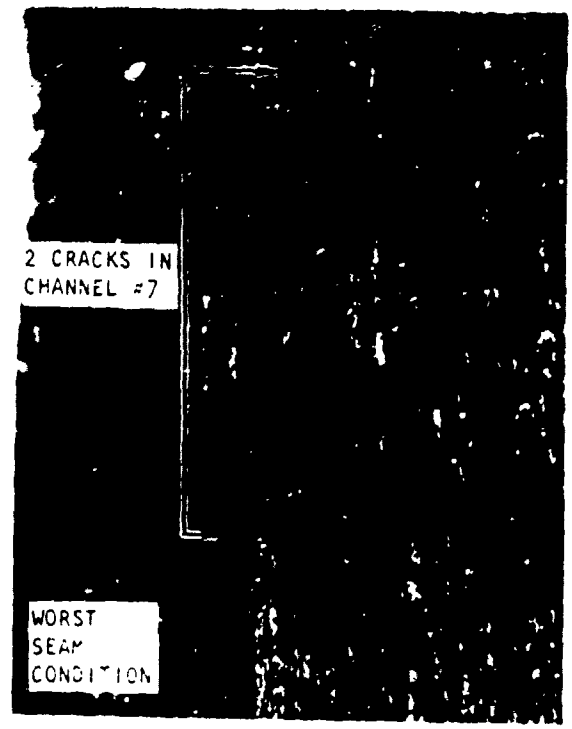

100X CHANNEL 7
(REVERSED)

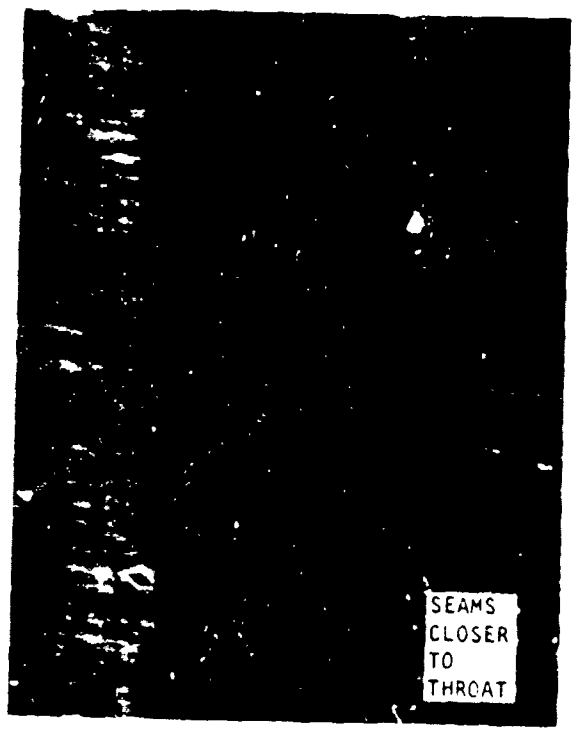

CHANNEL 7 15X

Figure 51.

Photographs Showing Stringer Initiated Cracks and Linear Tears in Typical Channel of NARloy-Z Chamber

THROAT

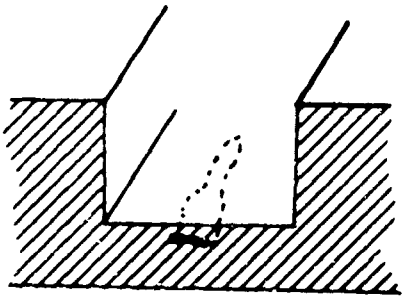

STRINGER IN
ORIGINAL MATERIAL

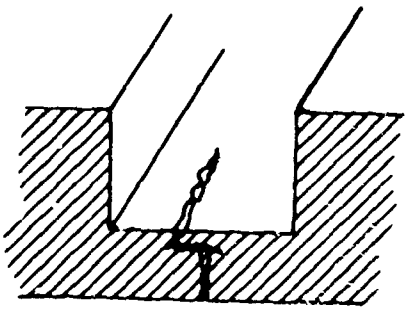

CRACK PROPAGATION
FROM STRINGER

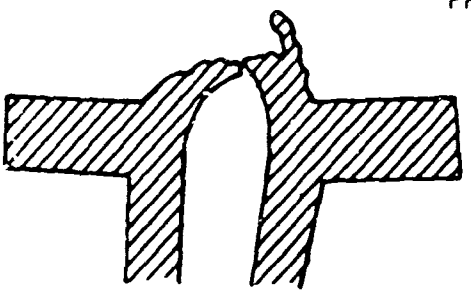

APPEARANCE AFTER
OPENING BY BENDING

8X

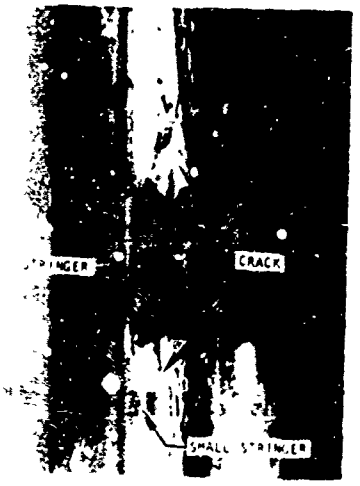

20X

STRINGER INITIATED CRACK EXPOSED BY BENDING
ENTIRE CRACK SURFACE BLACKENED BY HOT GAS

Figure 52. Evolution of a Stringer Crack

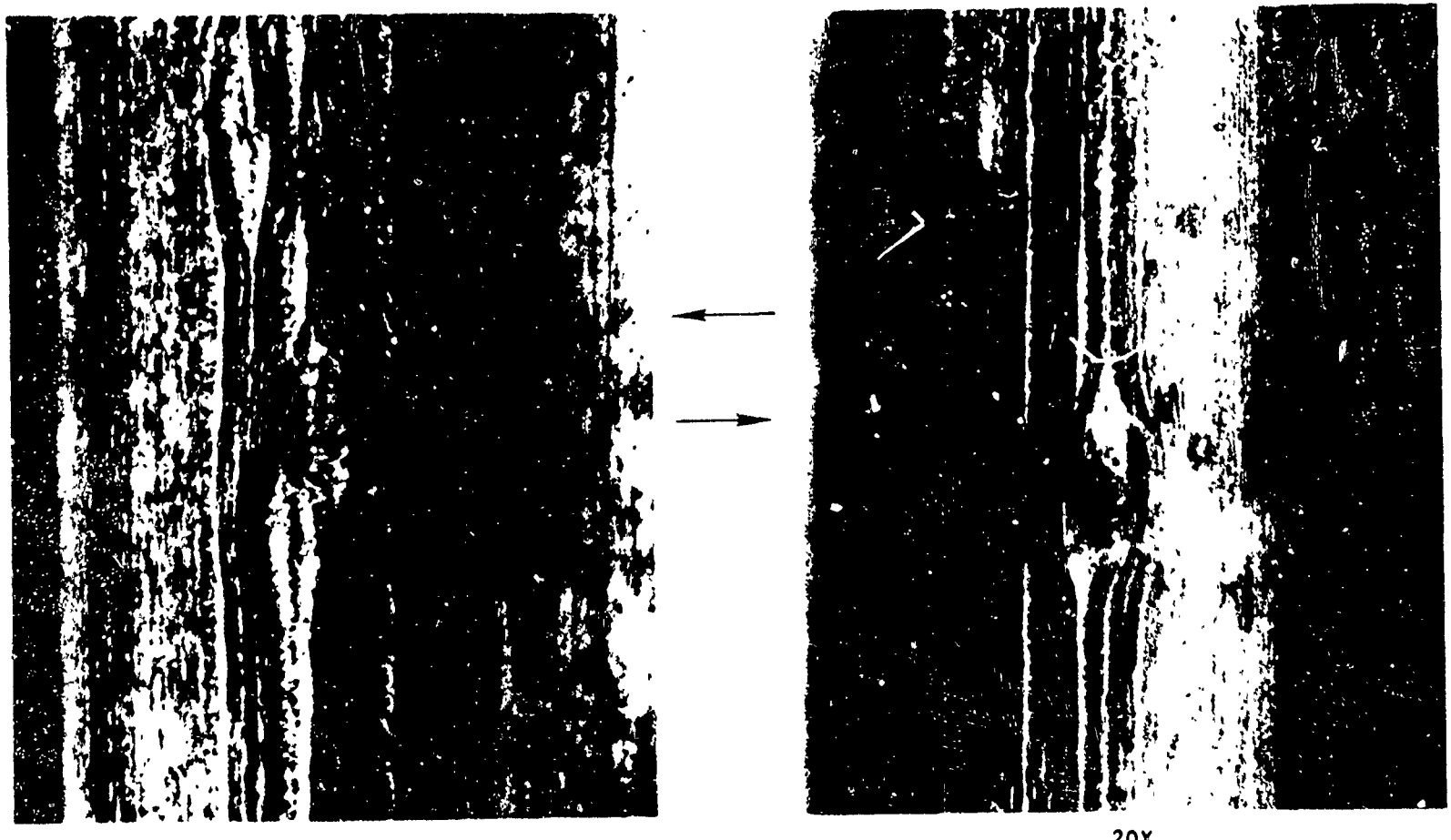

20X

20X

OXIDE STRINGERS EXPOSED BY BENDING AT
CRACK SITES ON COLD WALL. NEITHER
CRACK EXTENDED THROUGH TO THE
COMBUSTION ATMOSPHERE.

Figure 53. Oxide Stringers Exposed by Bending at Crack Sites on Cold Wall. Neither Crack Extended through to the Combustion Atmosphere

A number of typical stringers are shown in the microspecimen of Fig. 54 through 59. At relatively low magnification the stringers appear as dark patches, with the smaller particles being the metallic zirconium rich phase. The difference between the metallic and the non-metallic phases is very apparent at higher magnification.

These transverse sections shown in Fig. 60 are through the channel wall at the worst linear tear locations that were found in the NARloy-Z chamber. The wide, blunt ended type of crack was the only mode of propagation found in either the machine mark tears or the stringer cracks. The very small stringer crack found in the same sample shows this same blunt characteristic.

The distortion of the hot gas wall of the zirconium copper chamber is evident in the photographs of Fig. 61. The channels were initially of rectangular cross section as shown by the NARloy-Z photograph.

Post-Test Thermal and Cycle Life Analysis. As a part of the post-test analysis effort the cyclic life capability of the two copper alloy chambers was recalculated using actual test data. This was accomplished using a typical cycle test, Test No. 11, from the NARloy-Z test series.

From heat transfer data obtained from the water-cooled calorimetric chamber tests and regeneratively cooled copper alloy chamber tests, the cyclic thermal strain experienced was determined by analytically correlating measured backwall temperatures. These temperatures were measured at various axial chamber locations. In the thermal analysis performed, the following assumptions were made:

1. Chamber pressure versus time was a step-function from zero to design chamber pressure.
2. Coolant flow as constant during a cycle.
3. Analytical coolant-side film coefficient was correct.

CHAMBER SURFACE AT 50X

NOTE GROSS DISTORTION OF SURFACE

CHAMBER SURFACE AT 200X

CRACKS IN AREA OF INCLUSION

Figure 54. Hot Gas Surface of Zirconium Copper Chamber

CRACK IN INCLUSION AREA - CRACK PROPAGATING INTO CLEAN MATERIAL AREA (40X)

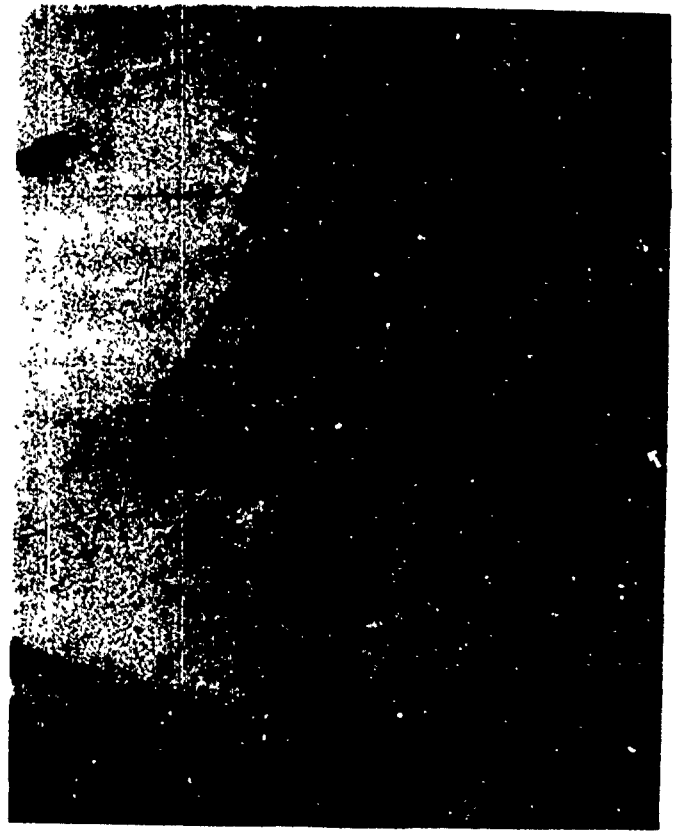

CRACK IN INCLUSION AREA AXIAL (100X)

Figure 55. Hot Gas Surface of Zirconium-Copper Chamber

VIEW SHOWING TAIL END OF CRACK IN PARENT METAL
(50X)

Figure 56. Hot Gas Surface of Zirconium-Copper Chamber

PHOTO SHOWING SMALL REGULAR GRAIN STRUCTURE AND TYPICAL OF STRINGERS ON HOT GAS SURFACE (SMALL DARK SPOTS ARE METALLIC ZIRCONIUM) (50X)

SECTION THROUGH HOT GAS WALL (LIGHT SPOTS ARE METALLIC ZIRCONIUM (500X)

Figure 57. Oxide Inclusions in NARloy-Z Chamber

SECTION THROUGH HOT GAS WALL
SHOWING START OF CRACKS (500X)

Figure 58. Inclusion in NARloy-Z Chamber

HOT GAS SURFACE AT 50X SHOWING
CRACKS IN INCLUSION

VIEW SHOWING RELATIONSHIP
OF CRACK TO INCLUSION (200X)

Figure 59. Hot Gas Surface of NARloy-Z Chamber

CHANNEL #7 - TRANSVERSE
MICRO 2-1068 100X

SAME SPECIMEN BUT ~0.050"
TOWARDS THROAT

OXIDE INITIATED
CRACK JUST BELOW
COLD WALL SURFACE

CHANNEL #4
MICRO 2-1068 500X

Figure 60. Photomicrographs of MARloy-2 Chamber Channel Cross Section Showing Tears and Cracks on Cold Wall Side

ZIRCONIUM COPPER CHAMBER

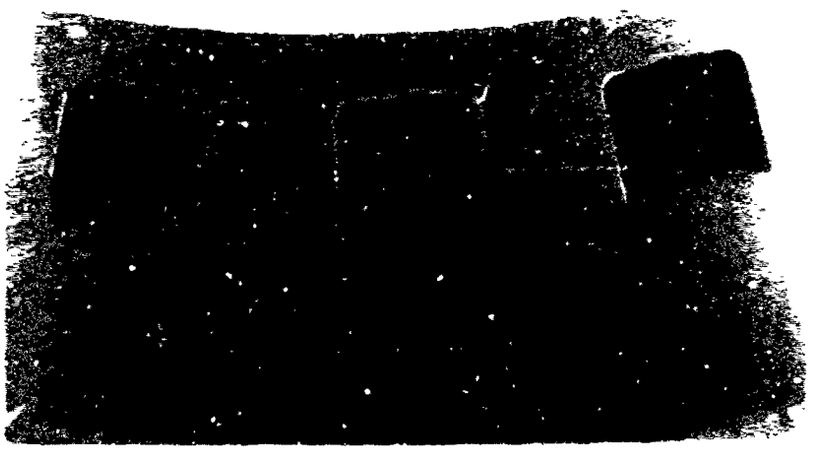

NARLOY-Z CHAMBER

Figure 61. Chamber Cross Sections at Throat

4. Water-cooled chamber test data were directly applicable

$$\frac{\Delta T_{\text{Inlet to Desired Station}}}{\Delta T_{\text{Combustor}}} = \text{Constant During the Cycle}$$

5. Axial heat conduction was neglected.

Typical measured test data are shown in Fig. 62 and 63 for run number 11 which was at approximately 750 psia chamber pressure and a mixture ratio of approximately 5.0. To match the measured transient backwall temperature profiles, coolant bulk temperature versus time was determined at the desired location and the predicted coolant-side film coefficient was corrected for the coolant temperature and the measured coolant flowrate. Then the gas-side coefficient was varied until a reasonable correlation with the measured backwall temperature was achieved. Predicted wall temperature transients for three axial locations are presented in Fig. 64 through 66. The maximum thermal gradient (gas-side to backwall) occurred at approximately 0.15 second into the cycle.

Fairly good agreement were obtained for the start to the steady-state portion of the cycle; however, for the shutdown the predicted temperature did not decay as rapidly as the measured value for the X = -1.0 inch and -0.1 inch locations. (X = 0 is throat plane and - X indicates distance upstream of the throat). This may be the result of some axial heat conduction occurring through the backwall on shutdown. Typical wall temperature distributions at various times in the cycle are shown in Fig. 67 through 69.

From these thermal data an analysis was undertaken to determine the maximum effective strain imposed on the hot gas wall during the start cycle. Results, plotted in Fig. 70 showed that a peak strain of ~1.4 percent occurred at a point 1.0 inches upstream of the throat and at a time 0.3 seconds into the run. Steady state strain value at the same plane is ~1.25 percent. The strain is higher during the start transient than at steady state conditions since the hot gas wall responds much faster than the back wall, resulting in a greater temperature differential across the chamber wall during the transient.

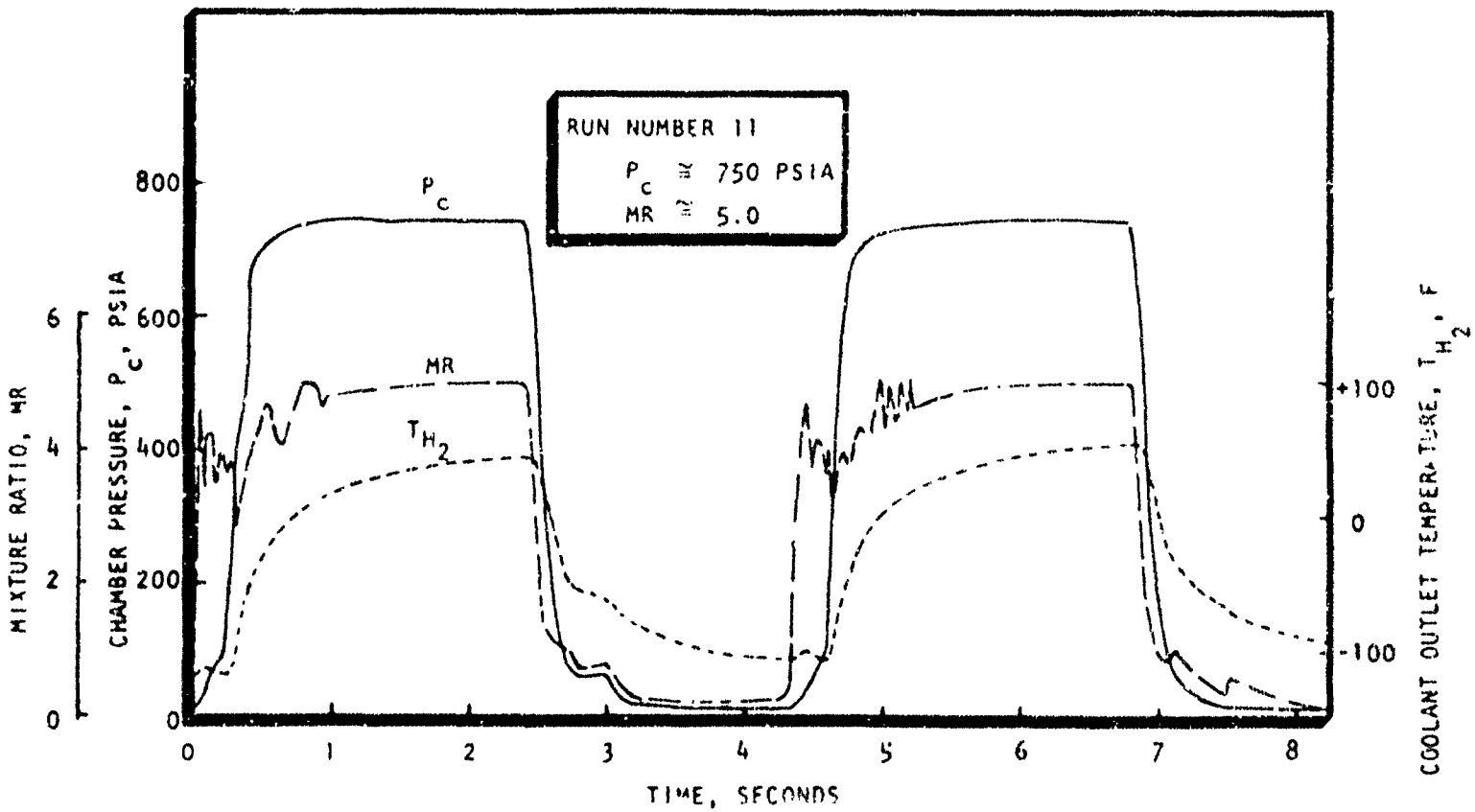

Figure 62. Typical Thermal Fatigue Chamber Test (Run No. 11)

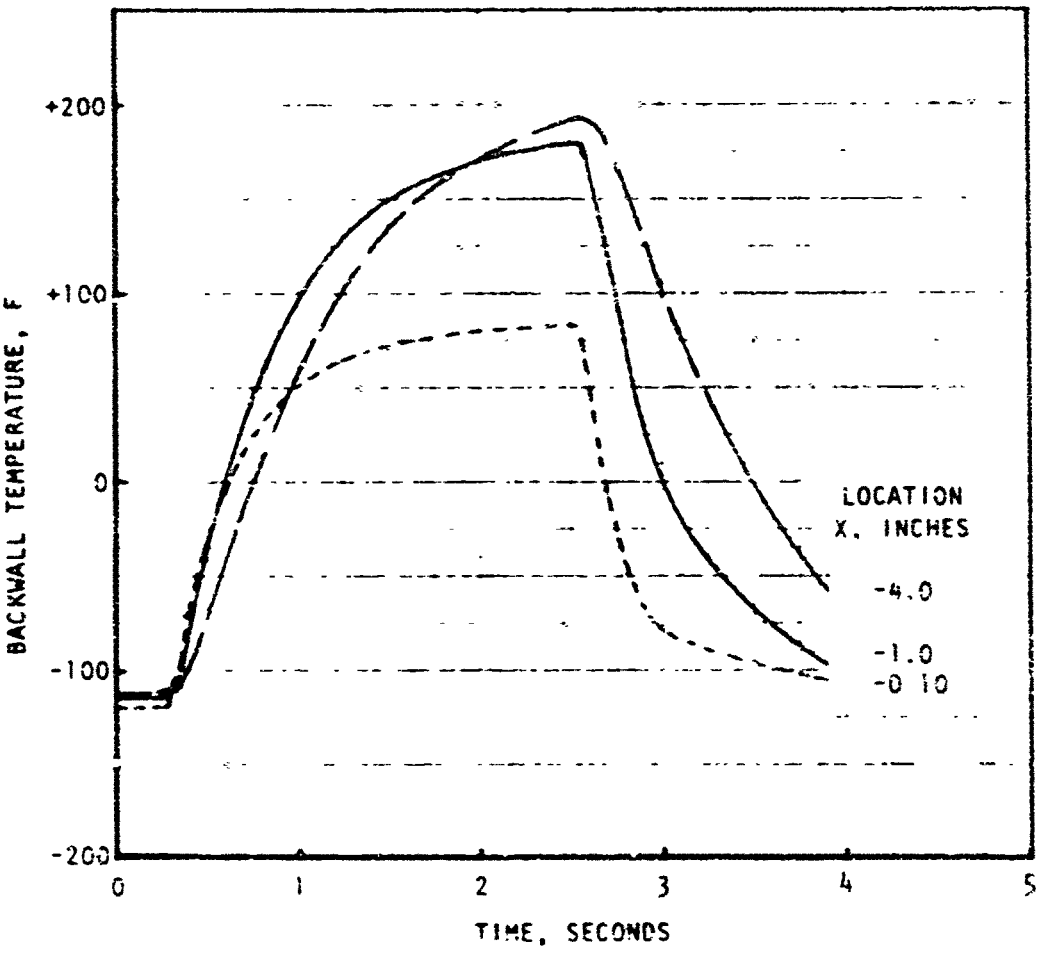

Figure 63. Typical Measured Backwall Temperatures (Run No. 11)

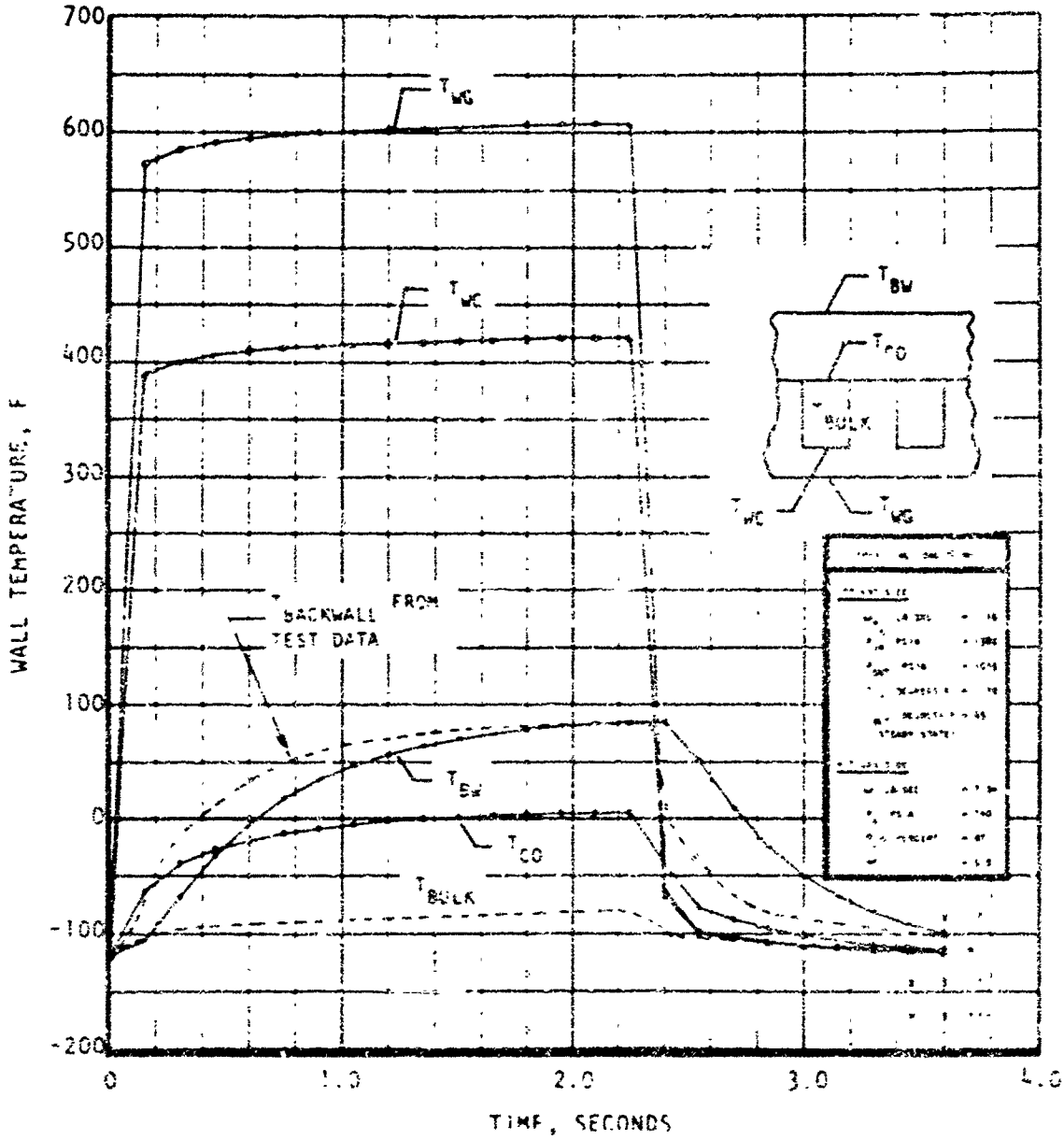

Figure 64. Predicted Transient Wall Temperature Distribution at X = -0.1 inch (Run No. 11)

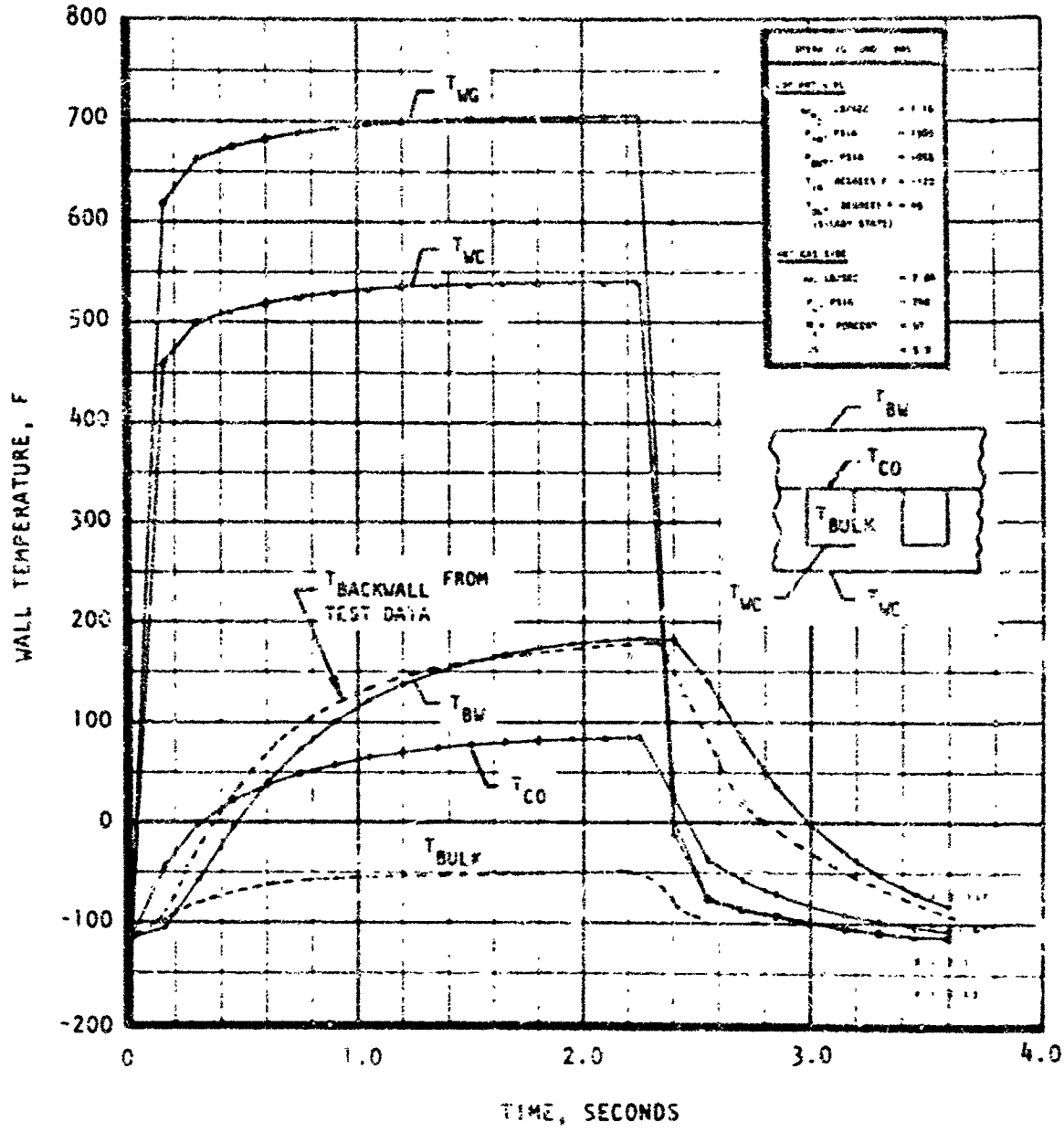

Figure 65 Predicted Transient Wall Temperature Distribution at X = -1.0 inches (Run No. 11)

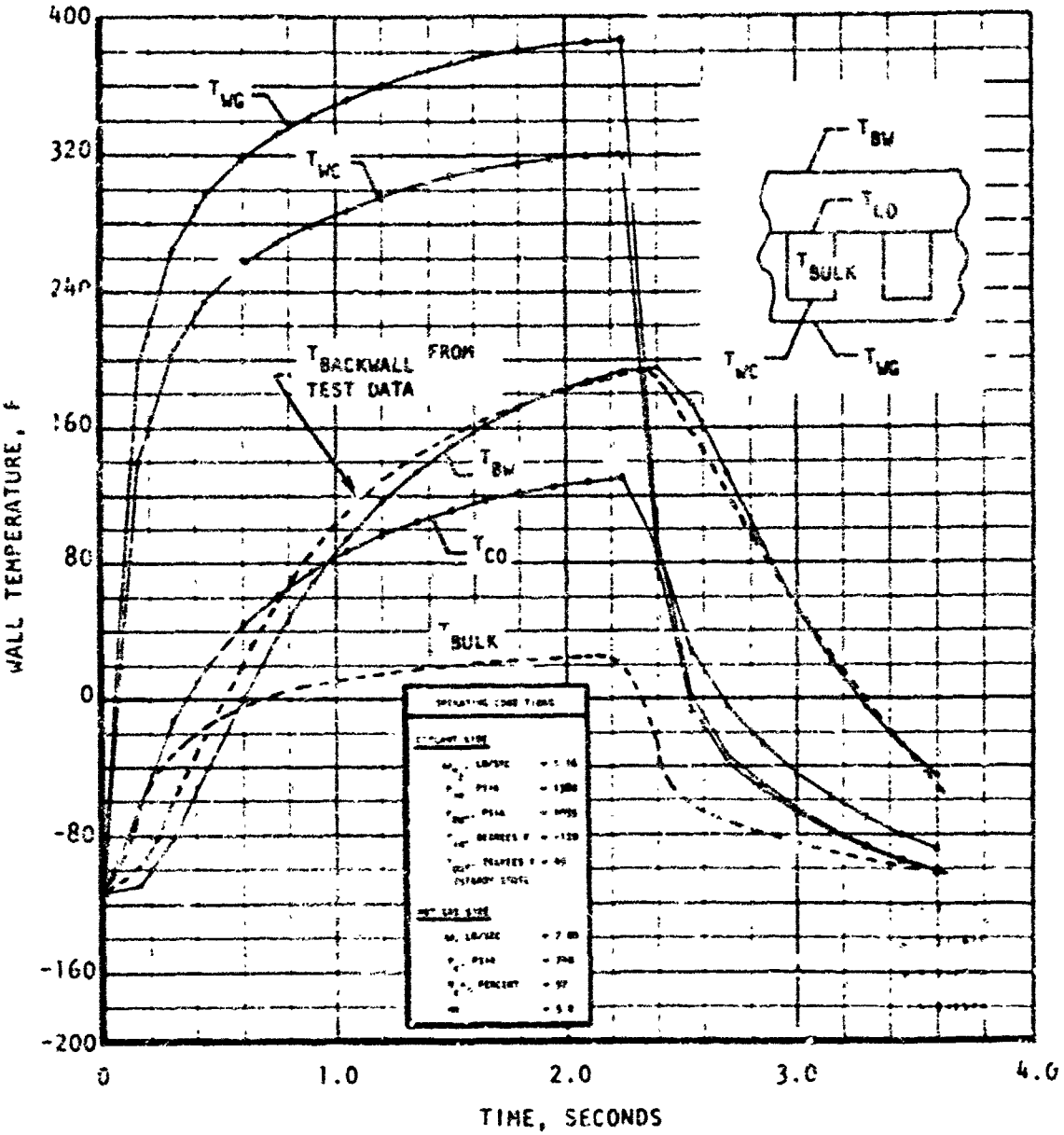

Figure 66. Predicted Transient Wall Temperature Distribution at X = -4.0 inch (Run No. 11)

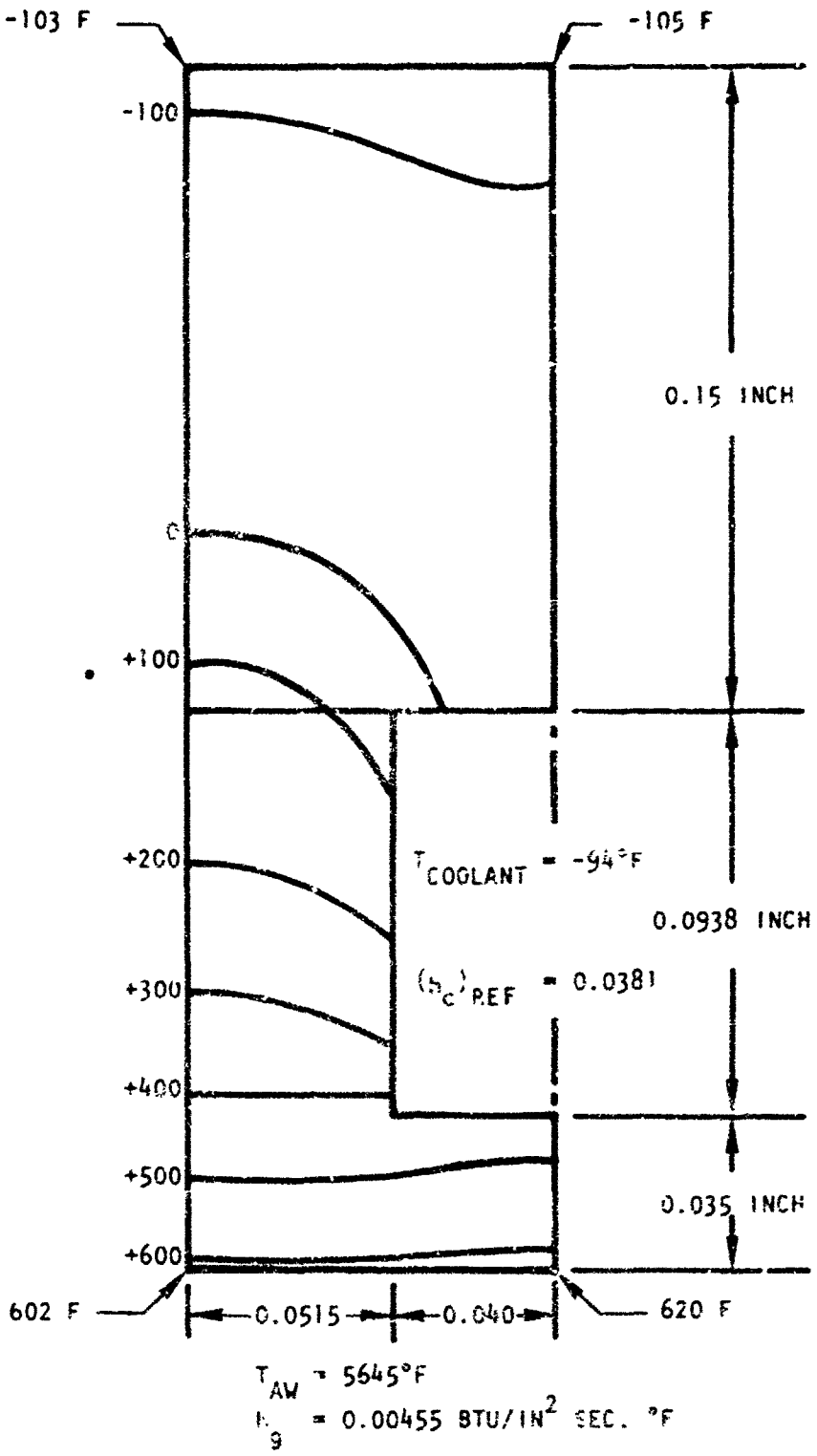

Figure 67. Thermal Fatigue Chamber Wall Temperature Distribution at X = -1.0 inches and t = 0.15 second (Run No. 11)

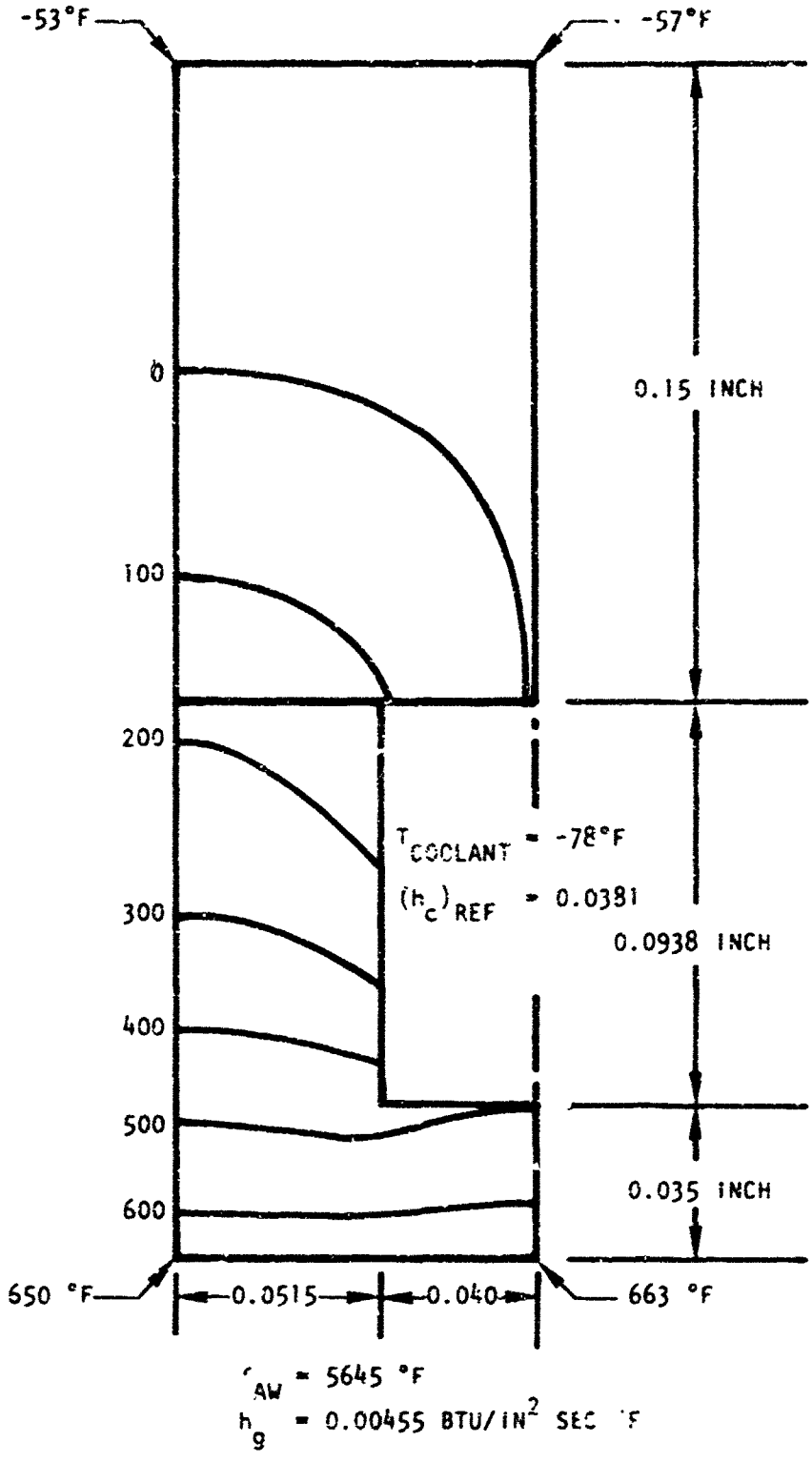

Figure 68. Thermal Fatigue Chamber Wall Temperature Distribution at X = -1.0 inches and t = 0.3 second (Run No. 11)

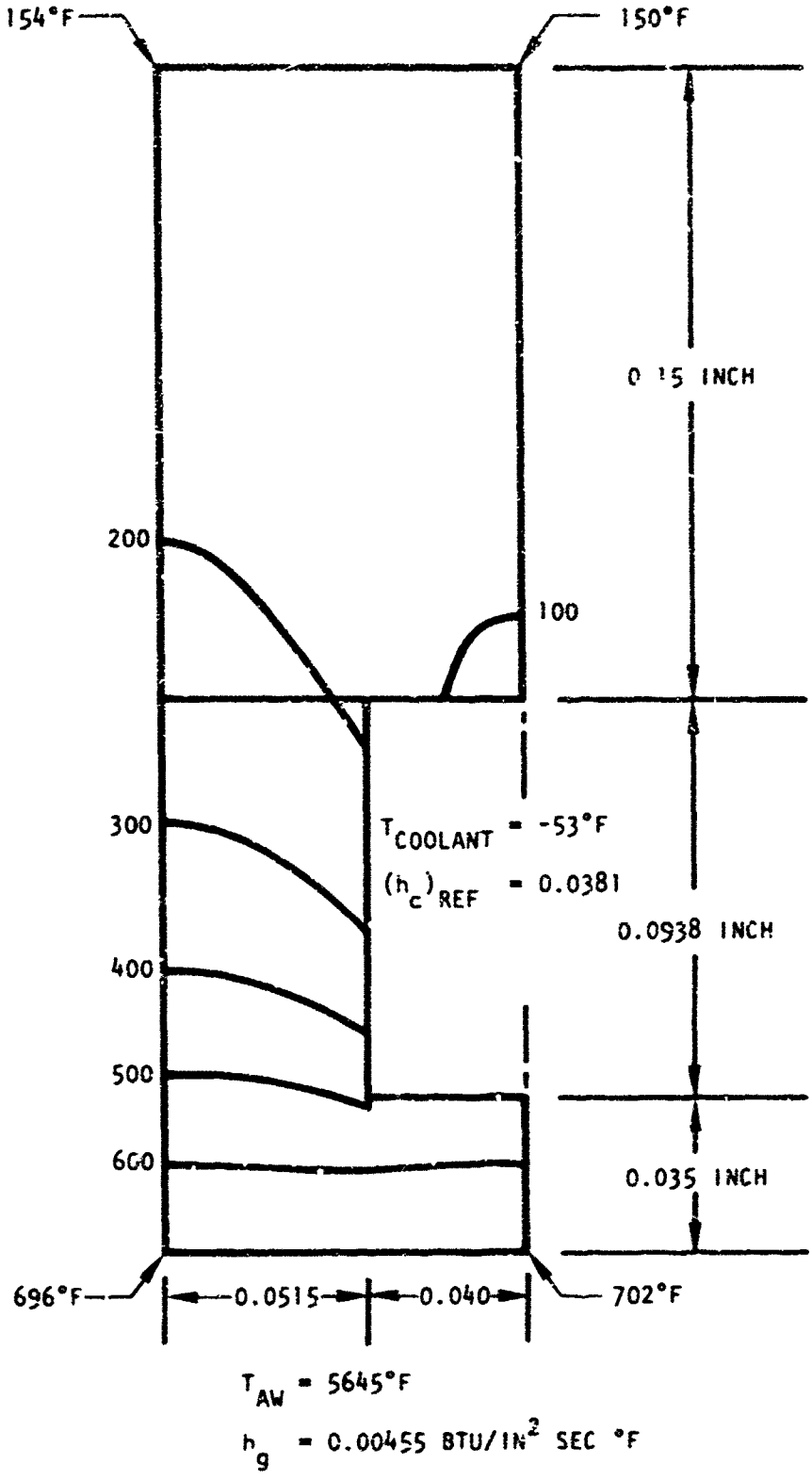

Figure 69. Thermal Fatigue Chamber Wall Temperature Distribution at X = -1.0 inches and t = 1.35 seconds (Run No. 11)

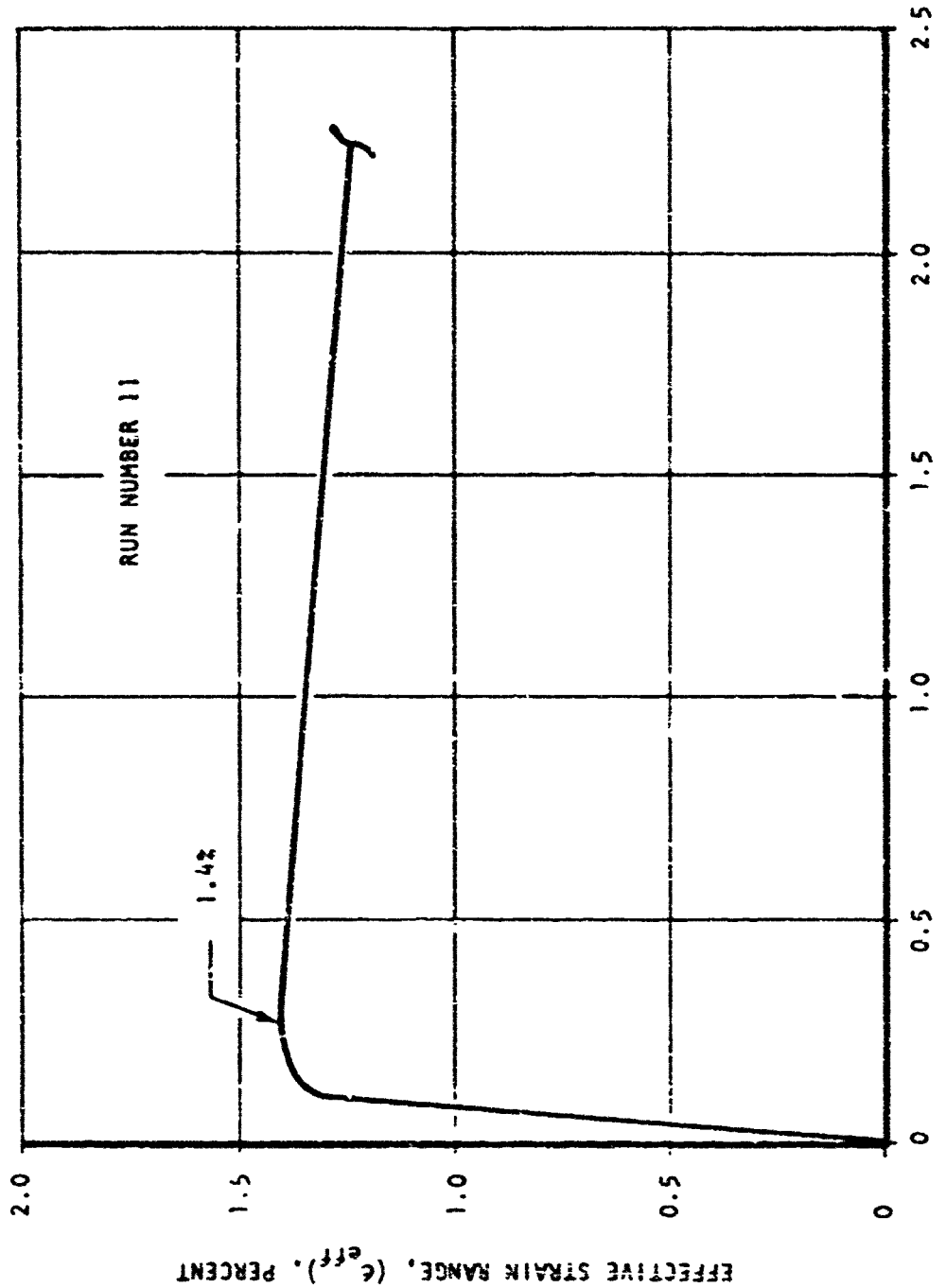

Figure 70. Effective Strain on Hot Gas Wall of NARloy-Z Chamber

In parallel with this, the isothermal fatigue data reported in Volume I was cross plotted to determine cycles to failure capability versus temperatures for several effective strain ranges as shown in Fig. 71. These data were then used to determine cycles to failure versus effective strain for the incrementally averaged data. Results are shown in Fig. 72. Also, upper and lower bounds were established based on the data scatter resulting from the isothermal fatigue tests. These data are for heat D5402, the heat of NARloy-Z used in the isothermal fatigue testing. These data were then adjusted for heat D5415, (the ingot used to make the thrust chamber) by the differences in basic material properties; accomplished by using the Universal Slopes equation as discussed in Volume I. These results, presented in Fig. 73 result in a plot of cycles to failure versus effective strain for the NARloy-Z chamber that was cyclic tested. Entering this curve at 1.4 percent effective strain shows a predicted life for the NARloy-Z chamber of 3100 to 15,000 cycles. These values are indicative of the cyclic life capability of a NARloy-Z chamber which has no inclusions as was experienced on the hardware listed here.

A comparable analysis on the zirconium copper chamber yielded a predicted life range for clean material of 2000 to 6300 cycles.

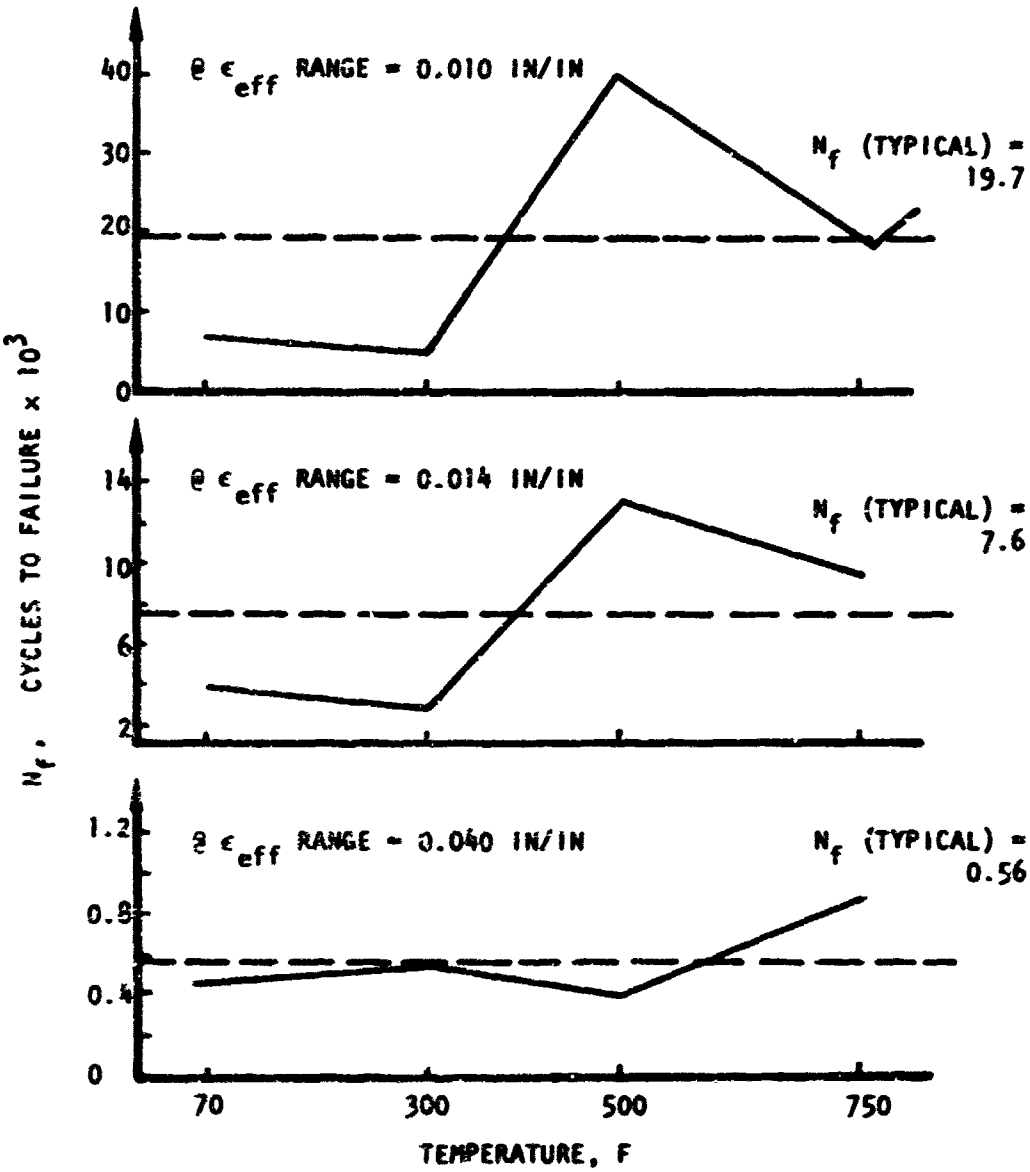

Figure 71. Cycles to Failure vs Temperature at Constant Effective Strain Range

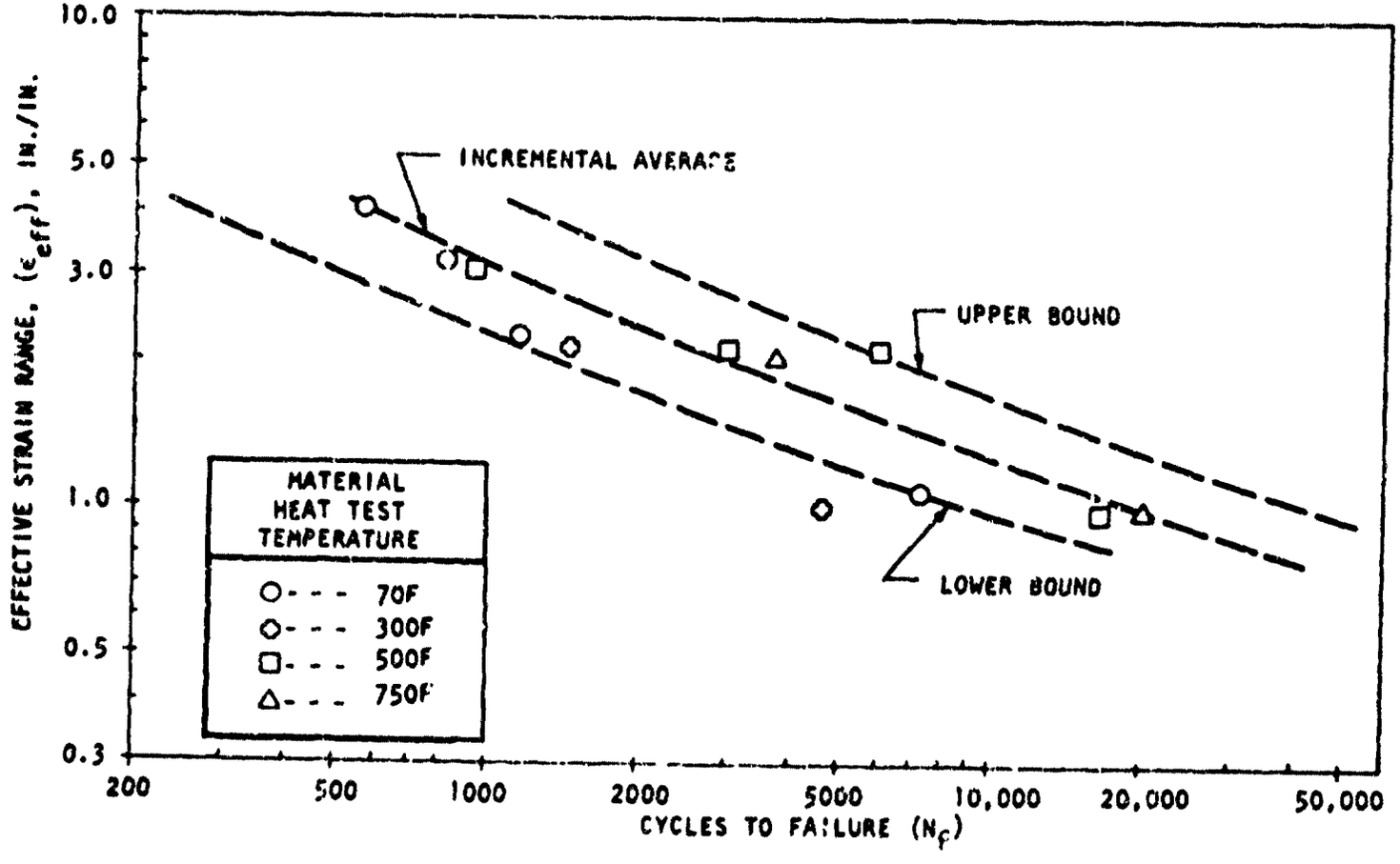

Figure 72. Thermal Fatigue Thrust Chamber Effective Strain vs Cycles to Failure Based on Incremental Averaging of All Test Data

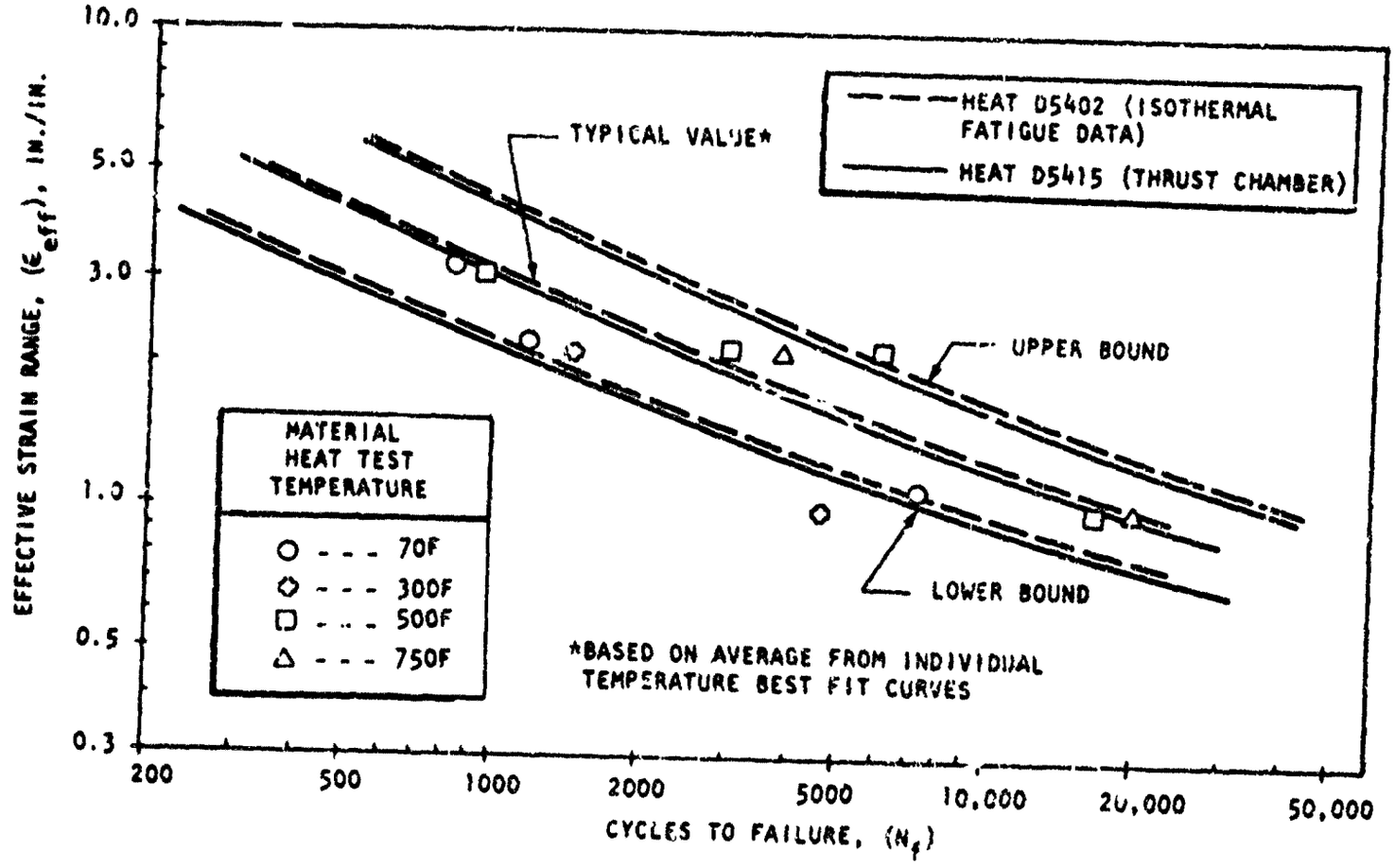

Figure 73. Thermal Fatigue Thrust Chamber Effective Strain vs Cycles to Failure

CONCLUSIONS AND RECOMMENDATIONS

It can be concluded from this test program that the copper alloy chambers do exhibit good life characteristics. This is typified by the fact that the zirconium copper chamber accumulated 398 cycles prior to occurrence of a through crack, while the NARloy-Z chamber ran 410 cycles before a similar crack occurred. The chambers were both subsequently tested for many more cycles, and although additional cracks occurred, they were capable of additional testing when the test program was terminated, due to the injector problem. It is recognized that the cracks occurred in the chambers quite early compared to the predicted values, based on the isothermal fatigue test data; however, as discussed previously, there is some lack of correlation between the two, since the effect of the inclusions is quite different on the chambers than on the isothermal fatigue specimens. On both the isothermal fatigue specimens and in the chamber these inclusions, in the form of stringers, were axially oriented. This coincides with the direction of loading for the isothermal fatigue specimens thus minimizing their effect on life. Conversely on the thrust chambers, the circumferential loads are transverse to the major stringer dimension, with a resulting major contribution to cyclic life capability. It is apparent that additional work needs to be done in laboratory testing to establish the cyclic life capability of material in a condition more nearly representative of that experienced by a thrust chamber. Also refinement of the processing of the two copper alloys is necessary to eliminate these inclusions such that the life capability can be increased to a value more nearly corresponding to that of the isothermal fatigue test specimens.

It is recommended that additional effort be accomplished in this area to (1) refine the processing of the material, and (2) conduct laboratory test effort more nearly representative of that which is experienced by a thrust chamber. This could be accomplished through the testing of small panels which experience a thermal gradient comparable to that of the thrust chamber, and would be more nearly representative of the chamber operating conditions than that of the isothermal fatigue specimens.

APPENDIX A

PROCESSING AND INSPECTION OF INCLUSION FREE ZIRCONIUM COPPER

The zirconium copper thrust chamber liner was to be fabricated by shear and form spinning from a preform forged disk 20 inches diameter x 1 inch thick. This forged disk configuration was selected as the most suitable for ultrasonic inspection of internal quality. The prior ingot stage was impossible to ultrasonic inspect because of coarse grain size and the final liner stage represented excessive cost if the material proved unsuitable. The forged disk represented the earliest stage of fabrication that the material would be potentially suitable for ultrasonic inspection.

Initially, three disks available from another program were evaluated. The disks were ultrasonically inspected in accordance with Rocketdyne Spec. RAC115-012 Class AA "Ultrasonic Inspection of Wrought Metals" (3/64 inch flat-bottom hole standard). The attenuation and hash level was so great in these parts that inspection even to a Class A level (5/64 inch flat-bottom hole standard) was impossible. No further action was taken on these forgings.

It is known that ultrasonic attentuation in copper alloys is significantly affected by the hot-work history of the forging. For this reason it was decided to procure zirconium copper ingots which could be forged under conditions which could be observed. Table A-1 outlines pertinent material information and two forging procedures employed. Two disks were forged according to Procedure I, of Table A-1. One disk was forged according to Procedure II, of Table A-1. The basic difference in the two procedures was the number of heating cycles given the forgings. Procedure I disks were made in one heat cycle. Procedure II disk was made with two heat cycles. The material in both cases was cross-worked with a high percentage of forging reduction. The intermediate heat cycle of Procedure II was introduced to cause recrystallization from any cold work that may have been introduced. The recrystallized structure, assuming no serious grain growth, might be expected to have lowered attentuation characteristics.

TAPLE A-1. MATERIAL AND FORGING PROCEDURES USED TO PRODUCT ZIRCONIUM COPPER DISKS FOR THERMAL FATIGUE LINER SPINNINGS

MATERIAL: 8-inch diameter direct chill cast ingot rough machined to 7-1/. inch diameter

Heat No. HT 329-6

Three pieces approximately 100 pounds each 7-1/2 inch diameter x 7 inch long

Ingot procured from AMPCO Metals, Pennsylvania

Ingot produced by AMAX Copper, New Jersey

FORGING PROCEDURE:

All operations performed on a 6000 pound open frame steam hammer.

PROCEDURE I - Two pieces forged

a. Heat material to 1500 F

b. Forge 7-1/2 inch diameter cross section to 5 inch square x 12 inches long

c. Break corners to 5 inch round

d. Upset 12 inch length to 20 inch diameter x 1 inch thick

e. All forging operations were completed in one heat. Temperature of part after forging was complete was below 1000 F.

PROCEDURE II - One piece forged

a. Heat material to 1500 F

b. Forge 7-1/2 inch diameter cross section to 5 inch square x 12 inches long

c. Break corners to 5 inch round

d. Upset 12 inch length to 5 inches x 9 inches diameter

e. Reheat to 1500 F

f. Upset 5 inch length to 20 inch diameter x 1 inch thick

g. Material did not go below 1000 F during forging operations

Three disks rough machined to clean up both faces with a 125 rms finish.

The forgings were rough machined on both faces and subsequently ultrasonically inspected in accordance with RA0115-012 Class AA at a locally approved inspection source (Sonic Testing and Engineering). None of the disks could be inspected with standard test blocks because of high attenuation. Forging Procedure II seemed to produce lower attenuation characteristics, however, the attenuation level was still too high for precise inspection without special test blocks. Singular ultrasonic responses were found in all three forgings when the instrumentation was calibrated to standard test blocks. The size of the indications were estimated to be larger than a 3/64 (.050 inch) flat-bottom hole standard. As many as 47 indications were found in one of the disks.

One disk (Forging Procedure I) was selected for more detailed evaluation at Rocketdyne. Special copper test blocks having attenuation characteristics similar to the forgings were used for the evaluation. The forging was scanned using a frequency of 5.0 MHz and 2.25 MHz. The hash level was too great at 5.0 MHz but a satisfactory inspection was possible at 2.25 MHz. This disk was found to have a total of 17 indications greater than 3/64 standard. Eight of these indications were greater than responses from a 5/64 test standard. The indications were estimated to range in size between 0.045 inch and 0.150 inch cross section.

Two of the 5/64 indications were isolated by sectioning the forging. The area was examined metallographically and inclusions were found. Figure A-1 shows the size and form of one of the inclusions. The long axis of the inclusion was oriented in the radial direction of the disk. The inclusion shown in the figure had a length of approximately 0.060 inch. The maximum length of the inclusion measured 0.078 inch at an earlier stage of examination. Grinding and polishing for photography caused the length of the inclusion to diminish.

Results of this investigation showed that:

1. The commercially produced zirconium-copper alloy contained large quantities of randomly dispersed oxide inclusions.

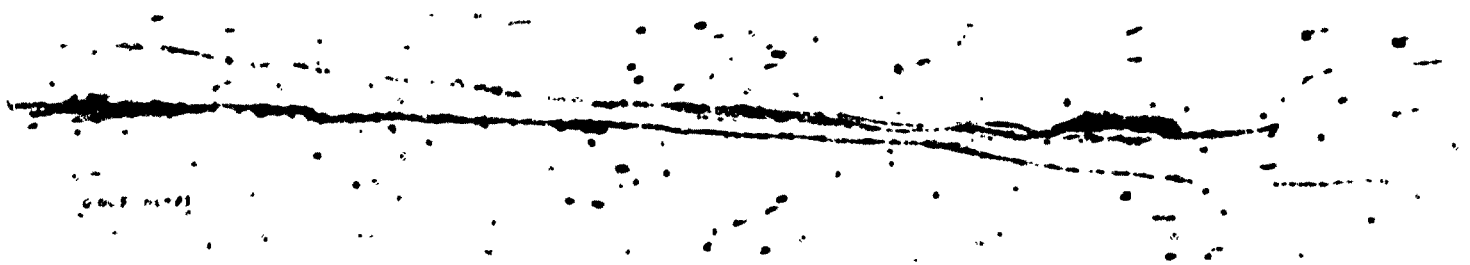

OXIDE INCLUSIONS IN ZIRCONIUM - COPPER ALLOY HEAT NUMBER HT329-6.

MATERIAL — DISK 20" DIA. X 1-1/4" FORGED FROM 8 INCH DIAMETER INGOT AS - FORGED CONDITION.

INCLUSIONS FOUND BY ULTRASONIC INSPECTION USING REST STANDARDS HAVING ATTENUATION EQUIVALENT TO THIS MATERIAL.

ULTRASONIC RESPONSE FROM THIS INCLUSION WAS GREATER THAN A 5/64" FLAT BOTTOM HOLE STANDARD.

Figure A-1. Oxide Inclusion in Zirconium-Copper Heat Number HT329-6

2. Inclusions in zirconium-copper found by this investigation ranged between an estimated .045 inch to .150 inch nominal diameter as determined ultrasonically by comparison with standards of known area.

3. Special melting and casting techniques will be required to produce inclusion-free zirconium-copper alloy suitable for rocket nozzles.

4. Zirconium-copper alloy in one-inch section thickness was difficult, if not impossible, to inspect ultrasonically to the Class AA level (3/64 inch flat-bottom hole standard equivalent to inclusions of approximately 0.050 inch diameter).

Inclusions of similar character had been observed in some of the early NARloy-Z ingots. Microprobe analysis identified these inclusions as primarily zirconium oxide. It was reasonable to assume that the inclusions in the zirconium-copper alloy had the same composition.

Ultrasonic evaluation of many heats of NARloy-Z have demonstrated that the forged material is readily inspected by ultrasonic technique and displays none of the annoying attentuation problems encountered in this evaluation of zirconium-copper alloy. Further, singular ultrasonic responses in NARloy-Z have been verified many times to be generated from oxide films and not be extraneous micro-structural phenomena. The technique has demonstrated effectiveness in detecting inclusions and conversely it can be assumed that an ultrasonically clean forging is free of these defects.

It is difficult to assess the causes of erratic attenuation and ultrasonic difficulties in the zirconium-copper alloy. Grain size and grain distribution can have a significant effect. However, the forging practices employed to produce the disks were conducive to producing a fine-grain forging. Similar forging operations in NARloy-Z have produced uniform equiaxed grain size with sonic attenuation equivalent to or lower than the standard test blocks used for normal inspection. Verbal communication with AMAX Copper, producer of the alloy, indicated that sonic inspection was a problem in the limited experience of commercial applications. They could offer no explanations for the difficulties.

Other copper alloys such as naval brass and OFHC copper have displayed attenuation problems. Rocketdyne experience with naval brass for wear rings found it impossible under any circumstance to inspect the material even to a Class A level (5/64 inch standard). No forging practice could be established which would alleviate the attenuation problem in this material. Grain size in this case was influential but not the total problem. No satisfactory explanation was determined.

Zirconium-copper alloy is not in the same category as naval brass, however, reliable inspection (Class AA level) in all but thin sections (1/2 inch-to-1/4 inch) may be a continual problem from the attenuation standpoint.

It was concluded from this effort that if zirconium-copper alloy was to be considered for long life thrust chamber liner applications, refinements in present mill practice or alternate methods of producing the material were mandatory. Development work on melting and casting NARloy-Z had evolved techniques capable of producing material free of ultrasonic indications and thus inclusions when inspected to the Class AA level. These techniques were evaluated for zirconium-copper fabrication.

It was subsequently determined that consumable electrode remelting of zirconium-copper ingots dramatically improved the ingot quality, making it available for use in long life thrust chambers.

This process involves a two-step melting procedure as illustrated in Fig. A-2. The basic ingot is produced by vacuum induction melting as shown. The ingot is then remelted and recast under vacuum by passing an electrical current through the ingot as illustrated. In this manner all inclusions are driven to the top of the ingot where they are subsequently machined away prior to ingot forging.